Statistical Inference in Multivariate Settings

A DISSERTATION
SUBMITTED TO THE FACULTY OF THE GRADUATE SCHOOL
OF THE UNIVERSITY OF MINNESOTA
BY

Daniel J. Eck

IN PARTIAL FULFILLMENT OF THE REQUIREMENTS
FOR THE DEGREE OF
DOCTOR OF PHILOSOPHY

Charles J. Geyer and
R. Dennis Cook, Advisers

June 2017

Acknowledgements

I am very thankful for my advisers, Charles Geyer and Dennis Cook. I am grateful for the energy they have spent and the encouragement they have given to make this dissertation possible. They have taught me many lessons on how to approach the problem at hand while simultaneously thinking about the big picture of our Statistics discipline. They were also very patient and took time to teach me the tools I needed to complete this dissertation and will need in the future. Both Charles and Dennis gave me academic freedom and allowed me to pursue problems that I found interesting. Again, thank you.

I would like to specially thank Ruth Shaw. Time and time again, she went out of her way to provide summer research opportunities, edit my work, and teach me the science relevant to aster modeling.

Thank you Christopher Nachtsheim for teaching me design of experiments and his contributions to algorithms and writing in Chapter 7. The examples in Chapter 7 would not be possible without him. Thank you William Sudderth for teaching me game theory during your retirement. Thank you Ian McKeague for introducing me to the subject matter that led to the work in Chapter 8 and the corresponding paper.

One of the main reasons I came here was the people that I met on my visit day. I have very much enjoyed my peers at the School of Statistics from start to finish. I thank all of the fellow students in the School of Statistics that I have met throughout the years. Special thanks to Brandon Whited, Dootika Vats, Ben Sherwood, Xin Zhang, Abhirup Mallik, Shubho Majumdar, Henry Wyneken, Brad Price, Felipe Acosta, Adam Maidman, Karl Oskar Ekvall, Sakshi Arya, Yang Yang, Lindsey Dietz, Megan Heyman, and Craig Rolling. Special thanks to Amber Eula-Nashoba of Ruth Shaw's group for providing edits of my technical report corresponding to the combination of aster and envelope models.

I would also like to thank professors Lan Wang, Adam Rothman, Yuhong Yang, Charles Doss, Lan Liu, and Nathaniel Helwig. Special thanks to professor Snigdhansu Chatterjee

who provided encouragement and edits to the work in Chapter 6.

The most important thank you goes out to my family. My parents and brother have been supportive, especially when support was needed. Most of all thanks to my future wife, Stephanna, for her support over the past four years.

Dedication

This dissertation is dedicated to my family

Abstract

Precise and reliable inferences are among one of the main tenets of the statistical practice. The ability to make such inferences in modeling can only be made when collected data satisfies the assumptions of the model chosen for inference. The topics covered in this dissertation are varied, but precise and reliable inference for multiple variables under realistic modeling assumptions is a unifying theme. When data come from a discrete exponential family, an inferential framework is developed for when the maximum likelihood estimator does not exist in the usual sense. Envelope methodology is incorporated with aster models so that expected Darwinian fitnesses can be estimated precisely. A residual bootstrap routine for a weighted envelope estimator which accounts for model selection volatility is developed. A residual bootstrap routine is developed in the context of the multivariate linear regression model. These routines show that the variability of the respective estimators is estimated consistently by bootstrapping. Engineering dimension analysis is extended to the multivariate design of experiments context. Outside of the main theme, a central limit theorem under additive deformations is provided in the last chapter.

Contents

List of Tables

List of Figures

Chapter 1

Introduction

Statistical inference is the process of drawing conclusions about a population on the basis of measurements or observations made on a sample of units from the population (Everitt and Skrondal, 2010). The primary focus of this dissertation is the study of statistical inference when multiple variables are of interest. In particular, we focus on estimation of an unknown parameter vector of a data generating model and estimation of the estimator's variability. The topics studied in this dissertation are varied but this is a main unifying theme. It is of specific interest to place realistic assumptions on the data generating model so that statistical inferences are reliable when made by practitioners in applications.

Outside of the common theme of multivariate statistical inference under realistic assumptions of the data generating model, the topics studied in this dissertation have little in common. The work in Chapters 2 through 4 put inferential interest in the canonical and mean-value parameter vectors of an exponential family. In Chapter 2, the exponential family is required to be discrete. In Chapters 3 and 4, the exponential family can be a mixture of discrete and continuous parts. The theory in Chapter 2 provides an inferential framework when observed data from a discrete exponential family is on the boundary of the support of the exponential family. Our theorems allow for practitioners to make relatively fast statistical inferences in this setting. Chapter 3 provides the backdrop of aster models, their usefulness in life history analysis, and contains a thorough real data example of them. The methods in Chapter 4 allow practitioners of life history analyses to estimate parameters of interest consistently and with less variability than existing methods can.

In Chapters 4 and 5, inferential interest is placed on consistent estimation and variance reduction through envelope methodology. In both chapters, model selection variability and post-selection inference are taken into account. The focus in these chapters is not to develop a framework for consistent model selection. Rather, models are averaged where the weight corresponding to a particular model reflects our belief that that particular model is the data generating model.

Bootstrapping techniques for inference in multivariate models are studied in Chapters 4 through 6. In Chapter 4, Efron (2014)'s parametric double bootstrap was used for inferences. In Chapter 5, a residual bootstrap of our construction was used for inferences. In Chapter 6, we extend the work of Freedman (1981) to show that the variability of the ordinary least squares regression coefficient matrix in the multivariate linear regression model is estimated consistently by the same residual bootstrap procedure as Freedman (1981).

In Chapter 7, we extend the work of Albrecht, Nachtsheim, Albrecht, and Cook (2013) to the multivariate design of experiments context. This provides a framework for practitioners to design efficient experiments when inference is desired for multiple responses that are measured in units that are otherwise not comparable. This work provides needed design of experiments methodology for a class of problems where appropriate and efficient designs were previously not well understood.

The work in Chapter 8 does not fit the multivariate theme or the same statistical inference theme as the work in the previous six chapters. However, it is work that I found interesting and completed during my tenure at the University of Minnesota. In this chapter, central limit theorems are developed when random variables are combined via a general binary operator instead of addition. Such central limit theorems are appropriate in physical applications.

All of the proofs in this dissertation are original to the author of this dissertation, except for the proof of Theorem 8. Theoretical derivations not made by this author are referenced.

Chapter 2

Maximum Likelihood Estimation in Exponential Families

2.1 Introduction

We develop an inferential framework for discrete exponential family problems when observed data lies on the boundary of the support of the exponential family. In such settings, it may be the case that the maximum likelihood estimator (MLE) need not exist in the traditional sense but may exist in a completion of the exponential family. Completions for families with finite and countable support were considered by Barndorff-Nielsen (1978, 154-156) and Brown (1986, 191-201) respectively. Csiszár and Matúš (2005) generalized the notion of completion of exponential families and provided weak convergence results within their construction. Geyer (2009) developed an inferential framework for when MLEs exist in the completion of the exponential family. Geyer (2009) assumed the conditions mentioned in Brown (1986) and referred to the completion of the exponential family as the Barndorff-Nielsen completion of the exponential family. We will make the same reference. When it is the case that the MLE exists in the Barndorff-Nielsen completion of the exponential family, the traditional theory of MLEs and computational methods will lead their users astray (Geyer, 2009). Further complicating the issue is the fact that statistical software provides users with no reliable detection methods and solutions when the MLE exists in the Barndorff-Nielsen completion.

Geyer (1990, 2009) provided a theoretical solution to this problem. Geyer (1990, Chapter 2) gave an algorithm that uses linear programming to calculate the MLE in a closed convex exponential family by recursively calculating limiting conditional models (LCMs) determined by directions of recession calculated by linear programming. A direction of recession is a direction that increases the likelihood of an exponential family as one goes further in that direction. An LCM is a model that is conditional on the subset of domain that is orthogonal to the direction of recession. Geyer (2009) gives an algorithm that uses linear programming to calculate the MLE in full regular exponential families satisfying a number of assumptions (Geyer, 2009, Section 3.7), by non-recursively calculating one LCM determined by a *generic* direction of recession calculated by linear programming. The algorithm in Geyer (1990, Chapter 2) is more general; the algorithm in Geyer (2009) is more efficient for the special cases to which it applies. Neither is very fast, and neither scales to very large problems. According to the documentation for the `cddlib` computational geometry library, to which the R package `rcdd` provides an R interface, it can handle problems having number of variables in the low hundreds and number of constraints in the thousands. Put in the context of exponential family problems discussed by Geyer (2009) this corresponds to generalized linear models with a few hundred regression coefficients and less than ten thousand cases. But for problems even that large, the computational geometry calculations will be very slow. Computational geometry calculations using `rcdd` do have the virtue that they are exact, using infinite-precision rational arithmetic. They find exact directions of recession.

A much faster alternative is to just let maximum likelihood estimation find directions of recession. If we have a sequence θ_n that maximizes the likelihood, we will have convergence to the unique MLE distribution, provided it exists in the Barndorff-Nielsen completion. We justify this approach to maximum likelihood estimation by showing that cumulant generating functions (CGFs) evaluated at such a sequence of iterates converges to the CGF of the MLE distribution.

It is then shown that moments of all orders converge along the maximizing likelihood sequence θ_n. Inference about the canonical parameter vector of an exponential family

can therefore be made when the MLE does not exist in the traditional sense. The CGF convergence that we develop is reliant on a measure-theoretic formulation of exponential families and on properties of sequences of affine functions. Both topics are thoroughly discussed before our convergence results are stated and examples are given.

Theorem 5 of Geyer (2009) in Section 2.4.5 and the following discussion state how taking limits in the generic direction of recession maximizes the likelihood. The LCM resulting from taking limits supports values of the canonical statistic that are orthogonal to the generic direction of recession. Therefore the direction of recession is a null eigenvector of the Fisher Information matrix of the LCM. Convergence of moments of all orders along maximizing likelihood sequences implies that we can estimate Fisher Information in the LCM without using directions of recession.

2.2 Motivating Example

Consider the case of perfect separation in the logistic regression model as an example of a discrete exponential family with data on the boundary of its support. In this example, suppose that we have a univariate response variable y and a single predictor x and suppose that $x_j = 10j$ and $y_j = I_{\{x>45\}}(x_j)$ for $j = 1, ..., 8$. Let $\beta \in \mathbb{R}$ be the unknown regression coefficient. The logistic regression model for this data has log likelihood given by

$$\begin{aligned} l(\beta) &= \sum_{j=1}^{8} y_j \log\left(\frac{e^{\beta x_j}}{1+e^{\beta x_j}}\right) + (1-y_j)\log\left(\frac{1}{1+e^{\beta x_j}}\right) \\ &= \sum_{j=1}^{8} y_j \left\{\log\left(\frac{e^{\beta x_j}}{1+e^{\beta x_j}}\right) - \log\left(\frac{1}{1+e^{\beta x_j}}\right)\right\} + \sum_{j=1}^{8} \log\left(\frac{1}{1+e^{\beta x_j}}\right) \\ &= \langle Y, M\beta\rangle - c(\beta) \\ &= \langle M^T Y, \beta\rangle - c(\beta) \end{aligned} \tag{2.1}$$

where Y is the vector of observed responses, $M = (10, ..., 80)^T$ is the model matrix, and $c(\beta) = -\sum_{j=1}^{8} \log\left(\frac{1}{1+e^{\beta x_j}}\right)$ is the cumulant function of the exponential family. In the final parameterization of the model (2.1), we say that $M^T Y$ is the canonical statistic and β is

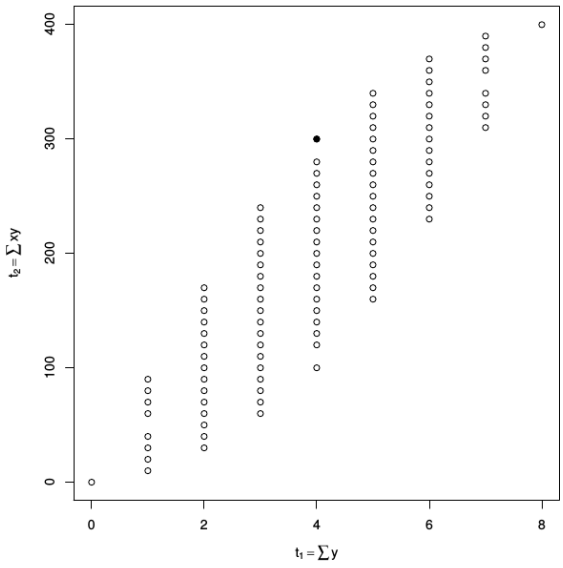

Figure 2.1: All possible values of the canonical statistic M^TY for the logistic regression example in the Motivating Example section. The solid dot is the observed value of M^TY.

the canonical parameter of the exponential family. Because of perfect separation of the observed data, the MLE of β does not exist in the traditional sense. Consult Figure 2.1 to see that the canonical statistic exists on the boundary of its support in this example. Our theory provides an inferential context in this specific "perfect separation" in logistic regression setting as well as a more general setting where the MLE does not exist in the traditional sense.

2.3 Laplace transforms and standard exponential families

We motivate exponential families through their measure-theoretical formulation starting with the log Laplace transform of the generating measure for the family. In this context, the log Laplace transform is called the cumulant function of the exponential family. The reason for this level of generality is that the CGF convergence we develop requires that the log density of the exponential family be an affine function of the data.

Let λ be a nonzero positive Borel measure on a finite-dimensional vector space E (positive means $\lambda(B) \geq 0$ for all Borel sets B and nonzero means $\lambda(B) \neq 0$ for some Borel set B). The *log Laplace transform* of λ is the function $c : E^* \to \overline{\mathbb{R}}$ defined by

$$c(\theta) = \log \int e^{\langle x, \theta \rangle} \, \lambda(dx), \qquad \theta \in E^* \tag{2.2}$$

(Geyer, 1990, Section 2.1), where E^* is the dual space of E (Geyer, 1990, Appendix A.1), $\langle \cdot, \cdot \rangle$ is the canonical bilinear form placing E and E^* in duality (same appendix), and $\overline{\mathbb{R}}$ is the extended real number system (Geyer, 1990, Appendix A.6), which adds the values $-\infty$ and $+\infty$ to the real numbers.

If one prefers, one can take $E = E^* = \mathbb{R}^p$ for some p, and define

$$\langle x, \theta \rangle = \sum_{i=1}^{p} x_i \theta_i, \qquad x \in \mathbb{R}^p \text{ and } \theta \in \mathbb{R}^p,$$

(and Geyer, 2009, does this), but here, like everywhere else linear algebra is used, the coordinate-free view of vector spaces offers more generality, is cleaner, and is more elegant. Also, as we are about to see, if E is the sample space of a standard exponential family, then a subset of E^* is the canonical parameter space, and the distinction between E and E^* helps remind us that we should not consider these two spaces to be the same space.

A log Laplace transform is a lower semicontinuous convex function that nowhere takes the value $-\infty$ (the value $+\infty$ is allowed and occurs where the integral in (2.2) does not exist) (Geyer, 1990, Theorem 2.1). The *effective domain* of an extended-real-valued convex function c on E^* is

$$\operatorname{dom} c = \{ \, \theta \in E^* : c(\theta) < +\infty \, \}.$$

For every $\theta \in \operatorname{dom} c$, the function $f_\theta : E \to \mathbb{R}$ defined by

$$f_\theta(x) = e^{\langle x, \theta \rangle - c(\theta)}, \qquad x \in E, \tag{2.3}$$

is a probability density with respect to λ. Densities (2.3) have log likelihood

$$l(\theta) = \langle x, \theta \rangle - c(\theta). \tag{2.4}$$

The set $\mathcal{F} = \{ f_\theta : \theta \in \Theta \}$, where Θ is any nonempty subset of $\operatorname{dom} c$, is called a *standard exponential family of densities with respect to* λ. This family is *full* if $\Theta = \operatorname{dom} c$.

It is useful to have terminology relating the family $\mathcal{F}$ to the measure λ. We say $\mathcal{F}$ is the standard exponential family *generated by* λ having canonical parameter space Θ, and we say λ is the *generating measure* of $\mathcal{F}$.

A general exponential family (Geyer, 1990, Chapter 1) is a family of probability distributions having a sufficient statistic X taking values in a finite-dimensional vector space E that induces a family of distributions on E that have a standard exponential family of densities with respect to some generating measure. Reduction by sufficiency loses no statistical information, so the theory of standard exponential families tells us everything about general exponential families (Geyer, 1990, Section 1.2).

In the context of general exponential families X is called the *canonical statistic* and θ the *canonical parameter* (the terms *natural statistic* and *natural parameter* are also used). In the context of standard exponential families, we only use the canonical parameter and statistic. The set Θ is the canonical parameter space of the family, the set $\operatorname{dom} c$ is the canonical parameter space of the full family having the same generating measure. A full exponential family is said to be *regular* if its canonical parameter space $\operatorname{dom} c$ is an open subset of E^*.

The distributions F_θ corresponding to the densities (2.3) are given by

$$F_\theta(B) = \int_B e^{\langle x, \theta \rangle - c(\theta)} \, \lambda(dx), \qquad B \in \mathcal{B}, \tag{2.5}$$

where $\mathcal{B}$ is the Borel sigma-algebra of E. The CGF k_θ of the distribution F_θ, provided this

distribution has a CGF, is given by

$$\begin{aligned} k_\theta(t) &= \log \int e^{\langle x,t\rangle} f_\theta(x)\, \lambda(dx) \\ &= c(\theta + t) - c(\theta) \end{aligned} \tag{2.6}$$

and this is a CGF provided it is finite on a neighborhood of zero, that is if $\theta \in \operatorname{int}(\operatorname{dom} c)$. We see that every distribution in a full family has a CGF if and only if the family is regular. Derivatives of k_θ evaluated at zero are the cumulants of F_θ. These are the same as derivatives of c evaluated at θ.

2.4 Generalized affine functions

2.4.1 Characterization on affine spaces

Exponential families defined on affine spaces are of particular interest for the convergence we develop. In the previous section, we motivated the development of the exponential family through its generating measure λ. The log likelihood of the exponential family corresponding to this measure-theoretic formulation is an affine function of the data as seen in (2.4). What we will call the *Barndorff-Nielsen completion* of the exponential family, following Geyer (2009), is the set of all limits of distributions in the family. We take limits in the sense of pointwise convergence of densities, following Geyer (1990, Chapters 2 and 4) and Geyer (2009). Other authors, including Barndorff-Nielsen (1978) and Brown (1986), have taken limits in the sense of convergence in distribution, but discussed no examples where convergence in distribution gave different results from pointwise convergence of densities.

Of course, if $e^{h_n} \to e^h$ pointwise, then $h_n \to h$ pointwise, and vice versa. Hence the idea of completing an exponential family naturally leads to the the study of limits of sequences of affine functions. Here we assume that the limiting function may be extended-real-valued (the extended real number system, denoted $\overline{\mathbb{R}}$, is the two-point compactification of the real number system, which adds $-\infty$ at one end and $+\infty$ at the other). A real-valued function is affine if and only if it is both convex and concave. Since limits preserve convexity and

concavity, we are led to the study of extended-real-valued functions that are both convex and concave. These functions are called *generalized affine functions*.

Geyer (1990, Chapter 3) studies generalized affine functions on both finite-dimensional and infinite-dimensional affine spaces, but here we only study generalized affine functions on finite-dimensional affine spaces. That is all that is needed for exponential family theory.

Definition 1

An extended-real-valued function h on a finite-dimensional affine space E is *generalized affine* if it is both convex and concave. □

This means that (Rockafellar, 1970, Section 4; Rockafellar and Wets, 1998, Section 2.A)

$$h\big(x + t(y - x)\big) \le (1 - t)h(x) + th(y),$$
$$\text{whenever } 0 < t < 1 \text{ and } h(x) < \infty \text{ and } h(y) < \infty,$$

and

$$h\big(x + t(y - x)\big) \ge (1 - t)h(x) + th(y),$$
$$\text{whenever } 0 < t < 1 \text{ and } h(x) > -\infty \text{ and } h(y) > -\infty.$$

The former says h is convex. The latter says h is concave. The following two theorems provide a characterization of generalized affine functions on affine spaces. In preparation, we use the notation

$$h^{-1}(\mathbb{R}) = \{\, x \in E : h(x) \in \mathbb{R} \,\}$$
$$h^{-1}(\infty) = \{\, x \in E : h(x) = \infty \,\}$$
$$h^{-1}(-\infty) = \{\, x \in E : h(x) = -\infty \,\}$$

Theorem 1

An extended-real-valued function h on a finite-dimensional affine space E is generalized

affine if and only if one of the following cases holds

(a) $h^{-1}(\infty) = E$,

(b) $h^{-1}(-\infty) = E$,

(c) $h^{-1}(\mathbb{R}) = E$ and h is an affine function,

(d) There is a hyperplane H such that $h(x) = \infty$ for all points on one side of H, $h(x) = -\infty$ for all points on the other side of H, and h restricted to H is a generalized affine function. □

The proof of Theorem 1 is in Geyer (1990). The intention is that this theorem is applied recursively. If we are in case (d), then the restriction of h to H is another generalized affine function to which the theorem applies. More on this later.

2.4.2 Topology

Now we need to understand the topology of the space of generalized affine functions on a finite-dimensional affine space E with the topology of pointwise convergence. Call that $G(E)$.

Theorem 2

The space of generalized affine functions on a finite-dimensional affine space with the topology of pointwise convergence is a compact Hausdorff space. □

The proof of Theorem 2 is in Geyer (1990).

Theorem 3

$G(E)$ is a first countable topological space. □

The proof of Theorem 3 is in Geyer (1990). The space $G(E)$ is not metrizable, unless E is zero-dimensional (Geyer, 1990, penultimate paragraph of Section 3.3). So we cannot use δ-ε arguments, but we can use arguments involving sequences, in particular, a compact and

first countable topological space is sequentially compact (every sequence has a convergent subsequence) (Kelley, 1955, Chapter 5, Problem E, Part (d)). This is instrumental for our treatment of maximum likelihood estimation.

2.4.3 Characterization on vector spaces

The convergence results that we discover are aimed for application in generalized linear regression model problems with data that is assumed to be realized from a full discrete exponential family. In these applications, data and parameters are assumed to be elements of a finite-dimensional vector space. The conclusions of Theorem 3 hold when $G(E)$ is the space of generalized affine functions on a finite-dimensional vector space E with the topology of pointwise convergence. The next Theorem provides a characterization of generalized affine functions defined on finite-dimensional vector spaces.

Theorem 4

An extended-real-valued function h on a finite-dimensional vector space E is generalized affine if and only if there exist finite sequences (perhaps of length zero) of vectors $\eta_1, \ldots, \eta_j$ being a linearly independent subset of E^*, the dual space of E, and scalars $\delta_1, \ldots, \delta_j$ such that h has the following form. Define $H_0 = E$ and, inductively, for integers i such that $0 < i \leq j$

$$
\begin{aligned}
H_i &= \{\, x \in H_{i-1} : \langle x, \eta_i \rangle = \delta_i \,\} \\
C_i^+ &= \{\, x \in H_{i-1} : \langle x, \eta_i \rangle > \delta_i \,\} \\
C_i^- &= \{\, x \in H_{i-1} : \langle x, \eta_i \rangle < \delta_i \,\}
\end{aligned}
$$

all of these sets (if any) being nonempty. Then $h(x) = +\infty$ whenever $x \in C_i^+$ for any i, $h(x) = -\infty$ whenever $x \in C_i^-$ for any i, and h is either affine or constant on H_j, where $+\infty$ and $-\infty$ are allowed for constant values. □

Proof: First, assume h satisfies the conditions of Theorem 1 on E. We then show that h satisfies the conditions of Theorem 4 by induction on the dimension of E. The induction

hypothesis, H(p), is that the conclusions of Theorem 1 imply that the conclusions of Theorem 4 hold when $\dim(E) = p$. We now show that H(0) holds. In this setting, $E = \{0\}$. Thus Theorem 4 holds with $j = 0$ and h is constant on E. The basis of the induction holds.

Let $\dim(E) = p + 1$. We now show that H(p) implies that H($p + 1$) holds. In the event that h is characterized by case (a) or (b) of Theorem 1 then Theorem 4 holds with $j = 0$. If case (c) of Theorem 1 characterizes h then there is an affine function f_1 defined by $f_1(x) = \langle x, \eta_1 \rangle - \delta_1$, $x \in E$, such that $h(x) = +\infty$ for x such that $f_1(x) > 0$, $h(x) = -\infty$ for x such that $f_1(x) < 0$, and h is generalized affine on the hyperplane $H_1 = \{x : f_1(x) = 0\}$. The hyperplane H_1 is p-dimensional affine subspace of E. Now, for some arbitrary $\zeta_1 \in H_1$, define

$$\begin{aligned} V_1 &= \{x - \zeta_1 : x \in H_1\} \\ &= \{y \in E : \langle y, \eta_1 \rangle = \delta_1 - \langle \zeta_1, \eta_1 \rangle\} \\ &= \{y \in E : \langle y, \eta_1 \rangle = 0\} \end{aligned}$$

where the last equality follows from $\zeta_1 \in H_1$. The space V_1 is a p-dimensional vector subspace of E since every affine space containing the origin is a vector subspace (Rockafellar, 1970, Theorem 1.1) and because every translate of an affine space is another affine space (Rockafellar, 1970, pp. 4). Let

$$h_1(y) = h(y + \zeta_1), \qquad y \in V_1. \tag{2.7}$$

The function h_1 is convex since the composition of a convex function with an affine function is convex. To see this, let $0 < \lambda < 1$, pick $y_1, y_2 \in V_1$ and observe that

$$\begin{aligned} h_1(\lambda y_1 + (1 - \lambda) y_2) &= h(\lambda y_1 + (1 - \lambda) y_2 + \zeta_1) \\ &\leq \lambda h(y_1 + \zeta_1) + (1 - \lambda) h(y_2 + \zeta_1) \\ &= \lambda h_1(y_1) + (1 - \lambda) h_1(y_2). \end{aligned}$$

A similar argument shows that h_1 is concave. Therefore h_1 is generalized affine. From our induction hypothesis, the conclusions of Theorem 1 imply that the conclusions of Theorem 4 hold for the generalized affine function h_1. These conditions are that there exist finite sequences of vectors $\tilde{\eta}_2$, ..., $\tilde{\eta}_j$ being a linearly independent subset of V_1^*, the dual space of V_1, and scalars $\tilde{\delta}_2$, ..., $\tilde{\delta}_j$ such that h_1 has the following form. Define $\widetilde{H}_1 = V_1$ and, inductively, for integers i such that $2 < i \leq j$

$$\begin{aligned} \widetilde{H}_i &= \{\, x \in \widetilde{H}_{i-1} : \langle x, \tilde{\eta}_i \rangle = \tilde{\delta}_i \,\} \\ \widetilde{C}_i^+ &= \{\, x \in \widetilde{H}_{i-1} : \langle x, \tilde{\eta}_i \rangle > \tilde{\delta}_i \,\} \\ \widetilde{C}_i^- &= \{\, x \in \widetilde{H}_{i-1} : \langle x, \tilde{\eta}_i \rangle < \tilde{\delta}_i \,\} \end{aligned} \tag{2.8}$$

all of these sets (if any) being nonempty. Then $h_1(x) = +\infty$ whenever $x \in \widetilde{C}_i^+$ for any i, $h_1(x) = -\infty$ whenever $x \in \widetilde{C}_i^-$ for any i, and h_1 is either affine or constant on $\widetilde{H}_j$, where $+\infty$ and $-\infty$ are allowed for constant values.

It remains to show that the conditions of Theorem 4 hold with respect to h. The vectors $\tilde{\eta}_i$, $i = 2, ..., j$ can be extended to form a set of vectors η_i, $i = 2, ..., j$ in E^* by the Hahn-Banach Theorem (Rudin, 1973, Theorem 3.6). The vectors η_i, $i = 2, ..., j$, form a linearly independent subset of E^*. To see this, let $\sum_{k=2}^{j} a_k \eta_k = 0$ on E for scalars a_k, $k = 2, ..., j$. Then $\sum_{k=2}^{j} a_k \eta_k = 0$ on V_1 which implies that $a_k = 0$ for $k = 2, ..., j$ by the definition of linearly independent. Let $H_0 = E$, and, for $i = 2, ..., j$, define

$$\begin{aligned} H_i &= \{\, x \in H_{i-1} : \langle x, \eta_i \rangle = \delta_i \,\} \\ C_i^+ &= \{\, x \in H_{i-1} : \langle x, \eta_i \rangle > \delta_i \,\} \\ C_i^- &= \{\, x \in H_{i-1} : \langle x, \eta_i \rangle < \delta_i \,\} \end{aligned} \tag{2.9}$$

where $\delta_i = \tilde{\delta}_i - \langle \zeta_1, \eta_i \rangle$ for $i = 2, ..., j$ and $\widetilde{H}_i = H_i + \zeta_1$ as a result. We see that $h(x) = h_1(x - \zeta_1) = +\infty$ whenever $\langle x + \zeta_1, \eta_i \rangle > \tilde{\delta}_i$. Therefore $h(x) = +\infty$ for all $x \in C_i^+$ for any i. The same derivation shows that $h(x) = -\infty$ whenever $x \in C_i^-$ for any i. The generalized affine function h is either affine or constant on H_j, where $+\infty$ and $-\infty$ are allowed for constant values since the composition of an affine function with an affine function is affine.

We now show that the vectors $\eta_1, ..., \eta_j$ are linearly independent. Assume that $\sum_{k=1}^{j} a_k \eta_k = 0$ on E for scalars a_k, $k = 1, ..., j$. This assumption implies that $\sum_{k=1}^{j} a_k \tilde{\eta} = 0$ on V_1^* where $\tilde{\eta}_1$ is the restriction of η_1 to V_1. Thus $\tilde{\eta}_1$ is an element of V_1^* and $\tilde{\eta}_1 = 0$ on V_1 since $\langle y, \tilde{\eta}_1 \rangle = \langle y, \eta_1 \rangle = 0$ on V_1. Therefore $\sum_{k=2}^{j} a_k \tilde{\eta}_k = 0$ where $a_k = 0$ for $k = 2, ..., j$ from what has already been shown. In the event that $a_1 = 0$, we can conclude that $\eta_1, ..., \eta_j$ are linearly independent. Now consider $a_1 \neq 0$. In this case, $\sum_{k=1}^{j} a_k \eta_k = 0$ implies that $\eta_1 = \sum_{k=2}^{j} b_k \eta_k$ where $b_k = -a_k/a_1$. This states that $\sum_{k=2}^{j} b_k \tilde{\eta}_k = 0$ on V_1. Therefore, $b_k = 0$ for all $k = 2, ..., j$ which implies that η_1 is the zero vector, which is a contradiction. Thus $a_1 = 0$ and we can conclude that $\eta_1, ..., \eta_j$ are linearly independent. This completes one direction of the proof.

Now assume that h satisfies the conclusions of Theorem 4 and show that these conclusions imply that Theorem 1 holds by induction on j. The induction hypothesis, H(j), is that the conclusions of Theorem 4 imply that the conclusions of Theorem 1 hold for sequences of length j. For the basis of the induction let $j = 0$. We now show that H(0) holds. The generalized affine function h is either affine or constant on E where $+\infty$ and $-\infty$ are allowed for constant values. This characterization of h is the same as cases (a) of (b) of Theorem 1. The basis of the induction holds.

We now show that H(j) implies that H($j+1$) holds. When the length of sequences is $j+1$, there exist vectors $\eta_1, ..., \eta_{j+1}$ and scalars $\delta_1, ..., \delta_{j+1}$ such that h has the following form. Define $H_0 = E$ and, inductively, for integers i, $0 < i \leq j+1$, such that the sets in (2.9) are all nonempty. Then $h(x) = +\infty$ whenever $x \in C_i^+$ for any i, $h(x) = -\infty$ whenever $x \in C_i^-$ for any i, and h is either affine or constant on H_{j+1}, where $+\infty$ and $-\infty$ are allowed for constant values. From the definition of the sets H_1, C_1^+, and C_1^-, there is an affine function f_1 defined by $f_1(x) = \langle x, \eta_1 \rangle - \delta_1$, $x \in E$, such that $h(x) = +\infty$ for all $x \in E$ such that $f_1(x) > 0$ and $h(x) = -\infty$ for all $x \in E$ such that $f_1(x) < 0$. This is equivalent to the case (c) characterization of h in Theorem 1, provided we show that the restriction of h to H_1 is a generalized affine function.

Define $V_1 = H_1 - \zeta_1$ for some arbitrary $\zeta_1 \in H_1$. Let $\dim(E) = p$. The space V_1 is a $(p-1)$-dimensional vector subspace of E. Define h_1 as in (2.7). Let $\tilde{\eta}_i$ be the restriction

of η_i to V_1 so that $\tilde{\eta}_i$ is an element of V_1^* for $1 < i \leq j+1$. Now let $\widetilde{H}_1 = V_1$ and, for $1 < i \leq j+1$, we can define the sets as in (2.8) where $\tilde{\delta}_i = \delta_i - \langle \zeta_1, \tilde{\eta}_i \rangle$. We see that $h_1(x) = h(x + \zeta_1) = +\infty$ whenever $\langle x + \zeta_1, \eta_i \rangle > \tilde{\delta}_i$. Therefore $h_1(x) = +\infty$ for all $x \in \widetilde{C}_i^+$ for any i. The same derivation shows that $h_1(x) = -\infty$ whenever $x \in \widetilde{C}_i^-$ for any i. The generalized affine function h_1 is either affine or constant on H_{j+1}, where $+\infty$ and $-\infty$ are allowed for constant values. Therefore h_1 meets the conditions of Theorem 4 with sequences of length j. From H(j), we know that the conclusions of Theorem 1 hold with respect to h_1. This completes the proof. □

2.4.4 Affine functions and exponential families

A family of probability distributions having densities with respect to a positive Borel measure λ on a finite-dimensional affine (vector) space is a *standard generalized exponential family* if the densities of these distributions with respect to λ have the form e^g where g is a generalized affine function. This definition is the same as Section 2 except for the replacement of *exponential family* by *generalized exponential family* and the replacement of *affine function* by *generalized affine function*.

Let $x \in E$ be observed data realized from a closed convex standard exponential family with log likelihood (2.4). Let the parameter space $\Theta \subseteq E^*$ and define $m(x) = \sup_{\theta \in \Theta} l(\theta)$. Then, for any x such that $m(x) < \infty$, there is a sequence $\theta_n \in \Theta$ such that

$$l(\theta_n) \to m(x), \qquad \text{as } n \to \infty. \tag{2.10}$$

From sequential compactness of $G(E)$, which arises as a consequence of Theorem 3, there is a subsequence θ_{n_k} such that the sequence of affine functions defined by

$$h_{\theta_{n_k}}(x) = \langle x, \theta_{n_k} \rangle - c(\theta_{n_k}), \qquad y \in E,$$

converges pointwise to a generalized affine function $h \in G(E)$. Since

$$h_{\theta_{n_k}}(x) = \langle x, \theta_{n_k} \rangle - c(\theta_{n_k}) = l(\theta_{n_k}) \to m(x),$$

we have $h(x) = m(x)$ where e^h is a density corresponding to a generalized exponential family. This treatment of maximum likelihood estimation is different from the usual situation in which we find the parameter value which maximizes the likelihood. Instead, a sequence of log densities, interpreted as affine functions, converges to the maximum likelihood estimator $m(x)$. In this case, the MLE is a generalized affine function $h \in G(E)$.

If we take a pointwise limit of a sequence of densities e^{h_i} in the family, the limit will have the form e^g, where g is a generalized affine function. From Fatou's lemma, we know that $\int e^g \, d\lambda \leq 1$. Thus we say such limits are *subprobability densities*. In general, one does get subprobability densities that are not probability densities as limits of sequences in exponential families (Geyer, 1990, Examples 4.1, 4.2, 4.3, 4.4, and 4.5). But one does not get subprobability densities that are not probability densities as limits of sequences in discrete closed convex exponential families, including discrete full exponential families (Geyer, 1990, Theorem 2.7).

To establish CGF convergence in the next section, we represent the likelihood maximizing sequence in the coordinates of the linearly independent η vectors that characterize the generalized affine function h according to its Theorem 4 representation. Let h be represented as in Theorem 4 with $j \leq p$. From Theorem 4, we have a linearly independent set of vectors $\eta_1, ..., \eta_j \in E^*$. We can extend this linearly independent set of vectors to form a basis for E^* by finding vectors $\eta_{j+1}, ..., \eta_p$ (Friedberg, et al., 2003, Corollary 2 to Theorem 1.10). Since $\eta_1, ..., \eta_p$ is a basis for E^*, we can express the sequence of iterates which maximizes the likelihood as

$$\theta_n = b_{1,n}\eta_1 + b_{2,n}\eta_2 + \cdots + b_{p,n}\eta_p. \tag{2.11}$$

Define $\psi_n = \sum_{i=j+1}^{p} b_{i,n}\eta_i$ and let c_i denote the log Laplace transform of the measure λ restricted to the hyperplane H_i for $i = 1, ..., j$. Lemma 1 provides properties about the numbers $b_{i,n}$, $i = 1, ..., p$ needed to prove CGF convergence.

Lemma 1

Suppose that a generalized affine function h on a finite dimensional vector space E is finite

at at least one point. Represent h as in Theorem 4, and extend $\eta_1, \ldots, \eta_j$ to be a basis $\eta_1, \ldots, \eta_p$ for E^*. Then there are sequences of scalars a_n and $b_{i,n}$ such that

$$h_n(y) = a_n + \sum_{i=1}^{j} b_{i,n} \left(\langle y, \eta_i \rangle - \delta_i \right) + \sum_{i=j+1}^{p} b_{i,n} \langle y, \eta_i \rangle, \qquad y \in E, \tag{2.12}$$

where the rightmost sum in (2.12) is empty when $j = p$ and, as $n \to \infty$, we have

(a) $b_{i,n} \to \infty$, for $1 \leq i \leq j$,

(b) $b_{i,n}/b_{i-1,n} \to 0$, for $2 \leq i \leq j+1$,

(c) $b_{i,n}$ converges, for $i > j$, and

(d) a_n converges

if and only if h_n converges to h on E. □

Proof: First suppose that h_n converges to h. The assumption that h is finite at at least one point guarantees that h is affine on H_j from Theorem 4. For all $y \in H_j$ we can write $h(y) = \langle y, \theta^* \rangle + a$ where $\langle y, \theta^* \rangle = \sum_{i=j+1}^{p} d_i \langle y, \eta_i \rangle$ and $s, d_i \in \mathbb{R}$. The convergence $h_n \to h$ implies that $b_{i,n} \to d_i$, $i = j+1, ..., p$ where the set of $b_{i,n}$s is empty when $j = p$ and that $a_n \to a$ as $n \to \infty$. Thus conclusions (c) and (d) hold. To show that conclusions (a) and (b) hold we will suppose that $j > 0$, because these conclusions are vacuous when $j = 0$. Both cases (a) and (b) will be shown by induction with the hypothesis H(m) that $b_{(j-m),n} \to +\infty$ and $b_{(j-m+1),n}/b_{(j-m),n} \to 0$ as $n \to \infty$ for $0 \leq m \leq j-1$. We now show that the basis of this induction holds. Pick $y \in C_j^+$ and observe that

$$h_n(y) = a_n + b_{j,n} \left(\langle y, \eta_j \rangle - \delta_j \right) + \sum_{k=j+1}^{p} b_{k,n} \langle y, \eta_k \rangle \to +\infty.$$

since $h(y) = +\infty$ and $h_n \to h$ pointwise. From this, we see that $b_{j,n} \to +\infty$ as $n \to \infty$ and $b_{j+1,n}/b_{j,n} \to 0$ as $n \to \infty$ from part (c). Therefore H(0) holds. It is now shown that H(m) implies that H($m+1$) holds. There exists a basis $y_1, ..., y_p$ in E^{**}, the dual

space of E^*, such that $\langle y_i, \eta_k \rangle = 0$ when $i \neq k$ and $\langle y_i, \eta_k \rangle = 1$ when $i = k$. The set of vectors $y_1, ..., y_p$ is a basis of E since $E = E^{**}$. Arbitrarily choose a $y \in H_{j-m-1}$ such that $y = \sum_{i=1}^{j-m-1} \delta_i y_i + c_1 y_{j-m}$ where $c_1 > \delta_{j-m}$. At this choice of y we see that $h(y) = +\infty$ and

$$\begin{aligned} h_n(y) &= a_n + \sum_{i=1}^{j-m+1} b_{i,n} \left(\langle y, \eta_i \rangle - \delta_i \right) \\ &= a_n + b_{(j-m),n} \left(\langle y, \eta_{j-m} \rangle - \delta_{j-m} \right) \\ &\to +\infty \end{aligned}$$

as $n \to \infty$. Therefore $b_{(j-m),n} \to +\infty$ as $n \to \infty$. Now arbitrarily choose $y = \sum_{i=1}^{j-m-1} \delta_i y_i + c_1 y_{j-m} + c_2 y_{j-m+1}$ where c_1 is defined as before and $c_2 < \delta_{j-m+1}$. At this choice of y we see that $h(y) = +\infty$ and

$$\begin{aligned} h_n(y) &= a_n + \sum_{i=1}^{j-m+1} b_{i,n} \left(\langle y, \eta_i \rangle - \delta_i \right) \\ &= a_n + b_{(j-m),n} \left(\langle y, \eta_{j-m} \rangle - \delta_{j-m} \right. \\ &\qquad \left. + \frac{b_{(j-m+1),n}}{b_{(j-m),n}} \left(\langle y, \eta_{j-m+1} \rangle - \delta_{j-m+1} \right) \right) \\ &= a_n + b_{(j-m),n} \left(c_1 - \delta_{j-m} - \frac{b_{(j-m+1),n}}{b_{(j-m),n}} \left(c_2 - \delta_{j-m+1} \right) \right) \\ &\to +\infty \end{aligned} \tag{2.13}$$

as $n \to \infty$. It follows from (2.13) that

$$\left(c_1 - \delta_{j-m} - \frac{b_{(j-m+1),n}}{b_{(j-m),n}} \left(c_2 - \delta_{j-m+1} \right) \right) \geq 0$$

for sufficiently large n. This implies that

$$\frac{b_{(j-m+1),n}}{b_{(j-m),n}} \leq \frac{c_1 - \delta_{j-m}}{\delta_{j-m-1} - c_2}$$

for sufficiently large n. From the arbitrariness of the constants c_1 and c_2 and (2.13), we can conclude that $b_{(j-m+1),n}/b_{(j-m),n} \to 0$ as $n \to \infty$. Therefore H$(m+1)$ holds and this completes one direction of the proof.

We now assume that conditions (a) through (d) and the h_n takes the form in (2.12). Let $\lim_{n\to\infty} \sum_{i=j+1}^{p} b_{i,n}\eta_i = \theta^*$ and $\lim_{n\to\infty} a_n = a$. Cases (a) through (d) then imply that

$$h_n(y) \to \begin{cases} -\infty, & y \in C_i^- \\ \langle y, \theta^* \rangle + a, & y \in H_j \\ +\infty, & y \in C_i^+ \end{cases} \tag{2.14}$$

for all $i = 1, ..., j$ where the right hand side of (2.14) is a generalized affine function in its Theorem 4 representation. This completes the proof. □

The results given in Lemma 1 are applicable to generalized affine functions in full generality. However, specifics of interest arise when e^h is a density corresponding to a generalized exponential family and $h_n = h_{\theta_n}$ corresponds to a likelihood maximizing sequence satisfying (2.10). Suppose that there are j hyperplanes characterizing h as in Theorem 4 and let θ^* be the maximum likelihood estimator corresponding to the model restricted to the hyperplane H_j. We now provide a brief extension of Lemma 1 that is consistent with this setup.

Corollary 1

For data x from a regular full exponential family defined on a vector space E, suppose θ_n is a likelihood maximizing sequence satisfying (2.10) with log densities h_n converging pointwise to a generalized affine function h. Characterize h as in Theorem 4 and represent the sequence θ_n in coordinate form as in (2.11). Define $\psi_n = \sum_{i=j+1}^{p} b_{i,n}\langle x, \eta_i \rangle$. Then conclusions (a) and (b) of Lemma 1 hold in this setting and

$$\psi_n \to \theta^*, \quad \text{as } n \to \infty,$$

where θ^* is the MLE of the exponential family restricted to H_j. □

Proof: The conditions of Lemma 1 are satisfied by our assumptions so all conclusions of

Lemma 1 are satisfied. As a consequence, $\psi_n \to \theta^*$ as $n \to \infty$. The fact that θ^* is the MLE of the LCM restricted to H_j follows from our assumption that θ_n is a likelihood maximizing sequence. □

Taken together, Theorem 4, Lemma 1, and Corollary 1 provide a theory of maximum likelihood estimation in exponential families motivated by properties of sequences of affine functions on finite-dimensional vector spaces. One key difference of this theory and the traditional theory is that the MLE is not a parameter value, $\theta \in \Theta$, but rather a log density $h \in G(E)$. These different formulations are the same when the data from a regular full exponential family are in the interior of their support set. In this case, we can write

$$h(x) = \langle x, \hat{\theta} \rangle - c(\hat{\theta})$$

where $\hat{\theta} \in \Theta$ is the MLE that satisfies $h(x) = m(x)$ and the generalized affine function h is affine. When we represent h as in Theorem 4 in this case, we have that $j = 0$. However, when the observed data are on the boundary of their support, the MLE does not exist in the traditional sense and may exist in the Barndorff-Nielsen completion. Our theory can find the MLE in the Barndorff-Nielsen completion of the exponential family in this setting when $m(x) < \infty$.

2.4.5 Comparisons with Geyer (2009)

We are not the only ones to investigate the existence of the MLE in the Barndorff-Nielsen completion of an exponential family when data are on the boundary of their support. Geyer (2009) investigated this issue and found the MLE in what is called a *limiting conditional model* (LCM). In practical settings, the support set for an LCM is determined by an estimated generic direction of recession (GDOR). The GDOR and LCM approach to this problem is similar to our approach, as evidenced by Theorem 5. Let K denote the convex support of the measure λ. The convex support of λ is the smallest closed convex set whose complement has λ measure zero (Barndorff-Nielsen, 1978, p. 90).

Theorem 5

For a full exponential family having log likelihood (2.4), densities (2.3), natural statistic X, observed value of the natural statistic x such that $x \in K$, and natural parameter space Θ, if η is a direction of recession,

$$H_\eta = \{w \in \mathbb{R}^p : \langle w - x, \eta \rangle = 0\},$$

and $\text{pr}(X \in H_\eta) > 0$ for some distribution in the family, and hence for all, then for all $\theta \in \Theta$

$$\lim_{s \to \infty} f_{\theta + s\eta} = \begin{cases} 0, & \langle X(w) - x, \eta \rangle < 0 \\ f_\theta(w) / \text{pr}_\theta(X \in H_\eta), & \langle X(w) - x, \eta \rangle = 0 \\ +\infty, & \langle X(w) - x, \eta \rangle > 0 \end{cases} \tag{2.15}$$

If η is not a direction of constancy, then $s \mapsto \text{pr}_{\theta + s\eta}(X \in H_\eta)$ is continuous and strictly increasing, and $\text{pr}_{\theta + s\eta}(X \in H_\eta) \to 1$ as $s \to \infty$. □

Proof: A proof is given in Geyer (2009). □

As stated in Geyer (2009, Section 3.4) there are three things to note about the right-hand side of (2.15). First, it is a probability density function with respect to the distribution having parameter value ψ. From Geyer (2009, Theorem 3 (d)), the set where it is $+\infty$ has probability zero. Second, it is the density with parameter value θ of the conditional distribution given that $X \in H_\eta$. Third, by Scheffe's lemma (Lehmann, 1959, pp. 351) pointwise convergence of densities implies convergence in total variation, which implies convergence in distribution. Denote the right-hand side of ((2.15)) by $f_\theta(w|X \in H_\eta)$. It is clear that the family

$$\{f_\theta(\cdot|X \in H_\eta) : \theta \in \Theta\} \tag{2.16}$$

is an exponential family with the same natural statistic and natural parameter as the original family. It need not be full. The natural parameter space of the full family containing it is

at least as large as

$$\Theta + \Gamma_{\lim} = \{\theta + \gamma : \theta \in \Theta \text{ and } \gamma \in \Gamma_{\lim}\}, \tag{2.17}$$

where θ is the natural parameter space of the original family and $\Gamma_{\lim}$ is the constancy space of the family (2.16). We will assume that (2.17) is the natural parameter space of the full family containing (2.16), and we will call this full family the LCM. It is clear that the log likelihood for (2.16)

$$l_{H_\eta}(\theta) = \langle x, \theta \rangle - c(\theta) - \log \mathrm{pr}_\theta(X \in H_\eta)$$

satisfies

$$l(\theta) < l_{H_\eta}(\theta), \qquad \theta \in \Theta.$$

Thus, if an MLE exists for the LCM, then it maximizes the likelihood in the family that is the union of the LCM and the original family, and it maximizes the likelihood in the family that is the set of all limits of sequences of distributions in the original family. When this happens, we say we have found an MLE in the Barndorff-Nielsen completion of the original family.

Refer back to the perfect separation case in logistic regression mentioned in Section 2.2. The GDOR for this examples is $\hat{\eta}_{\text{gdor}} = (-5, 0.1)^T$ and the LCM is degenerate at the observed data. The set H_η is the one point set containing only the observed value of the canonical statistic.

In Geyer (2009), the solution to finding an MLE in the Barndorff-Nielsen completion of the original family is dependent upon estimation of a direction of recession and then taking limits in that direction, as seen in Theorem 5. In our approach, we allow the iterates of a likelihood maximizing sequence (2.10) to find the MLE in the LCM. We compare methods from a practical standpoint in Section 5. In the next section, we provide convergence results necessary for inference when maximum likelihood estimation is obtained through an arbitrary likelihood maximizing sequence (2.10).

2.5 Convergence theorems

We now show CGF convergence along a likelihood maximizing sequence (2.10). First define $c_A(\theta) = \log \int_A e^{\langle y,\theta\rangle}\lambda(dy)$ for all $\theta \in \operatorname{dom} c_A = \{\theta : c_A(\theta) < +\infty\}$. Define the CGF with respect to the generalized affine function h by

$$\kappa(t) = \log \int e^{\langle y,t\rangle} e^{h(y)}\lambda(dy)$$

for all $t \in \mathbb{R}^p$ such that $\kappa(t)$ is finite. Define the CGF along the likelihood maximizing sequence (2.10) with respect to the log densities h_n by

$$\kappa_n(t) = \log \int e^{\langle y,t\rangle} e^{h_n(y)}\lambda(dy)$$

for all $t \in \mathbb{R}^p$ such that $\kappa(t)$ is finite where h_n converges to a generalized affine function h. In the next theorem, we state the conditions for which $\kappa_n(t) \to \kappa(t)$.

Theorem 6

Let E be a finite-dimensional vector space of dimension p. For data $x \in E$ from a regular full exponential family with natural parameter space $\Theta \subseteq E^*$ and generating measure λ. Assume that all LCMs are regular exponential families. Suppose that θ_n is a likelihood maximizing sequence satisfying (2.10) with log densities h_n converging pointwise to a generalized affine function h. Characterize h as in Theorem 4. When $j \geq 2$, and for $i = 1, ..., j-1$, define

$$\begin{aligned} D_i &= \{y \in C_i^- : \langle y, \eta_k\rangle > \delta_k, \text{ some } k > i\}, \\ F &= E \setminus \cup_{i=1}^{j-1} D_i = \{y : \langle y, \eta_i\rangle \leq \delta_i,\ 1 \leq i \leq j\}, \end{aligned} \tag{2.18}$$

and assume that

$$\sup_{\theta\in\Theta} \sup_{y\in\cup_{i=1}^{j-1} D_i} e^{\langle y,\theta\rangle - c_{\cup_{i=1}^{j-1} D_i}(\theta)} < \infty \quad \text{or} \quad \lambda\left(\cup_{i=1}^{j-1} D_i\right) = 0. \tag{2.19}$$

Then $\kappa_n(t)$ converges to $\kappa(t)$ pointwise for all t in a neighborhood of 0. □

Proof: First consider the case when $j = 0$, the sequences of η vectors and scalars δ are both of length zero. There are no sets C^+ and C^- in this setting and h is affine on E. From Lemma 1 we have $\psi_n = \theta_n$. From Corollary 1, $\theta_n \to \theta^*$ as $n \to \infty$. We observe that $c(\theta_n) \to c(\theta^*)$ from continuity of the cumulant function. The existence of the MLE in this setting implies that there is a neighborhood about 0 denoted by W such that $\theta^* + W \subset \text{int}(\text{dom}\, c)$. Pick $t \in W$ and observe that $c(\theta_n + t) \to c(\theta^* + t)$. Therefore $\kappa_n(t) \to \kappa(t)$ when $j = 0$.

Now consider the case when $j = 1$. Define $c_1(\theta) = \log \int_{H_1} e^{\langle y,\theta\rangle} \lambda(dy)$ for all $\theta \in \text{int}(\text{dom } c_1)$. In this scenario we have

$$\begin{aligned}
\kappa_n(t) &= c\left(\psi_n + t + b_{1,n}\eta_1\right) - c\left(\psi_n + b_{1,n}\eta_1\right) \\
&= c\left(\psi_n + t + b_{1,n}\eta_j\right) - c\left(\psi_n + b_{1,n}\eta_1\right) \pm b_{1,n}\delta_1 \\
&= \left[c\left(\psi_n + t + b_{1,n}\eta_1\right) - b_{1,n}\delta_1\right] - \left[c\left(\psi_n + b_{1,n}\eta_1\right) - b_{1,n}\delta_1\right].
\end{aligned}$$

From Geyer (1990, Theorem 2.2), we know that

$$\begin{aligned}
c\left(\theta^* + t + s\eta_1\right) - s\delta_1 &\to c_1\left(\theta^* + t\right), \\
c\left(\theta^* + s\eta_1\right) - s\delta_1 &\to c_1\left(\theta^*\right),
\end{aligned} \tag{2.20}$$

as $s \to \infty$ since $\delta_1 \geq \langle y, \eta_1\rangle$ for all $y \in H_1$. The left hand side of (2.20) is a convex function of θ and the right hand side is a proper convex function. If int(dom c_1) is nonempty, which holds whenever int(dom c) is nonempty, then the convergence in (2.20) is uniform on compact subsets of int(dom c_1) (Rockafellar and Wets, 1998, Theorem 7.17). Also (Rockafellar and Wets, 1998, Theorem 7.14), uniform convergence on compact sets is the same as continuous convergence. Using continuous convergence, we have that both

$$\begin{aligned}
c\left(\psi_n + t + b_{1,n}\eta_1\right) - b_{1,n}\delta_1 &\to c_1\left(\theta^* + t\right), \\
c\left(\psi_n + b_{1,n}\eta_1\right) - b_{1,n}\delta_1 &\to c_1\left(\theta^*\right),
\end{aligned}$$

where $b_{1,n} \to \infty$ as $n \to \infty$ by Lemma 1. Thus

$$\begin{aligned}\kappa_n(t) &= c(\theta_n + t) - c(\theta_n) \to c_1\left(\theta^* + t\right) - c_1\left(\theta^*\right) \\ &= \log \int_{H_1} e^{\langle y+t, \theta^* \rangle - c(\theta^*)} \lambda(dy) = \log \int_{H_1} e^{\langle y,t \rangle + h(y)} \lambda(dy) \\ &= \log \int e^{\langle y,t \rangle + h(y)} \lambda(dy) = \kappa(t).\end{aligned}$$

This concludes the proof when $j = 1$.

For the rest of the proof we will assume that $1 < j \leq p$ where $\dim(E) = p$. Represent the sequence θ_n in coordinate form as in (2.11) with scalars $b_{i,n}$, $i = 1, ..., p$. For $0 < j < p$, we know that $\psi_n \to \theta^*$ as $n \to \infty$ from Corollary 1. The existence of the MLE in this setting implies that there is a neighborhood about 0, denoted by W, such that $\theta^* + W \subset \text{int}(\text{dom}\, c)$. Pick $t \in W$, fix $\varepsilon > 0$, and construct ε-boxes about θ^* and $\theta^* + t$, denoted by $\mathcal{N}_{0,\varepsilon}(\theta^*)$ and $\mathcal{N}_{t,\varepsilon}(\theta^*)$ respectively, such that both $\mathcal{N}_{0,\varepsilon}(\theta^*), \mathcal{N}_{t,\varepsilon}(\theta^*) \subset \text{int}\,(\text{dom}\ c)$. Let $V_{t,\varepsilon}$ be the set of vertices of $\mathcal{N}_{t,\varepsilon}(\theta^*)$. For all $y \in E$ define

$$M_{t,\varepsilon}(y) = \max_{v \in V_{t,\varepsilon}} \{\langle v, y \rangle\}, \qquad \widetilde{M}_{t,\varepsilon}(y) = \min_{v \in V_{t,\varepsilon}} \{\langle v, y \rangle\}. \tag{2.21}$$

From the conclusions of Lemma 1 and Corollary 1, we can pick an integer N such that $\langle y, \psi_n + t \rangle \leq M_{t,\varepsilon}(y)$ and $b_{(i+1),n}/b_{i,n} < 1$ for all $n > N$ and $i = 1, ..., j-1$. For all $y \in F$, we have

$$\begin{aligned}\langle y, \theta_n + t \rangle - \sum_{i=1}^{j} b_{i,n}\delta_i &= \langle y, \psi_n + t \rangle + \sum_{i=1}^{j} b_{i,n} \left(\langle y, \eta_i \rangle - \delta_i\right) \\ &\leq M_{t,\varepsilon}(y)\end{aligned} \tag{2.22}$$

for all $n > N$. The integrability of $e^{M_{t,\varepsilon}(y)}$ and $e^{\widetilde{M}_{t,\varepsilon}(y)}$ follows from

$$\begin{aligned}\int e^{\widetilde{M}_{t,\varepsilon}(y)} \lambda(dy) &\leq \int e^{M_{t,\varepsilon}(y)} \lambda(dy) \\ &= \sum_{v \in V_{t,\varepsilon}} \int_{\{y:\ \langle y,v \rangle = M_{t,\varepsilon}(y)\}} e^{\langle y,v \rangle} \lambda(dy)\end{aligned}$$

$$\leq \sum_{v \in V_{t,\varepsilon}} \int e^{\langle y,v \rangle} \lambda(dy) < \infty.$$

Therefore,

$$\langle y, \psi_n + t \rangle + \sum_{i=1}^{j} b_{i,n} \left(\langle y, \eta_i \rangle - \delta_i \right) \to \begin{cases} \langle y, \theta^* + t \rangle, & y \in H_j, \\ -\infty, & y \in F \setminus H_j. \end{cases}$$

which implies that

$$c_F(\theta_n + t) - c_F(\theta_n) \to c_{H_j}(\theta^* + t) - c_{H_j}(\theta^*) \tag{2.23}$$

by dominated convergence. To complete the proof, we need to verify that

$$\begin{aligned} c(\theta_n + t) - c(\theta_n) &= c_F(\theta_n + t) - c_F(\theta_n) \\ &\quad + c_{\cup_{i=1}^{j-1} D_i}(\theta_n + t) - c_{\cup_{i=1}^{j-1} D_i}(\theta_n) \\ &\to c_{H_j}(\theta^* + t) - c_{H_j}(\theta^*). \end{aligned} \tag{2.24}$$

We know that (2.24) holds when $\lambda(\cup_{i=1}^{j-1} D_i) = 0$ in (2.19) because of (2.23). Now suppose that $\lambda(\cup_{i=1}^{j-1} D_i) > 0$. We have,

$$\langle y, \psi_n + t \rangle + \sum_{i=1}^{j} b_{i,n} \left(\langle y, \eta_i \rangle - \delta_i \right) \to -\infty, \qquad y \in \cup_{i=1}^{j-1} D_i, \tag{2.25}$$

and

$$\begin{aligned}
&\exp\left(c_{\cup_{i=1}^{j-1}D_i}(\theta_n+t)-c_{\cup_{i=1}^{j-1}D_i}(\theta_n)\right)\\
&\quad=\int_{\cup_{i=1}^{j-1}D_i} e^{\langle y,\theta_n+t\rangle-c_{\cup_{i=1}^{j-1}D_i}(\theta_n)}\lambda(dy)\\
&\quad\leq\int_{\cup_{i=1}^{j-1}D_i} e^{M_{t,\varepsilon}(y)-\widetilde{M}_{0,\varepsilon}(y)+\langle y,\theta_n\rangle-c_{\cup_{i=1}^{j-1}D_i}(\theta_n)}\lambda(dy)\\
&\quad\leq\sup_{y\in\cup_{i=1}^{j-1}D_i}\left(e^{\langle y,\theta_n\rangle-c_{\cup_{i=1}^{j-1}D_i}(\theta_n)}\right)\lambda\left(\cup_{i=1}^{j-1}D_i\right)\\
&\qquad\times\int_{\cup_{i=1}^{j-1}D_i} e^{M_{t,\varepsilon}(y)-\widetilde{M}_{0,\varepsilon}(y)}\lambda(dy)\\
&\quad\leq\sup_{\theta\in\Theta}\sup_{y\in\cup_{i=1}^{j-1}D_i}\left(e^{\langle y,\theta\rangle-c_{\cup_{i=1}^{j-1}D_i}(\theta)}\right)\lambda\left(\cup_{i=1}^{j-1}D_i\right)\\
&\qquad\times\int_{\cup_{i=1}^{j-1}D_i} e^{M_{t,\varepsilon}(y)-\widetilde{M}_{0,\varepsilon}(y)}\lambda(dy)\;<\;\infty
\end{aligned}\tag{2.26}$$

for all $n > N$ by the assumption given by (2.19). The assumption that the exponential family is discrete and full implies that $\int e^h(y)\lambda(dy) = 1$ (Geyer, 1990, Theorem 2.7). This in turn implies that $\lambda(C_i^+) = 0$ for all $i = 1, ..., j$ which then implies that $c(\theta) = c_F(\theta) + c_{\cup_{i=1}^{j-1}D_i}(\theta)$. Putting (2.22), (2.25), and (2.26) together we can conclude that (2.24) holds as $n \to \infty$ by dominated convergence and

$$\begin{aligned}
&c_{H_j}(\theta^*+t)-c_{H_j}(\theta^*)\\
&\quad=\log\int_{H_j} e^{\langle y,\theta^*+t\rangle}\lambda(dy)-\log\int_{H_j} e^{\langle y,\theta^*\rangle}\lambda(dy)\\
&\quad=\log\int e^{\langle y,t\rangle+h(y)}\lambda(dy)=\kappa(t).
\end{aligned}\tag{2.27}$$

for all $t \in W$. This verifies CGF convergence on neighborhoods of 0 which completes the proof. □

Discrete exponential families automatically satisfy (2.19) when

$$\inf_{y\in\cup_{i=1}^{j-1}D_i}\lambda(\{y\})>0.$$

In this setting, $e^{\langle y,\theta\rangle - c_{\cup_{i=1}^{j-1} D_i}(\theta)}$ corresponds to the probability mass function for the random variable conditional on the occurrence of $\cup_{i=1}^{j-1} D_i$. Thus,

$$\begin{aligned}
&\sup_{\theta\in\Theta} \sup_{y\in\cup_{i=1}^{j-1} D_i} \left(e^{\langle y,\theta\rangle - c_{\cup_{i=1}^{j-1} D_i}(\theta)} \right) \\
&\quad = \sup_{\theta\in\Theta} \sup_{y\in\cup_{i=1}^{j-1} D_i} \left(\frac{e^{\langle y,\theta\rangle}\lambda(\{y\})}{\lambda(\{y\}) \sum_{x\in\cup_{i=1}^{j-1} D_i} e^{\langle x,\theta\rangle}\lambda(\{x\})} \right) \\
&\quad \leq \sup_{y\in\cup_{i=1}^{j-1} D_i} (1/\lambda(\{y\})) < \infty.
\end{aligned}$$

Therefore, Theorem 6 is applicable for the non-existence of the maximum likelihood estimator that may arise in logistic and multinomial regression.

We show in the next Theorem that discrete families with convex polyhedron support also satisfy (2.19) under additional regularity conditions that hold in practical applications. When K is convex polyhedron, we can write K as,

$$K = \{y : \langle y, \alpha_i\rangle \leq a_i, \text{ for } i = 1, ..., m\}$$

as in Rockafellar and Wets (1998, Theorem 6.46). In the setting when the MLE does not exist, the data $x \in K$ is on the boundary of K. Denote the active set of indices corresponding to the boundary K containing x by $I(x) = \{i : \langle x, \alpha_i\rangle = a_i\}$. In preparation for Theorem 7, we define the normal cone $N_K(x)$ and tangent cone $T_K(x)$ as in Geyer (2009), and state the assumptions required on K for our theory to hold.

Definition 2

The normal cone of a convex set K in the finite dimensional vector space E at a point $x \in K$ is

$$N_K(x) = \{\eta \in E^* : \langle y - x, \eta\rangle \leq 0 \text{ for all } y \in K\}.$$

Definition 3

The tangent cone of a convex set K in the finite dimensional vector space E at a point

$x \in K$ is

$$T_K(x) = \text{cl}\{s(y - x) : y \in K \text{ and } s \geq 0\}$$

where $\text{cl}(\cdot)$ denotes the set closure operation. □

When K is a convex polyhedron, $N_K(x)$ and $T_K(x)$ are both convex polyhedra with formulas given in Rockafellar and Wets (1998, Theorem 6.46). These formulas are

$$T_K(x) = \{y : \langle y, \alpha_i \rangle \leq 0 \text{ for all } i \in I(x)\},$$
$$N_K(x) = \{c_1\alpha_1 + \cdots + c_m\alpha_m : c_i \geq 0 \text{ for } i \in I(x),\ c_i = 0 \text{ for } i \notin I(x)\}.$$

The assumptions required on K for our theory to hold are from Brown (1986, p. 193-197). We first define faces and exposed faces of convex sets.

Definition 4
A *face* of a convex set K is a convex subset F of K such that every (closed) line segment in K with a relative interior point in F has both endpoints in F. An *exposed face* of K is a face where a certain linear function achieves its maximum over K (Rockafellar, 1970, p. 162). □

The conditions of Brown required for our theory are:

(i) The support of the exponential family is a countable set X.

(ii) The exponential family is regular.

(iii) Every $x \in X$ is contained in the relative interior of an exposed face F of the convex support K.

(iv) The support of the measure $\lambda|F$ equals F, where λ is the generating measure for the exponential family.

Conditions (i) and (ii) are already assumed in Theorem 6. It is now shown that discrete exponential families satisfy (2.19) under the above conditions.

Theorem 7

Assume the conditions of Theorem 6 with the omission of (2.19) when $j \geq 2$. Let K denote the convex support of the exponential family. Assume that the support of the exponential family satisfies the conditions of Brown. Then (2.19) holds. □

Proof: Represent h as in Theorem 4. Denote the normal cone of the convex polyhedron support K at the data x by $N_K(x)$. We show that a sequence of scalars δ_i^* and a linearly independent set of vectors $\eta_i^* \in E^*$ can be chosen so that $\eta_i^* \in N_K(x)$, and

$$\begin{aligned} H_i &= \{y \in H_{i-1} : \langle y, \eta_i^* \rangle = \delta_i^*\}, \\ C_i^+ &= \{y \in H_{i-1} : \langle y, \eta_i^* \rangle > \delta_i^*\}, \\ C_i^- &= \{y \in H_{i-1} : \langle y, \eta_i^* \rangle < \delta_i^*\}, \end{aligned} \tag{2.28}$$

for $i = 1, ..., j$ where $H_0 = E$ so that (2.19) holds. We will prove this by induction with the hypothesis H(m), $m = 1, ..., j$, that (2.28) holds for $i \leq m$ where the vectors $\eta_i^* \in N_K(x)$ $i = 1, ..., m$.

We first verify the basis of the induction. The assumption that the exponential family is discrete and full implies that $\int e^h(y)\lambda(dy) = 1$ (Geyer, 1990, Theorem 2.7). This in turn implies that $\lambda(C_k^+) = 0$ for all $k = 1, ..., j$. This then implies that $K \subseteq \{y \in E : \langle y, \eta_1 \rangle \leq \delta_1\} = H_1 \cup C_1^-$. Thus $\eta_1 \in N_K(x)$ and the base of the induction holds with $\eta_1 = \eta_1^*$ and $\delta_1 = \delta_1^*$.

We now show that H($m+1$) follows from H(m) for $m = 1, ..., j-1$. We first establish that $K \cap H_m$ is an exposed face of K. This is needed to show that (2.28) holds for $i = 1, ..., m+1$. Let L_K be the collection of closed line segments with endpoints in K. Arbitrarily choose $l \in L_K$ such that an interior point $y \in l$ is such that $y \in K \cap H_m$. We can write $y = \gamma a + (1-\gamma)b$, $0 < \gamma < 1$, where a and b are the endpoints of l. Since $a, b \in K$ by construction, we have that $\langle a - x, \eta_m^* \rangle \leq 0$ and $\langle b - x, \eta_m^* \rangle \leq 0$ because $\eta_m^* \in N_K(x)$ by H(m). Now,

$$0 \geq \langle a - x, \eta_m^* \rangle = \langle a - y + y - x, \eta_m^* \rangle$$

$$= \langle a - y, \eta_m^* \rangle = \langle a - (\gamma a + (1-\gamma)b), \eta_m^* \rangle$$
$$= (1-\gamma)\langle a - b, \eta_m^* \rangle$$

and

$$0 \geq \langle b - x, \eta_m^* \rangle = \langle b - y + y - x, \eta_m^* \rangle$$
$$= \langle b - y, \eta_m^* \rangle = \langle b - (\gamma a + (1-\gamma)b), \eta_m^* \rangle$$
$$= -\gamma \langle a - b, \eta_m^* \rangle.$$

Therefore $a, b \in K \cap H_m$ and this verifies that $K \cap H_m$ is a face of K since l was chosen arbitrarily. The function $y \mapsto \langle y - x, \eta_m^* \rangle - \delta_m^*$, defined on K, is maximized over $K \cap H_m$. Therefore $K \cap H_m$ is an exposed face of K by definition. The exposed face $K \cap H_m = K \cap (H_{m+1} \cup C_{m+1}^-)$ since $\lambda(C_{m+1}^+) = 0$ and the convex support of the measure $\lambda | H_m$ is H_m by assumption. Thus, $\eta_{m+1} \in N_{K \cap H_m}(x)$.

The sets K and H_m are both convex and are therefore regular at every point (Rockafellar and Wets, 1998, Theorem 6.20). We can write $N_{K \cap H_m}(x) = N_K(x) + N_{H_m}(x)$ since K and H_m are convex sets that cannot be separated where $+$ denotes Minkowski addition in this case (Rockafellar and Wets, 1998, Theorem 6.42). The normal cone $N_{H_m}(x)$ has the form

$$\begin{aligned} N_{H_m}(x) &= \{\eta \in E^* : \langle y - x, \eta \rangle \leq 0 \text{ for all } y \in H_m\} \\ &= \{\eta \in E^* : \langle y - x, \eta \rangle \leq 0 \text{ for all } y \in E \\ &\qquad \text{such that } \langle y - x, \eta_i \rangle = 0,\ i = 1, ..., m\} \\ &= \left\{ \sum_{i=1}^m a_i \eta_i :\ a_i \in \mathbb{R},\ i = 1, ..., m \right\}. \end{aligned}$$

Therefore, we can write

$$\eta_{m+1} = \eta_{m+1}^* + \sum_{i=1}^m a_{m,i} \eta_i^* \tag{2.29}$$

where $\eta^*_{m+1} \in N_K(x)$ and $a_{m,i} \in \mathbb{R}$, $i = 1, ..., m$. For $y \in H_{m+1}$, we have that

$$\begin{aligned}\langle y, \eta^*_{m+1}\rangle &= \langle y, \eta_{m+1}\rangle - \sum_{i=1}^{m} a_{m,i}\langle y, \eta_i\rangle \\ &= \delta_{m+1} - \sum_{i=1}^{m} a_{m,i}\delta_i.\end{aligned}$$

Let $\delta^*_{m+1} = \delta_{m+1} - \sum_{i=1}^{m} a_{m,i}\delta_i$. We can therefore write

$$H_{m+1} = \left\{y \in H_m : \langle y, \eta^*_{m+1}\rangle = \delta^*_{m+1}\right\}$$

and

$$\begin{aligned}C^+_{m+1} &= \{y \in H_m : \langle y, \eta_{m+1}\rangle > \delta_{m+1}\} \\ &= \left\{y \in H_m : \langle y, \eta^*_{m+1}\rangle + \sum_{i=1}^{m} a_{m,i}\delta_i > \delta_{m+1}\right\} \\ &= \left\{y \in H_m : \langle y, \eta^*_{m+1}\rangle > \delta_{m+1} - \sum_{i=1}^{m} a_{m,i}\delta_i\right\} \\ &= \left\{y \in H_m : \langle y, \eta^*_{m+1}\rangle > \delta^*_{m+1}\right\}.\end{aligned} \tag{2.30}$$

A similar argument to that of (2.30) verifies that

$$C^-_i = \left\{y \in H_m : \langle y, \eta^*_{m+1}\rangle < \delta^*_{m+1}\right\}.$$

This confirms that (2.28) holds for $i = 1, ...m+1$ and this establishes that H$(m+1)$ follows from H(m).

Define the sets D_i in (2.18) with starred quantities replacing the unstarred quantities. Since the vectors $\eta^*_1, ..., \eta^*_j \in N_K(x)$, the sets $K \cap D_i$ are all empty for all $i = 1, ..., j-1$. Therefore (2.19) holds with $\lambda\left(\cup_{i=1}^{j-1} D_i\right) = 0$. This completes the proof. □

Theorems 6 and 7 both verify CGF convergence along likelihood maximizing sequences (2.10) on neighborhoods of 0. The next Theorems show that CGF convergence on neighborhoods of 0 is enough to imply convergence in distribution and of moments of all orders.

Therefore moments of distributions with log densities that are affine functions converge along likelihood maximizing sequences (2.10) to those of a limiting distribution whose log density is a generalized affine function. We establish some preliminaries before we state our theorems.

Suppose that X is a random vector in a finite-dimensional vector space E having a moment generating function (MGF) φ_X, then

$$\varphi_X(t) = \varphi_{\langle X,t\rangle}(1), \qquad t \in E^*,$$

regardless of whether the MGF exist or not. It follows that the MGF of $\langle X, t\rangle$ for all t determine the MGF of X and vice versa, when these MGF exist. More generally,

$$\varphi_{\langle X,t\rangle}(s) = \varphi_X(st), \qquad t \in E^* \text{ and } s \in . \tag{2.31}$$

This observation applied to characteristic functions rather than MGF is called the Cramér-Wold theorem. In that context it is more trivial because characteristic functions always exist.

If $v_1, \ldots, v_d$ is a basis for a vector space E, then there exists a unique dual basis $w_1, \ldots, w_d$ for E^* that satisfies

$$\langle v_i, w_j\rangle = \begin{cases} 1, & i = j \\ 0, & i \neq j \end{cases} \tag{2.32}$$

(Halmos, 1958, Theorem 2 of Section 15).

Theorem 8

If X is a random vector in E having an MGF, then the random scalar $\langle X, t\rangle$ has an MGF for all $t \in E^*$. Conversely, if $\langle X, t\rangle$ has an MGF for all $t \in E^*$, then X has an MGF. □

Proof: Suppose φ_X is an MGF, hence finite on a neighborhood W of zero. Fix $t \in E^*$. Then by (2.31) $\varphi_{\langle X,t\rangle}(s)$ is finite whenever $st \in W$. Continuity of scalar multiplication

means there exists an $\varepsilon > 0$ such that $st \in W$ whenever $|s| < \varepsilon$. That proves one direction.

Conversely, suppose $\varphi_{\langle X,t\rangle}$ is an MGF for each $t \in E^*$. Suppose $v_1, \ldots, v_d$ is a basis for E and $w_1, \ldots, w_d$ is the dual basis for E^* that satisfies (2.32). Then there exists $\varepsilon > 0$ such that $\varphi_{\langle X,w_i\rangle}$ is finite on $[-\varepsilon, \varepsilon]$ for each i.

We can write each $t \in E^*$ as a linear combination of basis vectors

$$t = \sum_{i=1}^{d} a_i w_i,$$

where the a_i are scalars that are unique (Halmos, 1958, Theorem 1 of Section 15). Applying (2.32) we get

$$\langle v_j, t\rangle = a_j,$$

so

$$t = \sum_{i=1}^{d} \langle v_i, t\rangle w_i,$$

and

$$\langle X, t\rangle = \sum_{i=1}^{d} \langle v_i, t\rangle \langle X, w_i\rangle.$$

Suppose

$$|\langle v_i, t\rangle| \le \varepsilon, \qquad i = 1, \ldots, d$$

(the set of all such t is a neighborhood of 0 in E^*). Let sign denote the sign function, which takes values -1, 0, and $+1$ as its argument is negative, zero, or positive, and write

$$s_i = \operatorname{sign}(\langle v_i, t\rangle), \qquad i = 1, \ldots, d.$$

Then we can write $\langle X, t\rangle$ as a convex combination

$$\langle X, t\rangle = \sum_{i=1}^{d} \frac{\langle v_i, t\rangle}{s_i \varepsilon} \cdot s_i \varepsilon \langle X, w_i\rangle + \left(1 - \sum_{i=1}^{d} \frac{\langle v_i, t\rangle}{s_i \varepsilon}\right) \cdot \langle X, 0\rangle.$$

So, by convexity of the exponential function,

$$\varphi_X(t) \le \sum_{i=1}^{d} \frac{\langle v_i, t\rangle}{s_i\varepsilon} \varphi_{\langle X, w_i\rangle}(s_i\varepsilon) + \left(1 - \sum_{i=1}^{d} \frac{\langle v_i, t\rangle}{s_i\varepsilon}\right) < \infty.$$

That proves the other direction. □

Theorem 9

Suppose X_n, $n = 1, 2, \ldots$ is a sequence of random vectors, and suppose their moment generating functions converge pointwise on a neighborhood W of zero. Then

$$X_n \xrightarrow{d} X, \tag{2.33}$$

□

and X has an MGF φ_X, and

$$\varphi_{X_n}(t) \to \varphi_X(t), \qquad t \in E^*.$$

Proof: The one-dimensional case of this theorem is proved in Billingsley (2012). We only need to show the general case follows by Cramér-Wold. It follows from the assumption that $\varphi_{\langle X_n, t\rangle}$ converges on a neighborhood W of zero for each $t \in E^*$. Then (2.33) follows from the one-dimensional case of this theorem and the Cramér-Wold theorem. And this implies

$$\langle X_n, t\rangle \xrightarrow{d} \langle X, t\rangle, \qquad t \in E^*.$$

By the one-dimensional case of this theorem, this implies $\langle X, t\rangle$ has an MGF for each t, and then Theorem 8 implies X has an MGF φ_X. By the one-dimensional case of this theorem, $\varphi_{\langle X_n, t\rangle}$ converges pointwise to $\varphi_{\langle X, t\rangle}$. So by (2.31) φ_{X_n} converges pointwise to φ_X. □

Theorem 10

Under the assumptions of Theorem 9, suppose $t_1, t_2, \ldots, t_k$ are vectors defined on E^*, the

dual space of E. Then $\prod_{i=1}^{k}\langle X_n, t_i\rangle$ is uniformly integrable so

$$\mathrm{E}\left\{\prod_{i=1}^{k}\langle X_n, t_i\rangle\right\} \to \mathrm{E}\left\{\prod_{i=1}^{k}\langle X, t_i\rangle\right\}.$$

Proof: From Theorem 9, we have that $\langle X_n, t_i\rangle \xrightarrow{d} \langle X, , t_i\rangle$. Continuity of the exponential function implies that $e^{\langle X_n, t_i\rangle} \xrightarrow{d} e^{\langle X, t_i\rangle}$. Now, pick an $\varepsilon > 0$ such that both $\varepsilon\sum_{i=1}^{k} t_i \in W$ and $\varepsilon\sum_{i=1}^{k} u_i \in W$ where $u_1 = -t_1$ and $u_i = t_i$ for all $i > 1$. This construction gives

$$e^{\langle X_n, \varepsilon\sum_{i=1}^{k} t_i\rangle} \xrightarrow{d} e^{\langle X, \varepsilon\sum_{i=1}^{k} t_i\rangle} \tag{2.34}$$

and

$$\mathrm{E}\left(e^{\langle X_n, \varepsilon\sum_{i=1}^{k} t_i\rangle}\right) \xrightarrow{d} \mathrm{E}\left(e^{\langle X, \varepsilon\sum_{i=1}^{k} t_i\rangle}\right). \tag{2.35}$$

Equations (2.34) and (2.35) imply that $e^{\langle X_n, \varepsilon\sum_{i=1}^{k} t_i\rangle}$ is uniformly integrable by Billingsley (1999, Theorem 3.6). A similar argument shows that $e^{\langle X_n, \varepsilon\sum_{i=1}^{k} u_i\rangle}$ is uniformly integrable. We now bound $|\varepsilon^k\prod_{i=1}^{k}\langle X_n, t_i\rangle|$ to show uniform integrability of $\prod_{i=1}^{k}\langle X_n, t_i\rangle$. Define

$$A_n = \{X_n : \prod_{i=1}^{k}\langle X_n, t_i\rangle \geq 0\}.$$

and let I_A be the indicator function. We have,

$$\varepsilon^k\prod_{i=1}^{k}\langle X_n, t_i\rangle \leq \prod_{i=1}^{k}\langle X_n, \varepsilon t_i\rangle I_{A_n} \leq e^{\langle X_n, \varepsilon\sum_{i=1}^{k} t_i\rangle} I_{A_n} \leq e^{\langle X_n, \varepsilon\sum_{i=1}^{k} t_i\rangle}$$

and

$$-\varepsilon^k\prod_{i=1}^{k}\langle X_n, t_i\rangle = \prod_{i=1}^{k}\langle X_n, \varepsilon u_i\rangle \leq \prod_{i=1}^{k}\langle X_n, \varepsilon u_i\rangle I_{A_n^c} \leq e^{\langle X_n, \varepsilon\sum_{i=1}^{k} u_i\rangle} I_{A_n^c} \leq e^{\langle X_n, \varepsilon\sum_{i=1}^{k} u_i\rangle}.$$

Therefore

$$|\varepsilon^k \prod_{i=1}^{k} \langle X_n, t_i \rangle| \leq e^{\langle X_n, \varepsilon \sum_{i=1}^{k} t_i \rangle} + e^{\langle X_n, \varepsilon \sum_{i=1}^{k} u_i \rangle}$$

The sum of uniformly integrable is uniformly integrable. This implies that $|\varepsilon^k \prod_{i=1}^{k} \langle X_n, t_i \rangle|$ is uniformly integrable. Scalings of uniformly integrable are also uniformly integrable, which states that $\prod_{i=1}^{k} \langle X_n, t_i \rangle$ is uniformly integrable. Our result follows from Billingsley (1999, Theorem 3.5) and this completes the proof. □

The combination of Theorems 6 through Theorem 10 provide a methodology for statistical inference along likelihood maximizing sequences when the MLE is in the Barndorff-Nielsen completion. In particular, we have convergence of moments of all orders along likelihood maximizing sequence. Thus, the estimated variability of the estimated canonical parameter vector converges to the variability of the estimated canonical parameter vector of the MLE distribution. When the MLE is in the Barndorff-Nielsen completion of the exponential family, the MLE is given as a generalized affine function h. When this is so, the η vectors corresponding to the hyperplanes that characterize h in its Theorem 4 representation, are directions of no variability. This is to say that the observed data is concentrated on the hyperplanes characterizing h in its Theorem 4 representation. Therefore, null eigenvectors of the estimated Fisher information matrix evaluated along the likelihood maximizing sequence are estimators of the η vectors corresponding to the hyperplanes that characterize h in its Theorem 4 representation.

2.6 Implementation and examples

The `glm` function in R statistical software (R Development Core Team, 2017) maximizes the likelihood of a generalized linear regression model via a Newton-Raphson (iteratively reweighted least squares) algorithm. When the observed data for a discrete generalized regression model are on the boundary of its support, the Newton-Raphson (iteratively reweighted least squares) algorithm in `glm` outputs a likelihood maximizing sequence of iterates. This sequence of iterates will never converge in finite time. However, the likelihood

asymptopes in this setting so that a reasonable approximate maximum likelihood estimator can be reported in finite time.

The Newton-Raphson (iteratively reweighted least squares) algorithm in `glm` can not find the MLE when it exists in the Barndorff-Nielsen completion of the exponential family. In this setting, the algorithm will either return the warning message "fitted probabilities numerically 0 or 1 occurred" in the case of logistic regression or "fitted rates numerically 0 occurred" in the case of Poisson regression, or `glm` will return nothing in the way of warnings. In this latter case, `glm` has not found the MLE and did not alert users of its failure to do so. This leaves users completely in the dark when using `glm` without a sophisticated means to check if the MLE is in the Barndorff-Nielsen completion of the exponential family.

We provide an idea for an implementation that checks whether or not the MLE exists in the Barndorff-Nielsen completion of the exponential family. If the MLE exists in the usual sense, then the implementation calls `glm` and the user continues with their analysis as originally intended. If the MLE exists in the Barndorff-Nielsen completion of the exponential family, then the implementation will return estimates of the null eigenvectors of the estimated Fisher information matrix $\hat{\eta}_1$,...,$\hat{\eta}_j$, where j is the number of null eigenvectors of the estimated Fisher information matrix. These null eigenvectors are estimates of the η vectors in the Theorem 4 representation of a generalized affine function h which is the log density of the exponential family when data is on the boundary of its support. The next Theorem, in combination with Theorems 5-10, justifies this approach.

Definition 5

Painlevé-Kuratowski set convergence (Rockafellar and Wets, 1998, Section 4.A) can be defined as follows (Rockafellar and Wets (1998) give many equivalent characterizations). If C_n is a sequence of sets in $\mathbb{R}^p$ and C is another set in $\mathbb{R}^p$, then we say $C_n \to C$ if

(i) For every $x \in C$ there exists a subsequence n_k of the natural numbers and there exists $x_{n_k} \in C_{n_k}$ such that $x_{n_k} \to x$.

(ii) For every sequence $x_n \to x$ in $\mathbb{R}^p$ such that there exists a natural number N such that $x_n \in C_n$ whenever $n \geq N$, we have $x \in C$. □

Theorem 11

Suppose that $A_n \in \mathbb{R}^{p\times p}$ is a sequence of positive semidefinite matrices and $A_n \to A$ componentwise. Fix $\varepsilon > 0$ less than half of the least nonzero eigenvalue of A unless A is the zero matrix in which case $\varepsilon > 0$ may be chosen arbitrarily. Let V_n denote the subspace spanned by the eigenvectors of A_n corresponding to eigenvalues that are less than ε. Let V denote the null space of A. Then $V_n \to V$. □

Proof: We first consider the case that A is positive definite and $V = \{0\}$. We can write $A_n = A+(A_n-A)$ where (A_n-A) is a perturbation of A for large n. From Weyl's inequality (Weyl, 1912), we have that all eigenvalues of A_n are bounded above zero for large n and $V_n = \{0\}$ as a result. Therefore, $V_n \to V$ as $n \to \infty$ when A is positive definite.

Now consider the case that A is not strictly positive definite. Without loss of generality, let $x \in V$ be a unit vector. For all $0 < \gamma \leq \varepsilon$, let $V_n(\gamma)$ denote the subspace spanned by the eigenvectors of A_n corresponding to eigenvalues that are less than γ. By construction, $V_n(\gamma) \subseteq V_n$.

From Rockafellar and Wets (1998, Example 10.28), if A has k zero eigenvalues, then for sufficiently large N_1 there are exactly k eigenvalues of A_n that are less than ε for all $n > N_1$. The same is true with respect to γ for all n greater than N_2. Thus $j_n(\gamma) = j_n(\varepsilon)$ which implies that $V_n(\gamma) = V_n$ for all $n > \max\{N_1, N_2\}$.

We now verify part (i) of Painlevé-Kuratowski set convergence with respect to $V_n(\gamma)$. Let N_3 be such that $x^T A_n x < \gamma^2$ for all $n \geq N_3$. Let $\lambda_{k,n}$ and $e_{k,n}$ be the eigenvalues and eigenvectors of A_n, with the eigenvalues listed in decreasing orders. Without loss of generality, we assume that the eigenvectors are orthonormal. Then,

$$x = \sum_{k=1}^{p} (x^T e_{k,n}) e_{k,n}, \qquad 1 = \|x\|^2 = \sum_{k=1}^{p} (x^T e_{k,n})^2,$$
$$x^T A_n x = \sum_{k=1}^{p} \lambda_{k,n} (x^T e_{k,n})^2.$$

There have to be eigenvectors $e_{k,n}$ such that $x^T e_{k,n} \geq 1/\sqrt{p}$ with corresponding eigenvalues $\lambda_{k,n}$ that are very small since $\lambda_{k,n}(x^T e_{k,n})^2 < \gamma$. But conversely, any eigenvalues $\lambda_{k,n}$ such

that $\lambda_{k,n} \geq \gamma$ must have

$$\lambda_{k,n}(x^T e_{k,n})^2 < \gamma^2 \implies (x^T e_{k,n})^2 < \gamma^2/\lambda_{k,n} \leq \gamma.$$

Define $j_n(\gamma) = |\{\lambda_{k,n} : \lambda_{k,n} \leq \gamma\}|$ and $x_n = \sum_{k=p-j_n(\gamma)+1}^{p}(x^T e_{k,n})e_{k,n}$ where $x_n \in V_n(\gamma)$ by construction. Now,

$$\begin{aligned}
\|x - x_n\| &= \|\sum_{k=1}^{p}(x^T e_{k,n})e_{k,n} - \sum_{k=p-j_n(\gamma)+1}^{p}(x^T e_{k,n})e_{k,n}\| \\
&= \|\sum_{k=1}^{p-j_n(\gamma)}(x^T e_{k,n})e_{k,n}\| \\
&\leq \sum_{k=1}^{p-j_n(\gamma)}|x^T e_{k,n}| \\
&\leq (p - j_n)\sqrt{\gamma} \\
&\leq p\sqrt{\gamma}
\end{aligned}$$

for all $n \geq N_3$. Therefore, for every $x \in V$, there exists a sequence $x_n \in V_n(\gamma) \subseteq V_n$ such that $x_n \to x$ since this argument holds for all $0 < \gamma \leq \varepsilon$. This establishes part (i) of Painlevé-Kuratowski set convergence.

We now show part (ii) of Painlevé-Kuratowski set convergence. Suppose that $x_n \to x \in \mathbb{R}^p$ and there exists a natural number N_4 such that $x_n \in V_n(\gamma)$ whenever $n \geq N_4$, and we will establish that $x \in V$. From hypothesis, we have that $x_n^T A_n x_n \to x^T A x$. Without loss of generality, we assume that x is a unit vector and that $|x_n^T A_n x_n - x^T A x| \leq \gamma$ for all $n \geq N_5$. From the assumption that $x_n \in V_n(\gamma)$ we have

$$x_n^T A_n x_n = \sum_{k=1}^{p}\lambda_{k,n}(x_n^T e_{k,n})^2 = \sum_{k=p-j_n(\gamma)+1}^{p}\lambda_{k,n}(x_n^T e_{k,n})^2 \leq \gamma \tag{2.36}$$

for all $n \geq N_4$. The reverse triangle inequality gives

$$||x_n^T A_n x_n| - |x^T A x|| \leq |x_n^T A_n x_n - x^T A x| \leq \gamma$$

Table 2.1: The estimated null eigenvector of inverse Fisher information matrix (column 2) and the gdor computed by Geyer (2009) (column 3). Only nonzero components are shown.

coefficient	$\hat{\eta}$	$\hat{\eta}_{\text{gdor}}$
intercept	-1	-1
$v1$	1	1
$v2$	1	1
$v3$	1	1
$v5$	1	1
$v1 : v2$	-1	-1
$v1 : v3$	-1	-1
$v1 : v5$	-1	-1
$v2 : v3$	-1	-1
$v2 : v5$	-1	-1
$v3 : v5$	-1	-1
$v1 : v2 : v3$	1	1
$v1 : v3 : v5$	1	1
$v2 : v3 : v5$	1	1

and (2.36) implies $|x^T Ax| \leq 2\gamma$ for all $n \geq \max\{N_4, N_5\}$. Since this argument holds for all $0 < \gamma < \varepsilon$, we can conclude that $x \in V$. This establishes part (ii) of Painlevé-Kuratowski set convergence with respect to $V_n(\gamma)$. Therefore $V_n \to V$ and this completes the proof. □

Theorem 11 states that the span of estimated null eigenvectors will converge to its population counterpart. In our case, the population counterpart is the span of the vectors that construct H_j in the Theorem 4 characterization of a generalized affine function h.

Geyer (2009) developed a different implementation to compute directions of recession. This implementation requires computationally expensive repeated linear programming algorithms, stated in Sections 3.10-3.13 and implemented in the `rcdd` package (Geyer and Meeden, 2008), that are slow in moderately sized problems and will not scale to larger problems. An advantage of our proposed implementation to that of Geyer (2009) is its relative speed, which is shown in our examples. A thorough development of a robust implementation is a research topic that falls outside of this dissertation.

2.6.1 Example 1: Example 2 from Geyer (2009)

As stated in Geyer (2009), this example consists of a $2 \times 2 \times \cdots \times 2$ contingency table with seven dimensions hence $2^7 = 128$ cells. The file `http://www.stat.umn.edu/geyer/gdor/catrec.txt` presents the data as eight vectors, seven categorical predictors $v_1, ..., v_7$ that specify the cells of the contingency table and one response y that gives the cell counts. Table 2.1 displays the estimated null eigenvector of the inverse Fisher information matrix using our implementation, denoted $\hat{\eta}$, and the estimated gdor in Geyer (2009), denoted $\hat{\eta}_{\text{gdor}}$. The $\hat{\eta}$ vector is identical to $\hat{\eta}_{\text{gdor}}$ up to six decimal places. Therefore, the inferences resulting from these two distinct approaches is identical up to rounding. The only material difference between our implementation and the linear programming in Geyer (2009) is computational time. Our implementation estimates η in 0.059 seconds of user time, while the call to `linearity` in the `rcdd` package estimates $\hat{\eta}_{\text{gdor}}$ in 7.259 seconds of user time.

2.6.2 Example 2

We simulate a big data example and show that our methods are much faster than the linear programming of Geyer (2009) for recovering directions of recession. This dataset consists of five categorical variables with four levels each and a response variable $Y \sim \text{Poisson}(\lambda = 1)$. A model with all four way interaction terms is fit to this data. It may seem that the four way interaction model is too large (1024 data points vs 781 parameters) but χ^2 tests select this model over simpler models, see Table 2.2. In Table 2.2, all considered models are nested.

Our implementation discovers and estimates a direction of recession, η in the four way interaction model. We estimate η in 15.639 seconds of user time, while the call to `linearity` in the `rcdd` package estimates no $\hat{\eta}_{\text{gdor}}$ in 2797.189 seconds of user time. The direction $\hat{\eta}$ estimated using our approach satisfies conditions (15a) and (15b) of Geyer (2009) which implies that it is a generic direction of recession.

Table 2.2: Model comparisons for Example 2. The model m1 is the main-effects only model, m2 is the model with all two way interactions, m3 is the model with all three way interactions, and m4 is the model with all four way interactions.

null model	alternative model	df	Deviance	$\Pr(>\chi^2)$
m1	m4	765	904.8	0.00034
m2	m4	675	799.2	0.00066
m3	m4	405	534.4	0.00002

Chapter 3

Aster Models

3.1 Introduction

The estimation of expected Darwinian fitness, the expected lifetime number of offspring an organism has, is a very important quantity in both biology and genetics. The importance of this quantity is not just limited to scientific disciplines, it is important for public policy. With genetic theory and simulation studies, Bürger and Lynch (1995) shows that, under certain conditions, a changing environment leads to extinction of species. Based on a field experiment on an annual plant, Etterson and Shaw (2001) inferred that predicted rates of evolutionary responses may be too slow to maintain adaptation in the face of climate change. In these papers, and all life history analyses of their kind, expected Darwinian fitness is the response variable. The interesting scientific conclusions are drawn from it. When Darwinian fitness is unable to be measured, a useful surrogate is measured in its place.

In many life history analyses, values of expected Darwinian fitness are plotted as a fitness landscape. A fitness landscape is the conditional expectation of Darwinian fitness plotted across phenotypic trait values. As such, the fitness landscape is a regression function. Lande and Arnold (1983) proposed an approach to estimation of the fitness landscape. Their modeling of an expected surrogate Darwinian fitness (survival probability) was conducted via ordinary least squares (OLS) regression with the assumption that the distribution of Darwinian fitness is normally distributed. This assumption is unlikely to be met in practice

(Mitchell-Olds and Shaw, 1987; Shaw, Geyer, Wagenius, Hangelbroek, and Etterson, 2008). The distribution of Darwinian fitness often has a large atom at 0 (corresponding to individuals that have died before reproducing), is multimodal (corresponding to breeding season), right-skewed, and integer-valued. These problems sternly call into question the appropriateness of OLS as a tool for inference on Darwinian fitness. The aster model was designed to fix all of these problems present with the Lande and Arnold (1983) approach. The aster model is the state-of-the-art model for all life history analyses in which the estimation of expected Darwinian fitness is the primary goal.

Researchers using an aster model in their analysis are estimating expected Darwinian fitness through maximum likelihood estimation. The aster model itself is a regular full exponential family. Properties of parameter estimation in this setting are well understood. Specifically, the maximum likelihood estimator for the aster model mean-value parameter vector $\hat{\tau}$ is asymptotically normal with asymptotic covariance matrix given by Fisher information Σ. Estimates of both τ and Σ are provided in the `R` contributed `aster` package (Geyer, 2014).

This chapter is divided into two sections. In the first section, the aster model is explained in detail and an interesting connection of aster models and Fisher (1930) is established. In the second section, a complete aster analysis of the *Manduca sexta* data is given (Eck, et al., 2015a). In this analysis, aster models are used to estimate both expected Darwinian fitness and the population growth rate for hypothetical individuals.

3.2 The aster model

The aster model is a graphical model obeying the following five assumptions:

A1. The graph is acyclic.

A2. A node has at most one predecessor node.

A3. The joint distribution is the product of conditional distributions, one conditional distribution for each arrow in the aster graph.

A4. Predecessor is sample size.

A5. Conditional distributions for arrows are one-parameter exponential family (possibly a different family for each arrow).

Assumptions A4 and A5 mean for an arrow $y_k \longrightarrow y_j$ that y_j is the sum of independent and identically distributed random variables from the exponential family for the arrow and there are y_k terms in the sum (the sum of zero terms is zero). These assumptions imply that the joint distribution of the aster model is an exponential family (Geyer, Wagenius, and Shaw, 2007, Section 2.3).

As an example of an analysis using aster models, consider a population of *Echinacea angustifolia*, plants where total flower head count is taken to be Darwinian fitness as in Geyer, et al. (2007). The graph for one individual is shown in panel A of Figure 3.1. There are nine response variables per individual. The first three indicate survival in each of three years. The next three indicate flowering (zero is no flowers, one is some flowers). The last three are flower head counts. The conditional distributions are Bernoulli for the indicator variables (first six) and zero-truncated Poisson for the rest (last three). These are all exponential families (property A5). Property A4 and sum of zero terms is zero imply that predecessor equals zero implies successor equals zero. Hence the aster model has dead individuals remaining dead, has dead individuals having no flowers, and has individuals with no flowers having zero flower head count. Thus the aster model contains the major dependencies in life histories. The combination of a Bernoulli arrow followed by a zero-truncated Poisson arrow gives a zero-inflated Poisson distribution (e. g., the conditional distribution of Y_7 given Y_1). This factorization of zero-inflated Poisson into product of zero-truncated Poisson and Bernoulli is required by A5 (one parameter per arrow).

The likelihood for the aster model corresponds to the graphical structure of the lifecycle. Variables in the aster model are denoted by Y_j where j ranges over the nodes of the graph. These variables correspond to components of fitness and Darwinian fitness. The

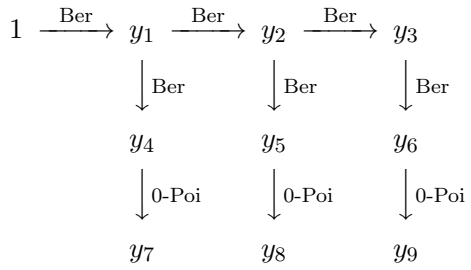

Figure 3.1: Graphical structure of the aster model for the *E. angustifolia* data.

joint distribution of all the random variables in an aster model follows the factorization

$$\text{pr}(Y_J|Y_F) = \prod_{G\in\mathcal{G}} \text{pr}(Y_G|Y_{p(G)}). \tag{3.1}$$

The index set J refers to the indices corresponding to the non-initial nodes of the graph, F corresponds to the set of initial nodes. The function $p(G)$ is defined to be the map $p : G \to J \cup F$ for all $G \in \mathcal{G}$ where $\mathcal{G}$ is the partition of J that determines the graphical structure. The interpretation of $p(G)$ is that the node $p(G)$ is the predecessor node for node $G \in \mathcal{G}$. The factorization of the joint distribution into conditional distributions $\text{pr}(Y_G|Y_{p(G)})$ for all $G \in \mathcal{G}$ then takes on special meaning when each conditional distribution is an exponential family. All the conditional distributions in (1) are now taken to be exponential families with canonical statistic Y_G and canonical parameter θ_G. There are $Y_{p(G)}$ independent and identically distributed copies of random variable Y_G where we require $P(Y_G = 0|Y_{p(G)} = 0) = 1$. This is the mathematical representation of the fourth aster model assumption. It has the interpretation that individuals that have died remain dead. With these assumptions met the log likelihood of the whole family has the form

$$\sum_{G\in\mathcal{G}} \left(\sum_{j\in G} Y_j\theta_j - Y_{p(G)}c_G(\theta_G) \right) = \sum_{j\in J} Y_j\theta_j - \sum_{G\in\mathcal{G}} Y_{p(G)}c_G(\theta_G) \tag{3.2}$$

where θ_G is the canonical parameter vector for the Gth conditional family, which has components $\theta_j, j \in G$, and c_G is the cumulant function for the Gth canonical family. Geyer, Wagenius, and Shaw (2007) demonstrate that this log likelihood can be reparameterized to capture the dependence structure of the graphical model by collecting terms with the same Y_j. This "collecting of terms" gives

$$\sum_{j \in J} Y_j \left(\theta_j - \sum_{G \in p^{-1}(j)} c_G(\theta_G) \right) - \sum_{G \in p^{-1}(F)} Y_{p(G)} c_G(\theta_G)$$

in place of (3.2). We arrive at a new aster model parameterization with

$$\varphi_j = \theta_j - \sum_{G \in p^{-1}(j)} c_G(\theta_G) \quad j \in J,$$

as the canonical parameters, Y_j as the canonical statistics, and

$$\sum_{G \in p^{-1}(F)} Y_{p(G)} c_G(\theta_G)$$

as the cumulant function. The log likelihood for the joint distribution simply becomes

$$l(\varphi) = \langle Y, \varphi \rangle - c(\varphi).$$

The method of collecting the same Y_j's and then switching from θ's to φ's to reparameterize the model is what is referred to as the aster transform. The resulting distribution is an exponential family with canonical statistic Y and canonical parameter φ. This current parameterization of the aster model has too many parameters and is of little scientific interest. We consider affine submodels of the form

$$\varphi = a + M\beta$$

where M is a known model matrix, a is a known offset vector, and β is a canonical parameter vector with dimension smaller than φ. This parameterization specifies an exponential family distribution with canonical statistic $M^T Y$. The dimension of this new model will be the dimension of β if M has full rank. In this case the offset vector a and the model matrix

M are assumed to not be stochastic. The analyses that we consider do not have an offset present. The log likelihood for the unconditional canonical submodel is

$$l(\beta) = \langle M^T Y, \beta \rangle - c_{sub}(\beta) \tag{3.3}$$

where β is the unconditional aster submodel canonical parameter vector. In this likelihood formulation it is understood that $c_{sub}(\beta) = c(a + M\beta)$. The exponential family form allows us to conveniently obtain the maximum likelihood estimator for our canonical parameter vector β using conventional software. First denote τ as our mean-value parameter vector. The map $h : \beta \mapsto \tau$ is a 1-1 invertible mapping where $h(\beta) = \nabla c_{sub}(\beta)$. We see that

$$\begin{aligned} \nabla l(\hat{\beta}) &= 0 \quad \text{occurs when} \\ \nabla c_{sub}(\hat{\beta}) &= M^T Y \quad \text{which is equivalent to} \\ \hat{\tau} &= M^T Y. \end{aligned}$$

We now have a MLE for our mean-value parameter τ. From invariance of maximum likelihood estimation we get $\hat{\beta}$ by solving $h^{-1}(\hat{\tau})$ using optimization software. The inverse map cannot be expressed in closed form. From the usual asymptotics of MLE and exponential families we have,

$$\sqrt{n}\left(\hat{\beta} - \beta\right) \xrightarrow{d} N\left(0,\, \Sigma^{-1}\right) \tag{3.4}$$

$$\sqrt{n}\left(\hat{\tau} - \tau\right) \xrightarrow{d} N\left(0,\, \Sigma\right), \tag{3.5}$$

where Σ is the Fisher information matrix for the canonical parameter vector β. The `aster` software in `R` will give us $\hat{\beta}, \hat{\tau}$, and $\hat{\Sigma}^{-1}$. Our procedures focus on the canonical parameterization of the unconditional aster submodel. However there are useful asymptotic results for either the canonical parameter β or the mean-value parameter τ. Expected Darwinian fitness is most closely associated with the μ parameterization. The relation between φ and μ is analogous to that of β and τ, see Figure 3.2. μ is the mean-value parameter for the

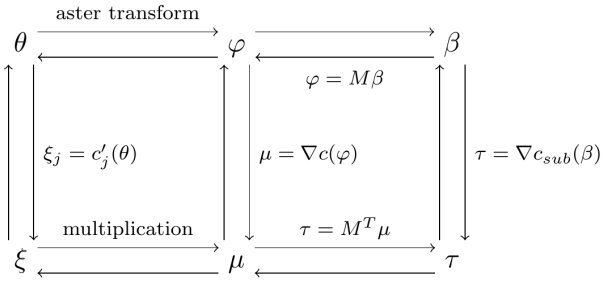

Figure 3.2: A depiction of the transformations necessary to change parameterizations.

full aster model. The MLE for μ is the canonical statistic for the full model. The canonical statistic for the full model is the response vector Y.

From (3.4) and the delta method we can obtain the asymptotic distribution for any function of $\hat{\beta}$ satisfying the conditions of the delta method. In particular, the asymptotic distribution for the MLE of expected Darwinian fitness is of interest. The asymptotic distribution for a differentiable mapping of β is

$$\sqrt{n}\left(g(\hat{\beta}) - g(\beta)\right) \xrightarrow{d} N\left(0,\ \nabla g(\beta)\Sigma^{-1}\nabla g(\beta)^T\right) \tag{3.6}$$

The asymptotic distribution for the maximum likelihood estimator of the mean-value parameter μ is

$$\sqrt{n}\left(\hat{\mu} - \mu\right) \xrightarrow{d} N\left(0,\ \nabla^2 c(M\beta)M\Sigma^{-1}M^T\nabla^2 c(M\beta)^T\right) \tag{3.7}$$

where $g(\beta) = \nabla c(M\beta)$.

3.2.1 Fisher's table of reproduction

When the aster model graphical structure takes the form of survival, adulthood, offspring, as is the case in the *E. angustifolia* example, an interesting connection to Fisher can be made. In Fisher (1930, pg. 24), the table of reproduction is defined. Fisher defines b_x as the rate of reproduction at age x. The quantity l_x is defined to be the number of

individuals in the population living to age x constituting unique phenotypic composition. This quantity is defined in Fisher (1930, pg. 23). For our purposes, l_x is interpreted as an individual's probability of living to age x. Fisher defines the table of reproduction to comprise $l_x b_x$ values. Define μ_x to be expected Darwinian fitness for age x where μ_x is also an unconditional aster model mean-value parameter for age x. We propose that $\mu_x = l_x b_x$ for organisms whose lifecycle follows a survival to reproduction pattern. The proof is obtained by the examination of the definitions and aster model reparameterizations. The unconditional expectation of fitness at age x is the expected value of the probability of surviving to age x multiplied by the conditional expectation of fecundity at age x for one individual, denoted ξ_x. These relationships are further explained in Geyer (2010).

Proposition 1
If the lifecycle follows a survival to reproduction pattern, then $\mu_x = l_x b_x$. □

Proof: Let y_x be observed offspring at age x so that $\mu_x = \mathrm{E}(y_x)$. We then have

$$\mu_x = \mathrm{E}(y_x) = \mathrm{E}(\mathrm{E}(y_x|y_{p(x)})).$$

From the predecessor is sample size property of the aster model we have that $\mathrm{E}(\mathrm{E}(y_x|y_{p(x)})) = \mathrm{E}(y_{p(x)}\,\mathrm{E}(y_x|y_{p(x)} = 1))$ where $\xi_x = \mathrm{E}(y_x|y_{p(x)} = 1)$. Putting it all together we see that,

$$\mu_x = \mathrm{E}(y_x) = \xi_x \mu_{p(x)} = \xi_x \xi_{p(x)} \xi_{p(p(x))} \ldots \mathrm{E}(y_{\text{initial}}).$$

Here, ξ_x is the expected fitness for an individual surviving to age x, $\xi_{p(x)}$ is the probability of survival to age x conditioned on reaching the previous age, $\xi_{p(p(x))}$ is the probability of survival to age $x-1$ conditioned on reaching the previous age, and so on. By definition, $\xi_x = b_x$. This pattern continues all the way to the initial node where all individuals are alive so that $\mathrm{E}(y_{\text{initial}}) = 1$ for one individual. The product of the other ξ terms is equal to the probability of living to age x which is denoted by l_x. Therefore, $\mu_x = b_x l_x$. The proof for case two follows a similar outline with the exception that ξ_x is expected fitness

conditioned on individuals reaching a reproduction stage in their lifecycle. There are living individuals in this model that are not reproducing. In this case $\xi_x \xi_{p(x)} = b_x$ where $\xi_{p(x)}$ is probability that the individual reaches its reproductive state at age x. The product of the other ξ terms is equivalent to l_x as in the previous case. Therefore, we can conclude that $\mu_x = l_x b_x$, completing the proof. □

With this equivalence, aster models can be thought of as "generalized Fisher table of reproduction models" since the aster model can appropriately model lifecycles outside of the survival to adulthood to offspring context. We now proceed with a detailed example of an aster analysis of the *M. Sexta* data.

3.3 *Manduca sexta* example

3.3.1 Introduction

There is abundant evidence for phenotypic and genotypic selection on quantitative traits in natural populations (Kingsolver, et al., 2001; Siepielski, et al., 2009). Most estimates of the strength and pattern of phenotypic selection — more than 90% — are based on individual components of fitness, rather than metrics of lifetime fitness (Kingsolver and Diamond, 2011). The resulting inferences may reflect the nature of phenotypic selection only weakly or not at all, to the extent that components of fitness differ in their relationships to traits. For studies that do evaluate lifetime fitness of individuals or genotypes, the distribution of fitness is generally not normal: it is typically highly skewed and often multimodal, with a large mode at zero, corresponding to individuals that die without reproducing. Thus, the assumption of normally distributed residuals required for the standard statistical analyses does not hold, making inference and hypothesis testing about selection problematic. Aster models were developed to address this challenge. This approach produces statistically valid models for fitness by taking into account the dependence of later expressed fitness components on those expressed earlier and also by employing appropriate probability models for each component (Geyer, et al., 2007; Shaw, et al., 2008). Aster models for inferring phenotypic selection have been validated by Shaw and Geyer (2010).

In many species, including most insects, variation in age at first reproduction is a major component of fitness that can have a large effect on the population growth rate and similar metrics of fitness (Roff, 2002). This information is typically difficult both to obtain and to incorporate into analyses of fitness. As a result, integrated analyses of phenotypic selection that consider variation in time to reproduction are currently limited to relatively few cases of long-term studies of birds, mammals and plants (Ozgul et al., 2009; Clutton-Brock and Sheldon, 2010; Ozgul et al., 2010; Charmantier and Gienapp, 2014; Childs, et al., 2004).

We extend previous Aster models to incorporate age at reproduction in the model for fitness. These new models (R package `aster2`, Geyer, 2010) allow us to specify "dependence groups" that represent different life history stages, as well as variation in the age at which individuals reach these stages, and include these in the model for fitness.

Holometabolous insects have distinct larval, pupal and adult (reproductive) life stages, and rates of growth and development within and across life stages have important effects on fitness. For example, Kingsolver, et al. (2012) used common garden field studies with *Manduca sexta* to estimate phenotypic selection on body size and age at different developmental stages. However, that study estimated selection via survival, reproduction, and generation time separately, and therefore could not quantify how selection operates over the entire life cycle, nor identify the interplay of fitness components in their contributions to lifetime fitness. Here we describe and apply `aster2` models to these data to gain an integrated view of phenotypic selection on size and age across development, along with insight into the interplay of fitness components, in this study system. We discuss the utility of these methods in clarifying selection in other systems. Our statistical results are fully reproducible (Eck, et al., 2015b)

3.3.2 Methods

Study System and Field Studies

The Tobacco Hornworm, *M. sexta*, is found in Central America and the southern US, with eastern populations extending north into New York and Massachusetts. In the southeastern

US, including North Carolina, cultivated tobacco and tomato are dominant host plants for *M. sexta*, which can be an important agricultural pest in these systems. Our field studies used tobacco cultivars (see below).

After hatching, *M. sexta* larvae grow and develop rapidly through five (occasionally more) larval instars, growing from $\sim$ 1 mg to $\sim$ 8–12 g in body mass in a few weeks under optimal conditions. Rates of larval growth and development are strongly influenced by environmental temperatures and host plant quality. Towards the end of the final instar, larvae stop feeding and wander off the host plant to pupate nearby in the soil. A facultative pupal diapause is determined by larval photoperiod, such that *M. sexta* populations have multiple generations per year in most areas (2–3 generations/year in North Carolina). Because pupae do not feed, maximum larval mass at wandering strongly determines pupal and adult size and the number of eggs (oocytes) produced by females.

For *M. sexta*, both host plant quality and larval susceptibility to natural enemies are important determinants of survival to adult reproduction. For example, in the southeastern US including North Carolina, the larval parasitoid *Cotesia congregata* (Hymenoptera: Braconidae) is often a major source of larval mortality. Thus, rapid rates of early larval growth and development may strongly influence survival to reproduction in this system.

Here we consider a field selection study of *M. sexta* conducted in a cultivated tobacco garden in the Mason Farm Biological Reserve, Chapel Hill NC, in July 2010. Details are fully described by Kingsolver, et al. (2012); we briefly summarize here. Prior to the study, the garden plot (12 m by 20 m in size) was tilled and fertilized. Tobacco plants (*Nicotiana tabacum*, var. LA Burley 21) were grown from seeds in pots in the greenhouse at UNC, and then they were transplanted to the field garden. A total of 60 plants in 6 rows were used in the study plot, with a single buffer row of tobacco plants around the perimeter of the study plot. The plants were allowed to establish for $\sim$ 4 weeks prior to the start of a study; plants that did not thrive after transplanting were replaced. The garden was watered daily, and insect herbivores were removed weekly by hand from each plant. To minimize larval predation by birds and social wasps, plants were covered with bridal veil netting just prior to the study. The netting excludes large predators but allows access to the caterpillars by

parasitoids, including *C. congregata*.

To initiate the study, *M. sexta* eggs were collected from pesticide-free tobacco plants at the NC State Agricultural Extension Farm, Clayton NC, approximately 100 km from Chapel Hill. Eggs were allowed to hatch in the lab and were maintained individually on tobacco leaves in an environmental chamber at 25 °C. with a 16L:8D light cycle during the 1st and 2nd larval instars. Body mass and age at the start of the 2nd and 3rd instars were measured. Following molt into the 3rd instar, each larva was randomly assigned to a plant (4 larvae per plant, to avoid larval competition for food) in the study plot. Each larva was marked using water-based nail polish on the tip of the dorsal horn (and re-applied after each molt). This allowed us to track individuals in the field throughout the study Kingsolver, et al. (2012).

During daily field censuses, we recorded the presence or absence of each larva. Recapture probabilities (given alive) for larvae consistently exceeded 90%. At the start of the 4th and 5th instar, the mass and age of each larva were recorded, and the larva was returned to its plant.

When larval mass late in the 5th instar exceeded 5 g (about 14–16 days), larvae were removed from the field and reared individually on tobacco leaves in petri dishes in an environmental chamber at 26.7 °C (16L:8D light cycle) until wandering. Mass and age at wandering were recorded, then each larva was placed in a wooden block (Yamamoto, 1969) at 25 °C to pupate. Pupal mass was measured at 7 days after wandering to ensure the pupal cuticle hardened prior to handling. Pupae were placed in Solo cups with moistened soil, kept at 20 °C, and checked daily each morning until eclosion (considered as age of reproduction). Estimates of potential fecundity for adult females (48 h after eclosion) were obtained by dissecting out and counting the number of ovarioles at stage 6 or later (Yamauchi and Yoshitake, 1984; Diamond and Kingsolver, 2010a).

Statistical Analyses

Our analyses evaluate the relationship between fitness and three traits, age (since hatching) at the second instar stage, mass at that age, and mass at eclosion. Individuals reproduce

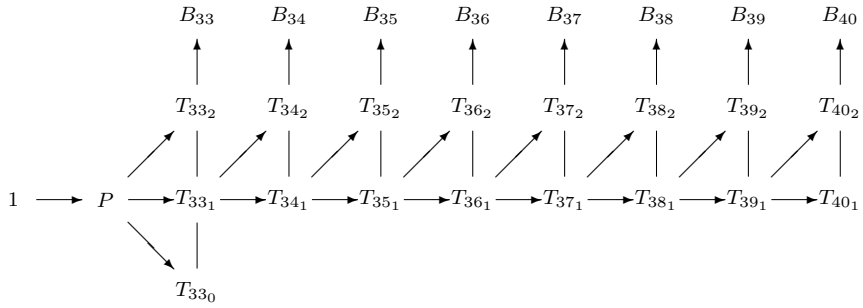

Figure 3.3: Aster Graph for Female *M. sexta*. Arrows go from predecessor nodes to successor nodes. Lines (that are not arrows) link dependence groups. Nodes are labeled by their associated variables. P node is pupation, T nodes are survival and eclosion indicators, B nodes are ovariole counts. Subscripts indicate age (in days), subsubscripts indicate variables in the same dependence group (0 = death, 1 = surviving but pre-eclosion, 2 = eclosion at this time). For simplicity, all deaths after pupation but before reproduction were modeled as occurring on day 33. No individuals survived past day 40.

only if they survive to eclosion and they eclose only if they survive to pupation. Thus there is inherent dependence of each component of fitness on survival to that life history stage. We here use an individual's ovariole count as the best proxy for its lifetime fitness. No measure of fitness is perfect, and this one has the limitation that the data do not span the complete life cycle, but they do span the great majority of it. Ovariole count will henceforth be referred to simply as observed fitness. The unconditional expectation of ovariole count for an individual at the beginning of the experiment will be referred to as expected fitness. To address the problem that lifetime fitness generally does not conform to any standard statistical distribution, in part because many individuals die without reproducing, Aster directly models this distribution by explicitly modeling the distributions of its underlying components, as well as their dependence structure.

The underlying dependence structure of development for females in this dataset can be represented by an Aster graph (Figure 3.3). The first arrow indicates an individual's survival to pupation, where survival is modeled as a Bernoulli random variable, shown as P in the graph. For an individual that survived to pupation, we account for the timing of metamorphosis by using dependence groups in the graphical model. For example, the next three nodes in this graph (T_{33_0}, T_{33_1}, and T_{33_2}) together represent a three-way switch where

a particular *M. sexta* can only transition into one of these three nodes. The T_{33_0} node is 1 if the individual died before reaching eclosion. For simplicity, all individuals that died following pupation and before eclosion are treated as dying at age 33 days, the day when the first individual in our study eclosed. The T_{33_1} node is 1 if the individual remained as a pupa on day 33, and the T_{33_2} node is 1 if the individual eclosed at age 33. In general, if the predecessor is 0, then every component in the dependence group is 0. However, if the predecessor is 1 then exactly one component of the response in the dependence group is 1 and the rest are 0. The dependence groups at each successive age follow a similar pattern, albeit with only two nodes because all mortality after pupation but before reproduction is treated as occurring on day 33. No individual survived past day 40. The dependence groups are modeled as multinomial with the number of categories equal to the number of nodes in the dependence group. For any age i when an individual has eclosed, $T_{i_2} = 1$, the ovariole counts, labeled B_i, are modeled with a zero-truncated Poisson distribution, given that females reaching eclosion are expected to have more than zero ovarioles.

To estimate fitness, we modeled both females and males, recognizing that the graph corresponding to males does not have ovariole count nodes, otherwise the graphs are the same. In order to model the probability of an individual female's survival to pupation we included the information for the males in our statistical model, because an individual can be sexed only once it reaches the pupal stage.

We use an unconditional aster model (Shaw, et al., 2008) to obtain comprehensive estimates of lifetime fitness by modeling these distinct fitness components jointly according to this graphical structure. Once the distributions of all the nodes in the aster model and their dependence structure are specified, phenotypic selection analysis proceeds by regressing the nodes considered to correspond to lifetime fitness, here female ovariole counts, on the phenotypic predictors of interest. This regression, conducted as an unconditional aster model, takes into account all life history stages. In the unconditional aster model unconditional expected fitness is a monotone function of fitness on the canonical parameter scale, which is modeled as a linear or quadratic function of the traits (Shaw and Geyer, 2010, Appendix, which is generalized our Appendix). To assess directional selection, as well

as the curvature of the fitness function, we consider two aster models having as predictors both of the mass traits as well as the individual's age when it reached the second instar larval stage. The first model is a general linear function of the traits (mass at second instar, mass at eclosion, and age at second instar) on the canonical parameter scale. The second model is a general quadratic function of the traits on the canonical parameter scale; as such, it includes squares of each trait and pairwise interactions between the traits (Blows and Brooks, 2003; Shaw and Geyer, 2010).

In order to compare models of interest, a Rao test is used where the reference distribution is χ^2 with degrees of freedom equal to the difference of free parameters between the two models. Fitness landscapes (Lande and Arnold, 1983; Shaw and Geyer, 2010) are then generated from the model selected by the Rao test. This is done by evaluating expected fitness for hypothetical individuals having various values of the phenotypic traits (mass at second instar, mass at eclosion, and age at second instar) ranging over a grid and then making a contour plot of these values (Figure 3.4).

The analyses described above account for variation in survival and ovariole counts but do not take into account that, in a growing population, earlier produced offspring contribute more to fitness than those produced later. To address this aspect of fitness, we extended the aster models described by Shaw and Geyer (2010). The population growth rate parameter (λ) for the observed population of *M. sexta* is estimated from the stable age equation (Fisher, 1930), which is equation (3.11) in the Appendix, as the basis of accounting for individuals' age at reproduction in their lifetime fitness.

We examine the effects of λ on fitness by refitting the data using the model determined by equations (3.8) and (3.10) in the Appendix with $q(\mathbf{z})$ indicating a function of the same form as was used in the fit that did not account for λ but with different regression coefficients. This makes expected fitness adjusted for population growth rate a monotone function of $q(\mathbf{z})$ as explained in the Appendix.

We then also adjust the fitness landscape to plot fitness adjusted for λ as given by equation (3.12) in the Appendix. Because the adjustment for λ involves dimensionless factors $e^{-\lambda t}$, this fitness landscape must be a relative fitness landscape (adjusted fitness

Table 3.1: Rao tests for smaller models. P-values and degrees of freedom for Rao tests of three smaller models against the larger model that includes linear, quadratic, and interaction term for the two mass traits and a linear term for age at second larval instar stage.

null model	df	P-value
removes quadratic terms for mass at second instar	2	3.37×10^{-10}
removes quadratic terms for mass at eclosion	2	$< 10^{-10}$
removes linear term for age at second instar	1	7.88×10^{-5}

divided by mean adjusted fitness).

3.3.3 Results

Larval mortality prior to pupation was 23%, including 2% mortality due to parasitism by *C. congregata*. Field studies suggest that rates of larval mortality vary seasonally in this region (Diamond and Kingsolver, 2010b; Kingsolver, et al., 2012).

The phenotypic selection analysis detected relationships between lifetime fitness and all three traits considered as predictors. The aster model that includes the linear and quadratic terms for the two mass traits and their interaction, as well as the linear term for age at second larval instar stage, was chosen based on the Rao test. This model is chosen over the model that is full quadratic (including interactions) in all three traits ($P = 0.105$, Rao test, 3 degrees of freedom). All Rao tests that considered immediately smaller models were rejected, see 1.

The fitness landscape generated from this model shows that absolute fitness not adjusted for population growth rate (unconditional expected ovariole count, left column of Figure 3.4) is predominantly explained by an individual's mass at eclosion. As mass at eclosion increases, unconditional expected ovariole count increases with a maximum found for female *M. sexta* weighing roughly 2 grams at eclosion, beyond which fitness declines. Considering mass at the second instar stage, the estimated contours viewed in relation to the observed data suggest that selection is largely directional with fitness inversely related to this trait, despite significant curvature of the fitness function in relation to this trait. In addition, unconditional expected ovariole counts decline with increasing age to 2nd instar

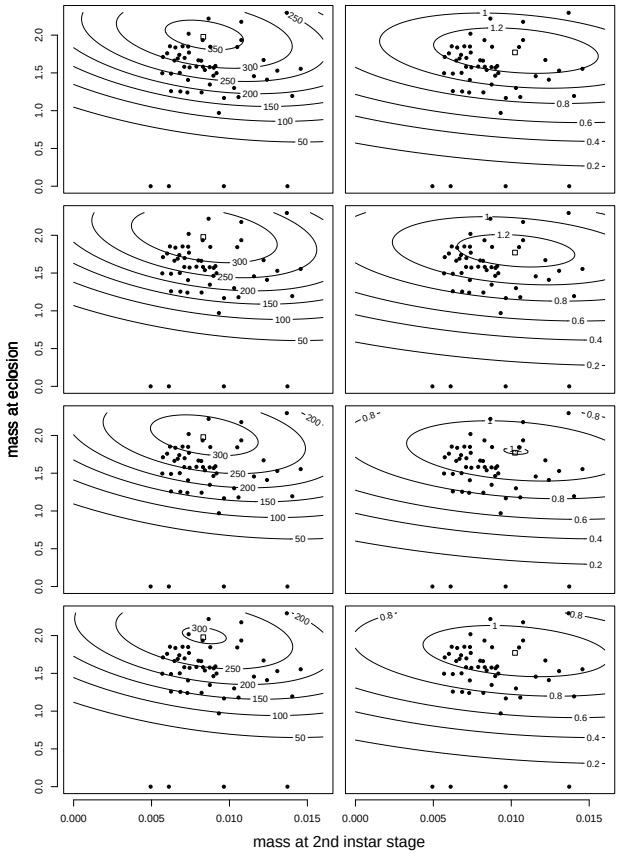

Figure 3.4: Fitness landscapes without (left column) and with (right column) adjustment for population growth rate λ. Rows top to bottom are 2nd instar stage reached at age 2, 3, 4, and 5. Numbers on contours are absolute fitness (unconditional expected ovariole counts) in the left column and are relative fitness (absolute fitness divided by its average over the population) in the right column. All plots display fitness as contours vs. mass at eclosion and mass at 2nd instar stage. Boxes denote locations of maxima. The maximum values for unconditional expected ovariole counts for each age are 363.6 (age 2), 342.4 (age 3), 322.4 (age 4), and 303.6 (age 5).

(left column of Figure 3.4). For example, the maximum unconditional expected ovariole counts declines by 16% as age to 2nd instar increases from 2 to 5 days. This effect is largely due to the effects of age at 2nd instar on survival to eclosion: slower development (later age at 2nd instar) is associated with lower survival.

Absolute fitness (unconditional expected ovariole count) predicted from the model for predictor values of individuals that survive to eclosion range from 102.7 to 301.37. But observed ovariole counts for these individuals are larger ranging from 173.8 to 350.3. The reason for the discrepancy is that the former take survival into account and the latter do not (they ignore individuals that did not survive to eclosion).

The preceding analysis accounts for survival and ovariole count as components of fitness, but does not account for the role of variation in timing of reproduction in fitness variation. To incorporate this effect we consider population growth rate.

From the estimates of unconditional expected ovariole count at each age produced by the aster model we obtain via the stable age equation (3.11) the estimate $\hat{\lambda} = 0.122$. The large positive value of λ indicates a growing population. Such overestimates of population growth rate are typical of experiments that do not have all sources of natural mortality and all sources of failure to reproduce, (cf., Shaw, et al., 2008, Example 1 reanalyzing data of Lenski and Service, 1982).

The relative fitness landscape taking into account population growth and timing of reproduction (right column of Figure 3.4) is qualitatively different from the landscape not so adjusted (left column of Figure 3.4). When population growth rate is taken into account, maximum fitness occurs at a lower mass at eclosion and at a higher mass at the second instar larval stage. In Figure 3.4 we can see that the strength of directional selection on mass at the second instar stage is decreased when the population growth rate is taken into account. This suggests that, in this study, variation in generation time does contribute importantly to patterns of phenotypic selection on the two mass traits.

3.3.4 Discussion

Variation in timing of reproduction is an important component of fitness variation in many organisms, and traits that influence it may undergo strong phenotypic selection. As a result, rates of development and other traits that affect age of first reproduction or reproductive schedules can importantly influence overall fitness. Our Aster models provide an integrated statistical framework for estimating selection on traits via their effects on survival, ovariole counts and timing of reproduction.

The selection analyses of *M. sexta* in our study population identify two key traits: mass at eclosion, and age at 2nd instar. We detected stabilizing selection on mass at eclosion with the optimum near to the top of the observed range of values for this trait, but still within the range, such that fitness declines at still greater values. Reaching 2nd instar at earlier ages is associated with greater fitness (Figure 3.4). However, these three traits contribute to fitness via different components: mass at eclosion via fecundity, earlier age at 2nd instar through survival and timing of reproduction. More rapid development rates (reaching second instar at earlier ages) may allow larvae to escape key parasitoids and other natural enemies and increase survival, as noted in Diamond and Kingsolver (2010b); Kingsolver, et al. (2012). For these data, variation in survival and ovariole counts appears to be more important than variation in timing of reproduction in determining selection on these traits (Figure 3.4). Fitness was more subtly (though significantly) related to mass at 2nd instar: though rate of early larval development is under substantial directional selection, mass at this early stage is selected more weakly, largely in the direction of lower values.

Life history tradeoffs among survival, fecundity and generation time are common in many organisms (Roff, 2002). Similarly, phenotypic and genetic correlations between traits can lead to opposing selection on the traits via different fitness components. The analyses presented here allow us to estimate phenotypic selection and fitness landscapes that integrate all three of these fitness components. A key result of these analyses is that incorporating generation time into fitness alters the pattern and strength of selection on larval and adult mass in *M. sexta*. In particular when population growth rate is taken into account,

the strength of directional selection on mass at the 2nd instar decreases, and maximum fitness occurs at a higher mass at the 2nd instar but at a lower mass at eclosion (Figure 3.4). These changes occur in part because age at 2nd instar is strongly positively correlated with age at eclosion and first reproduction, but is negatively correlated with mass at 2nd instar (Kingsolver, et al., 2012). These effects could not be detected in previous analyses that considered selection on each fitness component separately (Kingsolver, et al., 2012).

The Aster analyses presented here account for development rate by using the multinomial distribution to model transitions through stages; they thus illustrate a new capability of Aster modeling. This capability enables statistical modeling of selection via variation in the timing of life history events through the discounting of later produced offspring in a growing population, in addition to any direct association of development rate with absolute reproductive output. As theory shows (Fisher, 1930) and our analyses suggest, this discounting can play an important role in modulating individual fitness. Phenotypic variation in generation time and age of first reproduction occurs in many populations (Roff, 2002). In many temperate and tropical regions, variation in the number of generations per year is widespread in many insect populations. It will be of interest to learn from future empirical studies of phenotypic selection how discounting of age-specific reproduction influences fitness surfaces more generally.

Appendix: Adjusting Fitness for Population Growth Rate

The Appendix of Shaw and Geyer (2010) explains the multivariate monotone relationship between unconditional canonical parameters φ_j and unconditional mean value parameters μ_j in an aster model. The latter are the quantities of scientific interest, unconditional expectations of components of the response vector. The former are the ones specified by model formulas for many statistical reasons (Geyer, et al., 2007). Now we must extend equations (A2) and (A3) of Shaw and Geyer (2010) to allow for population growth rate.

We replace (A2) by

$$\varphi_j(\mathbf{x}, \mathbf{z}) = a_j(\mathbf{x}) + w_j q(\mathbf{z}), \qquad j \in J. \tag{3.8}$$

Here J is the set of nodes of the full aster graph; j runs over individuals and over nodes within individuals. The full aster graph has one subgraph for each individual in the data. In our data, each subgraph looks like Fig. 1 for a female or like Fig. 1 with the ovariole count nodes omitted for a male. In (3.8) $\mathbf{z}$ is the vector of phenotypic trait variables for an actual or hypothetical individual, $\mathbf{x}$ is a vector of other covariate variables, $\varphi_j(\mathbf{x}, \mathbf{z})$ is the canonical parameter value for node j. We have no other such variables $\mathbf{x}$ in our data, but the equations being rewritten from Shaw and Geyer (2010) allowed for them, so we keep them. This equation says that $\varphi_j(\mathbf{x}, \mathbf{z})$ is modeled as an arbitrary function of $\mathbf{x}$, which may vary from node to node, plus an arbitrary function of $\mathbf{z}$, which varies from node to node in only a very restricted way, the same function $q(\mathbf{z})$ being multiplied by node-specific weights w_j that do not depend on $\mathbf{z}$.

It then follows by the same argument that goes from (A2) to (A3) in Shaw and Geyer (2010) that (3.8) implies

$$q(\mathbf{z}_1) > q(\mathbf{z}_2) \quad \text{if and only if} \quad \sum_{j \in J} w_j \mu_j(\mathbf{x}, \mathbf{z}_1) > \sum_{j \in J} w_j \mu_j(\mathbf{x}, \mathbf{z}_2). \tag{3.9}$$

This argument holds for arbitrary real number weights w_j and arbitrary functions $q(\mathbf{z})$. We can think of $q(\mathbf{z})$ as the fitness landscape on the canonical parameter scale and of $\sum_{j \in J} w_j \mu_j(\mathbf{x}, \mathbf{z})$, considered as a function of $\mathbf{z}$ holding $\mathbf{x}$ fixed, as the fitness landscape on the mean value parameter scale.

In all previously published aster analyses, the weights w_j were zero or one so fitness on the mean value parameter scale is just the sum of terms with $w_j = 1$. This allows fitness to be the sum over only those nodes of the graph that contribute directly to fitness. In our data, this is the ovariole count nodes. (Other nodes contribute only indirectly through their effect on unconditional mean ovariole count.) For our data our first aster analyses were also of this form. But after population growth rate λ had been determined we refit the data using weights

$$w_j = f_j e^{-\lambda t_j} \tag{3.10}$$

where f_j are the zero or one weights indicating nodes that contribute directly to fitness and t_j is the age of the individual at node j. This weighting accounts for population growth rate (Charlesworth, 1980, p. 134).

In our data, there are no "other" (non-phenotypic) covariates $\mathbf{x}$, so $a_j(\mathbf{x})$ in (3.8) becomes a_j and $\varphi_j(\mathbf{x}, \mathbf{z})$ and $\mu_j(\mathbf{x}, \mathbf{z})$ in (3.8) and (3.9) become $\varphi_j(\mathbf{z})$ and $\mu_j(\mathbf{z})$.

To estimate λ we use the stable age equation (Fisher, 1930, p. 26) In our context, this is

$$1 = \frac{1}{n} \sum_{j \in J} \mu_j(\mathbf{z}_j) f_j e^{-\lambda t_j} \tag{3.11}$$

where n is the number of individuals in the data, $\mu_j(\mathbf{z}_j)$ is the mean value for node j with the phenotypic data for that individual plugged in, and the rest is as above.

Most applications of the stable age equation, starting with Fisher, the term $\mu_j(\mathbf{z}_j)$ in (3.11) is written as the product of probability of survival to age t_j and the conditional expectation of number of offspring at age t_j given survival to age t_j. We use the notation in (3.11) because $\mu_j(\mathbf{z}_j)$ is calculated directly by the aster software. Most applications of the stable age equation, starting with Fisher, do not average over all individuals in the data, as we do here. That is because those treatments do not allow for variation among individuals. Consequently, they use the same model for all individuals and apply the stable age equation to one individual (and hence to all because all are the same according to the model).

Having estimated λ and refit the aster model so fitness is adjusted for λ, we then take the fitness landscape adjusted for λ to be

$$w(\mathbf{z}) = \sum_{j \in K} \mu_j(\mathbf{z}) f_j e^{-\lambda t_j}, \tag{3.12}$$

where on the right-hand side everything is as in (3.11) except that now the summation runs over the set K of nodes for a single hypothetical female individual having phenotypic trait vector $\mathbf{z}$ (Charlesworth, 1980, p. 134).

Comparison of (3.11) and (3.12) shows that if we replace $\mathbf{z}$ for this hypothetical individ-

ual by the covariate vector values $\mathbf{z}_j$ for actual individuals and average over all individuals in the data, we get 1. Thus (3.12) is *relative fitness* (fitness divided by mean fitness). Call (3.12) expected relative fitness adjusted for population growth rate.

Chapter 4

Aster Models and Envelope Methodology

4.1 Introduction

We further improve on the aster model through the incorporation of general envelope methodology. Envelope models were developed as a variance reduction tool for the multivariate linear regression model. These models are especially useful when some characteristics of the response vector are unaffected by changes in the predictors. The MLE from the envelope model can be substantially less variable than OLS estimator, especially when the mean function varies in directions that are orthogonal to the directions of maximum variation for the response vector (Cook, et al., 2010). These efficiency gains can be massive. There are examples where the OLS estimator would require 10,000 times as many data points to replicate the standard errors obtained through envelope estimation. Su and Cook (2011) developed partial envelope models for analyses that have a distinction between parameters of interest and nuisance parameters. Cook and Zhang (2015a) developed the most general envelope framework to date, which assumes only a $\sqrt{n}$ consistent and asymptotically normal estimator of an unknown parameter vector and a $\sqrt{n}$ consistent estimator of its asymptotic covariance matrix.

From both the data analysis standpoint and the theoretical standpoint, we show that the assumptions and quantities needed for general envelope methodology are inherent in aster modeling and are easily obtained. Our envelope methodology, which seeks variance reduc-

tion of expected Darwinian fitness, is implemented with respect to mean value parameters instead of canonical parameters. We also construct envelope estimators by searching over reducing subspaces of the estimated covariance matrix. Variance reduction is assessed using parametric bootstrap algorithms developed in this exposition. These bootstrap algorithms are robust against model selection volatility by incorporating techniques in Efron (2014, Section 4). Our methodology provides the most precise estimation of expected Darwinian fitness to date when using aster models. Researchers using our methods can therefore draw stronger conclusions about the driving forces of Darwinian fitness from their life history analyses. The analyses we consider in this Chapter estimate expected Darwinian fitness for categorical variables and fitness landscapes (Shaw, Geyer, Wagenius, Hangelbroek, and Etterson, 2008; Shaw and Geyer, 2010). Fitness landscapes are the conditional expectation of Darwinian fitness given a wide range of predictor values. This tool is used to see which combination of predictor values yield the highest estimated expected Darwinian fitness. In a real data example and a simulated example, we show that our methodology leads to variance reduction in estimation of expected Darwinian fitness when compared with analyses that use aster models alone. These examples use our new envelope estimator constructed from reducing subspaces. Our examples are fully reproducible and the calculations necessary for its reproduction are included in Eck, et al. (2016a).

4.2 The aster model

The aster models to which we apply general envelope methodology are unconditional aster models and unconditional aster submodels (Geyer, Wagenius, and Shaw, 2007; Geyer, 2010). Parameters associated with unconditional aster models are displayed in the middle and right columns of Figure 3.2. The parameters in the left column of Figure 3.2 correspond to conditional aster models. Almost all uses of aster models are unconditional aster models and our methods are developed for these models exclusively. The response vector of an unconditional aster model has the same dimension as the canonical parameter vector φ that we are interested in estimating when using this model. These models are saturated

(one parameter per component of the response vector) and hence not useful. Therefore, the unconditional aster submodel is used where we write $\varphi = a + M\beta$, see Figure 3.2. We will refer to the unconditional aster submodel as an aster model. Here $\varphi \in \mathbb{R}^m$ is the unconditional aster model canonical parameter and β is the aster model canonical parameter vector where m is the dimension of the response vector. The number of responses is the number of nodes that appear in the graphical structure multiplied by the number of individuals sampled. $M \in \mathbb{R}^{m \times p}$ is a known model matrix assumed to be of full column rank where p is the dimension of the aster model, and $a \in \mathbb{R}^m$ is a known offset vector.

There are five parameters of interest that are present in the aster analyses we consider, four parameterizations and one function of one of these. These parameterizations are:

1) The aster model canonical parameter vector $\beta \in \mathbb{R}^p$.

2) The aster model mean-value parameter vector $\tau \in \mathbb{R}^p$.

3) The saturated aster model canonical parameter vector $\varphi \in \mathbb{R}^m$.

4) The saturated aster model mean-value parameter vector $\mu \in \mathbb{R}^m$.

5) The best surrogate of expected Darwinian fitness, which is a function of μ.

Relations among the parameterizations are shown in Figure 3.2. In the *E. angustifolia* example, see the previous Chapter, Darwinian fitness has one component per individual, which gives the total (over the three years) flower head count for that individual, so in this case it is a linear function.

The log likelihood for the aster model in canonical form is (3.3) with canonical statistic $M^T Y$ and $Y \in \mathbb{R}^m$ is the vector of responses depicted in the corresponding graphical structure. The response vector has one component for every node in the graph for every individual in the study. Our model, being a regular full exponential family, allows us to conveniently obtain the maximum likelihood estimator for our canonical parameter vector β. We obtain the model mean-value parameter τ by differentiation. We see that

$$\tau = \nabla_\beta c(a + M\beta) = M^T \nabla c(\varphi) = \mathrm{E}(M^T Y) = M^T \mu$$

and the MLE of τ, denoted $\hat{\tau}$, is $M^T Y$. The MLE of β is obtained from invariance of maximum likelihood estimation where $\hat{\beta} = f^{-1}(\hat{\tau})$ and $f : \beta \mapsto M^T \nabla c(a + M\beta)$, seen in Figure 3.2, is an invertible mapping (assuming the model is identifiable). From the usual asymptotics of MLE and exponential families we have,

$$\sqrt{n}\,(\hat{\tau} - \tau) \xrightarrow{d} N\,(0,\, \Sigma)\,, \tag{4.1}$$

where $\Sigma = \mathrm{Var}(M^T Y)$ is the Fisher information matrix associated with the canonical parameter vector β, which is the inverse Fisher information matrix for τ. The maximum likelihood estimator of β is asymptotically normal with variance given by Σ^{-1}. The `aster` software in `R` provides $\hat{\beta}$ and $\widehat{\Sigma}$ where $\widehat{\Sigma}$ is the maximum likelihood estimator of Σ. From (4.1) and the delta method we can obtain the asymptotic distribution for any differentiable function of $\hat{\tau}$. The asymptotic distribution for a differentiable function g of $\hat{\tau}$ is

$$\sqrt{n}\,(g(\hat{\tau}) - g(\tau)) \xrightarrow{d} N\left(0,\ \nabla g(\tau) \Sigma \nabla g(\tau)^T\right). \tag{4.2}$$

In particular, the asymptotic distribution of estimated expected Darwinian fitness is of interest, call it $h(\mu)$. Since $\beta = f^{-1}(\tau)$ and $\mu = \nabla c(a + M\beta)$,

$$g(\tau) = h\Big(\nabla c\big(a + M f^{-1}(\tau)\big)\Big)$$

gives expected Darwinian fitness as a function of τ and is differentiable if h is differentiable. So now our estimator $g(\hat{\tau})$ has asymptotic distribution given by (4.2).

4.3 Envelope methodology

Envelope methodology was developed originally in the context of the multivariate linear regression model (Cook, et al., 2010),

$$Y = \alpha + \beta X + \varepsilon, \tag{4.3}$$

where $\alpha \in \mathbb{R}^r$, the random response vector is $Y \in \mathbb{R}^r$, the fixed predictor vector $X \in \mathbb{R}^p$ is centered to have mean zero, and the error vector $\varepsilon \sim N(0, \Sigma)$. It was shown by Cook, et al. (2010) that the envelope estimator of the unknown coefficient matrix $\beta \in \mathbb{R}^{r\times p}$ in (4.3) has the potential to yield massive efficiency gains relative to the standard estimator of β. These efficiency gains can arise when the dimension u of the envelope, defined in the next section, is less than r. The main idea of envelope methodology is that the full spectral structure of the error covariance matrix Σ is not needed to estimate β. The spectral structure of Σ has two parts. One part is material to the estimation of β. The other part is immaterial and can be discarded since it serves no purpose towards estimation of β. This situation occurs when some characteristics of the response vector are unaffected by changes in the predictors (Cook, et al., 2010).

More carefully, suppose that we can find a subspace $\mathcal{S} \subseteq \mathbb{R}^r$ so that

$$\mathcal{Q}_{\mathcal{S}}Y \perp\!\!\!\perp \mathcal{P}_{\mathcal{S}}Y \mid X, \quad \text{and} \quad \mathcal{Q}_{\mathcal{S}}Y \mid X = x_1 \sim \mathcal{Q}_{\mathcal{S}}Y \mid X = x_2, \quad \text{for all} \quad x_1, x_2, \tag{4.4}$$

where $\sim$ means identically distributed, $\mathcal{P}_{(\cdot)}$ projects onto the subspace indicated by its argument and $\mathcal{Q} = I_r - \mathcal{P}$. For any $\mathcal{S}$ with the properties (4.4), $\mathcal{P}_{\mathcal{S}}Y$ carries all of the material information and perhaps some of the immaterial information, while $\mathcal{Q}_{\mathcal{S}}$ contains just immaterial information. Let $\mathcal{B} = \text{span}(\beta)$ and $d = \dim(\mathcal{B})$ so that $0 < d \leq \min(p, r)$. Then (4.4) holds if and only if $\mathcal{B} \subseteq \mathcal{S}$ and $\Sigma = \Sigma_{\mathcal{S}} + \Sigma_{\mathcal{S}^\perp}$, where $\Sigma_{\mathcal{S}} = \text{Var}(\mathcal{P}_{\mathcal{S}}Y)$ and $\Sigma_{\mathcal{S}^\perp} = \text{Var}(\mathcal{Q}_{\mathcal{S}}Y)$. The envelope is defined as the intersection of all subspaces $\mathcal{S}$ that satisfy (4.4) and is denoted by $\mathcal{E}_\Sigma(\mathcal{B})$ with dimension $u = \dim\{\mathcal{E}_\Sigma(\mathcal{B})\}$ satisfying $0 < d \leq u \leq r$.

The envelope model can be represented in terms of coordinates by parameterizing model (5.1) to incorporate conditions (4.4). Define $\Gamma \in \mathbb{R}^{r\times u}$ to be a semi-orthogonal basis matrix for $\mathcal{E}_\Sigma(\mathcal{B})$ and let $(\Gamma, \Gamma_o) \in \mathbb{R}^{r\times r}$ be an orthogonal matrix. Then the envelope model with respect to model (5.1) is parameterized as

$$Y = \alpha + \Gamma\eta X + \varepsilon, \qquad \varepsilon \sim N(0, \Sigma), \tag{4.5}$$

where $\Sigma = \Gamma\Omega\Gamma^T + \Gamma_o\Omega_o\Gamma_o^T$, $\Omega \in \mathbb{R}^{u\times u}$ and $\Omega_o \in \mathbb{R}^{(r-u)\times(r-u)}$ are positive definite, and

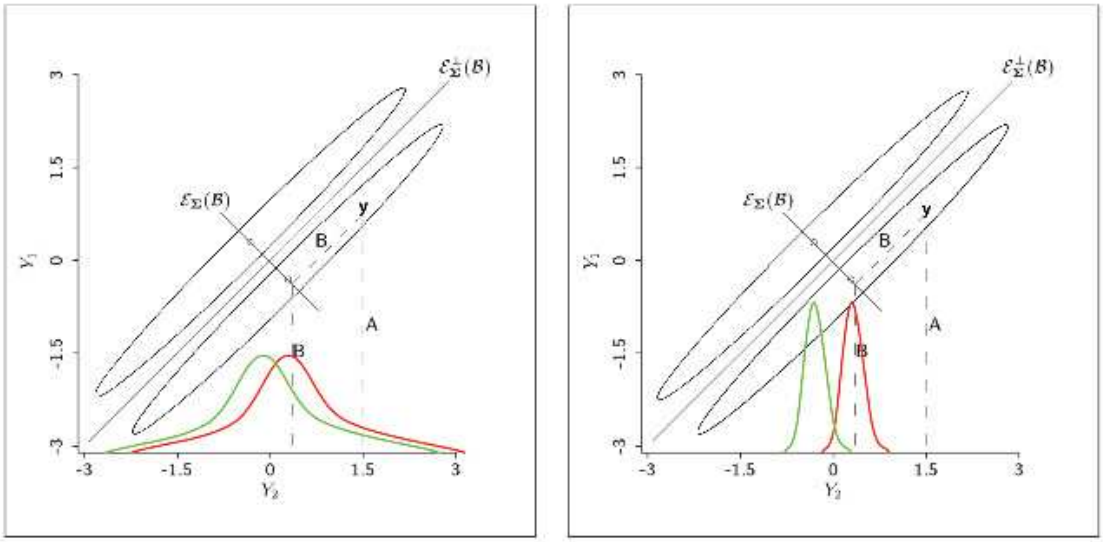

Figure 4.1: Visualization of the envelope model and the efficiency gains it is capable of producing.Graphic is taken from Su and Cook (2011).

$\eta \in \mathbb{R}^{u\times p}$ is $\beta = \Gamma\eta$ in the coordinates of Γ. We see from (4.5), that $\mathcal{E}_\Sigma(\mathcal{B})$ links the mean and covariance structures of the regression problem and it is this link that provides the efficiency gains. The gains can be massive when the immaterial information is large relative to the material information; for instance, when $\|\Omega\| \ll \|\Omega_o\|$, where $\|\cdot\|$ is a matrix norm (Cook, et al., 2010). Cook and Zhang (2015a) provided a more general framework for envelope methodology, which requires only a $\sqrt{n}$-consistent estimator $\hat{\theta}$ of an unknown parameter θ and a $\sqrt{n}$-consistent estimator of its asymptotic variability. Cook, et al. (2013) showed that partial least squares gives a moment-based envelope estimator that is $\sqrt{n}$-consistent. As partial least squares is widely used in chemometrics and elsewhere, the Cook, et al. (2013) finding indicates that envelope methodology is also widely applicable.

An illuminating depiction and explanation of how an envelope increases efficiency in multivariate linear regression problems was given by Su and Cook (2011, pgs. 134–135). We summarize some of that depiction here. To motivate intuition, consider Figure 4.1 taken from Su and Cook (2011). The data corresponding to Figure 4.1 comes from a population with two response variables and a single binary valued predictor. The predictor

variable indicates which subpopulation the responses are realized from. The two ellipses correspond to the contours of Σ for both predictor values. The standard analysis for the estimation of β_2, the second component of β, involves projecting the data clouds onto the horizontal axis. The left panel of Figure 4.1 shows that the two subpopulations can not be distinguished when this projection is made. The standard analysis will conclude that the two subpopulations are similar statistically. A greater sample size, possibly impractically large, is needed to determine statistical differences between these two subpopulations.

The right panel of Figure 4.1 shows the working mechanisms of the envelope structure. In this example $\Sigma \in \mathbb{R}^{2\times 2}$ and the parameter of interest resides within the smallest part of the spectral structure of Σ. Smallest means the eigenvector of Σ associated with the smallest eigenvalue. The span of this eigenvector is the envelope space, denoted $\mathcal{E}_\Sigma(\mathcal{B})$, where $B = \text{span}(\beta)$. In the envelope analysis, response values are projected into the envelope space and then projected onto the horizontal axis. We can now see a clear separation of the two subpopulations when this approach is employed.

Figure 4.1 provides a depiction of a scenario when envelope models provide efficiency gains for the estimation of β. The scope of envelope methodology was then expanded with the discovery of partial envelopes with the goal of variance reduction in the presence of nuisance parameters. Partial envelopes estimate "relevant" parameters using envelope methodology. The nuisance parameters are estimated using another conventional estimation approach. Partial envelopes are useful when the envelope estimator of the full coefficient matrix offers slight to no gains. These models can still discover massive efficiency gains when envelope methodology is restricted to the relevant parameters (Su and Cook, 2011).

All of these envelope modeling approaches extend from the general envelope framework outlined in Cook and Zhang (2015a). This general envelope framework, and its partial envelope analogue, is applicable to aster models. Once the intuition for general envelope model methodology is developed, its applications to aster models will be analyzed in detail. In order to use general envelope methodology one needs a $\sqrt{n}$ consistent estimator, $\hat{\varphi} \in \mathbb{R}^p$, $p > 1$, and knowledge of its asymptotic covariance matrix V_φ. In this setting we assume that for some $u \leq p$ there exists a subspace, call it $\mathcal{S}$, of V_φ of dimension u such that

a) $\text{span}(\varphi) \subset \mathcal{S}$

b) $V_\varphi = P_\mathcal{S} V_\varphi P_\mathcal{S} + Q_\mathcal{S} V_\varphi Q_\mathcal{S}$,

where $P_\mathcal{S}$ is the projection into the subspace $\mathcal{S}$ and $Q_\mathcal{S}$ is the projection into its orthogonal complement. Taken together, these conditions say that all the relevant information necessary for the estimation of φ is contained in $P_\mathcal{S} V_\varphi P_\mathcal{S}$. The above two conditions can be written in coordinate form. In coordinate form the two envelope model conditions are equivalent to,

a) $\text{span}(\varphi) \subset \text{span}(\Gamma)$

b) $V_\varphi = \Gamma \Omega \Gamma^T + \Gamma_o \Omega_o \Gamma_o^T$.

where $\Gamma \in \mathbb{R}^{p \times u}$ is a semi-orthogonal basis matrix for $\mathcal{E}$ satisfying $P_\mathcal{S} = \Gamma\Gamma^T$, Γ_o is the completion of Γ, $\Omega = \Gamma^T V_\varphi \Gamma$, $\Omega_o = \Gamma_o^T V_\varphi \Gamma_o$, and u is the dimension of the envelope. With u and $P_\mathcal{S}$ known we have two central limit theorem results,

$$\sqrt{n}(P_\mathcal{S}\hat{\varphi} - \varphi) \xrightarrow{d} N\left(0, P_\mathcal{S} V_\varphi P_\mathcal{S}\right),$$
$$\sqrt{n} Q_\mathcal{S} \hat{\varphi} \xrightarrow{d} N\left(0, Q_\mathcal{S} V_\varphi Q_\mathcal{S}\right),$$

which say that $P_\mathcal{S}\hat{\varphi}$ is asymptotically independent of $Q_\mathcal{S}\hat{\varphi}$. The V_φ envelope of φ, written as $\mathcal{E}_{V_\varphi}(\text{span}(\varphi))$ or $\mathcal{E}$ when convenient, is defined as the smallest space satisfying the two conditions above. It is the smallest reducing subspace of V_φ that contains $\text{span}(\varphi)$.

The cornerstone result from the framework of general envelope models as it applies to aster models is the sequential 1-dimension (1D for short) algorithm developed by Cook and Zhang (2015a,b). The sequential 1D algorithm, algorithm 2 in Cook and Zhang (2015a), provides an estimator of the semi-orthogonal basis matrix Γ that spans $\mathcal{E}$. It estimates Γ one dimension at a time, hence the name, by exploiting a powerful Lemma in envelope methodology. The algorithm requires $V_\varphi > 0$ (positive definite). The algorithm goes as follows. Let $g_k \in \mathbb{R}^p, k = 0, ..., u-1$ be the stepwise directions obtained. Let $G_k =$

$(g_1, ..., g_k)$, (G_k, G_{ok}) be an orthogonal basis matrix for $\mathbb{R}^p$, and set $g_o = G_o = 0$, then find

$$w_{k+1} = \arg\min_{w \in \mathbb{R}^{p-k}} J_k(w), \text{ subject to } w^T w = 1,$$
$$g_{k+1} = G_{ok} w_{k+1},$$

where $J_k(w) = \log(w^T G_{ok}^T V_\varphi G_{ok} w) + \log(w^T (G_{ok}^T (V_\varphi + U) G_{ok})^{-1} w)$ and $U = \varphi\varphi^T$ for $w \in \mathbb{R}^{p-k}$. It is a proposition that this algorithm returns a true basis matrix for the envelope when true parameter inputs are used (Cook, 2013, Proposition 6.3). The internal mechanism that makes the 1-d algorithm feasible is a key proposition in general envelope methodology (Cook, 2013, Proposition 5.7). This proposition says that

$$B_o \mathcal{E}_{B_o^T M B_o}(B_o^T \mathcal{S}) \subset \mathcal{E}_M(\mathcal{S})$$

where (B, B_o) is an orthogonal matrix and $\text{span}(B) \subset \mathcal{E}_M(\mathcal{S})$. So for every $v \in \mathcal{E}_{B_o^T M B_o}(B_o^T \mathcal{S})$ it is true that $B_o v \in \mathcal{E}_M(\mathcal{S})$. The sequential algorithm finds orthonormal vectors in $\mathcal{E}_M(\mathcal{B})$ one iteration at a time. At the first pass through the algorithm $G_o = I_p$ and the minimizer subject to the unit constraint, $\hat{w}_1$, of $\log(w^T V_\varphi w) + \log(w^T (V_\varphi + U)^{-1} w)$ is found. For this iteration $G_1 = g_1 = \hat{w}_1$ where $g_1 \in \mathcal{E}_M(\mathcal{S})$. For the second iteration, we construct G_{o1} orthogonal to g_1 and find the vector $\hat{w}_2$ that minimizes $J_1(w)$. Then we construct $g_2 = G_{o1}\hat{w}$ and $G_2 = (g_1, g_2)$. The vector $g_2 \in \mathcal{E}_M(\mathcal{S})$ and is orthogonal to g_1. The process is repeated until $k = u - 1$ and when finished, the algorithm returns $\Gamma = G_u = (g_1, g_2, ..., g_u)$. Γ consists of u orthonormal vectors all belonging to $\mathcal{E}$. Therefore, the 1-d algorithm returns a semi orthogonal basis matrix for $\mathcal{E}$ since $\mathcal{E}$ has dimension u. Once Γ is obtained, we can construct the projection into the envelope as $P_\mathcal{E} = \Gamma\Gamma^T$. The real utility of this algorithm comes from another proposition (Cook, 2013, Proposition 6.4). This proposition states that the 1-d algorithm returns a $\sqrt{n}$ consistent estimator of Γ when $\sqrt{n}$ consistent estimators $\hat{M}$ and $\hat{U}$ are used in place of M and U respectively.

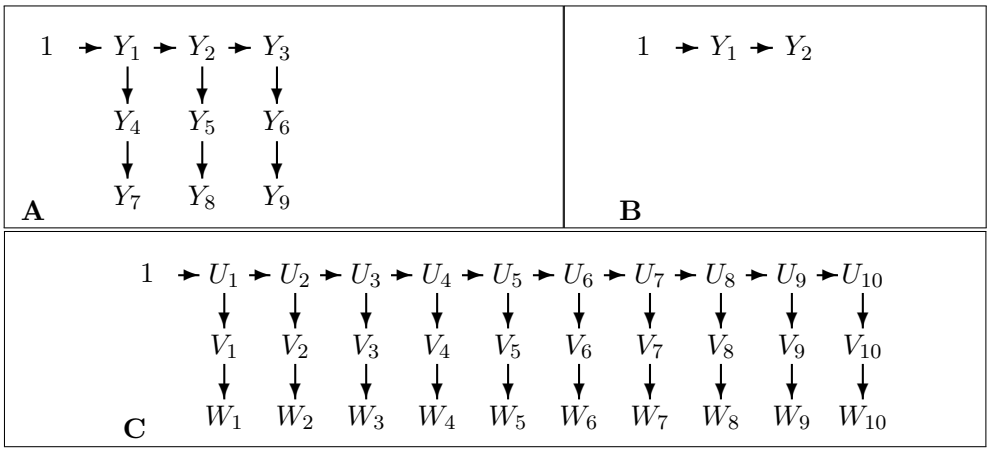

Figure 4.2: **(A)** Graphical structure of the aster model for one individual in the *E. angustifolia* data. The top layer corresponds to survival; these random variables are Bernoulli. The middle layer corresponds to flowering; these random variables are also Bernoulli. The bottom layer corresponds to flower head counts; these random variables are zero-truncated Poisson. **(B)** Graphical structure of the aster model for the data in Example 2. The first arrow corresponds to survival which is a Bernoulli random variable. The second arrow corresponds to reproduction count conditional on survival which is a zero-truncated Poisson random variable. **(C)** Graphical structure of the aster model for the simulated data in Example 1. The top layer corresponds to survival; these random variables are Bernoulli. The middle layer corresponds to whether or not an individual reproduced; these random variables are also Bernoulli. The bottom layer corresponds to offspring count; these random variables are zero-truncated Poisson.

4.4 Incorporation of general envelope methodology

The theory of general envelope methodology requires a $\sqrt{n}$ consistent and asymptotically normal estimator of an unknown parameter vector and a $\sqrt{n}$ consistent estimator of its asymptotic covariance matrix (Cook and Zhang, 2015a). Aster models, being an exponential family, satisfy these conditions. Our methods distinguish parameters of interest from nuisance parameters. The parameters of interest are those components of τ which correspond directly to the estimation of Darwinian fitness. We partition τ into $(\gamma^T, \upsilon^T)^T$ where $\gamma \in \mathbb{R}^{p-k}$ and $\upsilon \in \mathbb{R}^k$ are the vectors of nuisance parameters and parameters of interest respectively. Envelope models that involve this form of partitioning are referred to partial envelope models (Su and Cook, 2011). The maximum likelihood estimator of the parameters of interest, $\hat{\upsilon}$, has asymptotic covariance matrix $\Sigma_{\upsilon,\upsilon}$ which is the submatrix of Σ corresponding to the parameters of interest. The estimator of $\Sigma_{\upsilon,\upsilon}$ obtained from `aster` software is denoted by $\widehat{\Sigma}_{\upsilon,\upsilon}$.

Let $\mathcal{T} = \text{span}(\upsilon)$. The envelope subspace $\mathcal{E}_{\Sigma_{\upsilon,\upsilon}}(\mathcal{T})$ is defined as the intersection of all reducing subspaces of $\Sigma_{\upsilon,\upsilon}$ that contain T (a reducing subspace is a sum of eigenspaces). We will denote the envelope subspace as $\mathcal{E}$ when using it as a subscript. The envelope space satisfies both

1. $\mathcal{T} \subset \mathcal{E}_{\Sigma_{\upsilon,\upsilon}}(\mathcal{T})$
2. $\Sigma_{\upsilon,\upsilon} = P_{\mathcal{E}}\Sigma_{\upsilon,\upsilon}P_{\mathcal{E}} + Q_{\mathcal{E}}\Sigma_{\upsilon,\upsilon}Q_{\mathcal{E}}$

where $P_{\mathcal{E}}$ is the projection into the envelope subspace and $Q_{\mathcal{E}}$ is the projection into the orthogonal complement. In coordinate form, the two envelope conditions are equivalent to

a) $\mathcal{T} \subset \text{span}(\Gamma)$

b) $\Sigma_{\upsilon,\upsilon} = \Gamma\Omega\Gamma^T + \Gamma_o\Omega_o\Gamma_o^T$,

where (Γ, Γ_o) is a partitioned orthogonal matrix, the columns of Γ are a basis for $\mathcal{E}_{\Sigma_{\upsilon,\upsilon}}(\mathcal{T})$, and the dimensions of Ω and Ω_o are such that the matrix multiplications are defined.

The goal in envelope methodology is to estimate the basis matrix Γ of the envelope space $\mathcal{E}_{\Sigma_{\upsilon,\upsilon}}(\mathcal{T})$. The envelope space $\mathcal{E}_{\Sigma_{\upsilon,\upsilon}}(\mathcal{T})$ contains the parameter of interest and is a reducing

subspace of $\Sigma_{\upsilon,\upsilon}$. Intuitively, the envelope estimator reduces variability in estimation at no cost to consistency by making use of the defining properties of $\mathcal{E}_{\Sigma_{\upsilon,\upsilon}}(\mathcal{T})$. With the basis matrix Γ estimated, we can construct envelope estimators of υ and then map the resulting envelope estimators to the scale of Darwinian fitness. The variance reduction of estimated expected Darwinian fitness with respect to envelope estimation of υ is then assessed.

To gain intuition on the working mechanics of envelope methodology, consider the case when Γ is known beforehand. When Γ is known, the envelope estimator of υ is $P_{\mathcal{E}}\hat{\upsilon}$ with $P_{\mathcal{E}} = \Gamma\Gamma^T$, and

$$\sqrt{n}\left(P_{\mathcal{E}}\hat{\upsilon} - \upsilon\right) \xrightarrow{d} N\left(0, P_{\mathcal{E}}\Sigma_{\upsilon,\upsilon}P_{\mathcal{E}}\right).$$

Knowledge of $u = \dim\left(\mathcal{E}_{\Sigma_{\upsilon,\upsilon}}(\mathcal{T})\right)$ and $P_{\mathcal{E}}$ are both lacking in practice. Thus u and $P_{\mathcal{E}}$ are in need of estimation. The sequential 1D algorithm proposed in (Cook and Zhang, 2015a, Algorithm 2) estimates the basis matrix Γ for $\mathcal{E}_{\Sigma_{\upsilon,\upsilon}}(\mathcal{T})$ at u. The estimate of Γ is obtained by providing $\widehat{\Sigma}_{\upsilon,\upsilon}$ and $\hat{\upsilon}\hat{\upsilon}^T$ as inputs into the 1D algorithm. The resulting estimator of Γ obtained from the 1D algorithm, $\widehat{\Gamma}$, is $\sqrt{n}$ consistent and gives a $\sqrt{n}$ consistent estimator $P_{\hat{\mathcal{E}}}$ of the projection onto the envelope subspace $P_{\mathcal{E}}$ (Cook and Zhang, 2015a). The 1D algorithm finds the estimated basis $\widehat{\Gamma}$ by performing u optimizations. Each of these optimizations separately finds an estimated basis vector for the envelope subspace that is orthonormal to the basis vectors that preceded it.

We can compare envelope dimensions u by transforming envelope estimators $\hat{\upsilon}_{\text{env}} = P_{\hat{\mathcal{E}}}\hat{\upsilon}$ to the canonical parameterization where $P_{\hat{\mathcal{E}}}$ is obtained from the 1D algorithm at candidate values of u. The envelope estimator of τ is given as

$$\hat{\tau}_{\text{env}} = \begin{pmatrix} \widehat{\Gamma} \\ \hat{\upsilon}_{\text{env}} \end{pmatrix} = \begin{pmatrix} I & 0 \\ 0 & P_{\hat{\mathcal{E}}} \end{pmatrix} M^T Y = M_{\text{env}}^T Y$$

where

$$M_{\text{env}} = M \begin{pmatrix} I & 0 \\ 0 & P_{\hat{\mathcal{E}}} \end{pmatrix}$$

is the model matrix corresponding to the aster model that incorporates the partial envelope structure. The envelope estimator of τ is therefore a maximum likelihood estimate of the

mean-value parameter corresponding to the aster model with model matrix M_{env}. The fact that the envelope estimator of τ is also a maximum likelihood estimator is of importance. It justifies the use of the transformations seen in Figure 3.2 used to switch between MLEs of aster model parameterizations. However, the model matrix M_{env} is not of full column rank. This means that the transformations in Figure 3.2 are not 1-1. In particular, many distinct estimates of β map to $\hat{\tau}_{\text{env}}$. Each of these distinct estimated values of β maps to the same estimate of $\varphi = M_{\text{env}}\beta$, which in turn maps to a common estimate of expected Darwinian fitness.

The mapping $f : \tau \to \beta$ cannot be expressed in closed form and we must use the `aster2` package (Geyer, 2010) to carry out the transformation finding $\hat{\beta}_{\text{env}} = f(\hat{\tau}_{\text{env}})$. From here, likelihood based methods for comparing models such as AIC, BIC, or the likelihood ratio test (LRT) are used to select which envelope model dimension is appropriate. The LRT has the hypotheses:

$$H_o : u = u_o$$
$$H_a : u = k$$

where $u_o \leq k$ is some proposed dimension of $\mathcal{E}_{\Sigma_{v,v}}(\mathcal{T})$. (The alternative is use the aster model.) At the envelope dimension u or a larger dimension, we have

$$\sqrt{n}\left(\hat{v}_{\text{env}} - v\right) \xrightarrow{d} N\left(0,\ \Delta_1\right),$$

where Δ_1 is unknown. The asymptotic covariance matrix Δ_1 can be thought of as $\Delta_1 = P_{\mathcal{E}}\Sigma_{v,v}P_{\mathcal{E}} + C$ where $C > 0$ is the cost incurred from estimation.

However, inference with respect to v is not normally sought in life history analysis. What is sought, in this analysis, is the estimated expected Darwinian fitness considered as a function of phenotypic trait values for a hypothetical individual. This function is referred to as the fitness landscape when traits are continuous. In the setting of continuous traits, the fitness landscape is plotted. This plot is the primary graphical inferential tool for our analyses. The envelope estimator of expected Darwinian fitness for these hypothetical

individuals has asymptotic distributions given by

$$\sqrt{n}\left(g(\hat{\tau}_{\text{env}}) - g(\tau)\right) \xrightarrow{d} N\left(0,\ \nabla g(\tau)\Delta_2 \nabla g(\tau)^T\right), \tag{4.6}$$

where Δ_2 is the unknown asymptotic covariance matrix of $\hat{\tau}_{\text{env}}$. The asymptotic covariance matrix of estimated expected Darwinian fitness is estimated using a parametric bootstrap adjusting for model selection. The dimension of the envelope space is selected using model selection criteria and is not known in advance. Efron (2014, Section 4) provides a double bootstrap procedure which accounts for the randomness associated with model selection procedures. This double bootstrap procedure is used to estimate the variance of estimated expected Darwinian fitness using envelope methodology. At first, datasets are generated as a realization from the aster model distribution evaluated at the envelope estimator. The envelope dimension is determined for each of these generated datasets. The estimator of expected Darwinian fitness is then taken to be the average of all of the envelope estimators obtained from these datasets. To estimate the variability of this envelope estimator, we generate further datasets from the aster model distribution evaluated at each separate envelope estimator of expected Darwinian fitness used to calculate the aforementioned average. The steps of this procedure are presented in Algorithm 1 in Figure 4.3. More particulars on the application of the double bootstrap procedure outlined in Efron (2014) are included in the Discussion.

This algorithm requires that our aster model is fitted using a large enough sample size to provide a reliable maximum likelihood estimate of τ. This assumption is implicitly made when performing an aster analysis whether or not one incorporates an envelope model structure. When our bootstrap procedure has run for a total of B iterations we obtain the envelope estimator

$$\frac{1}{B}\sum_{b=1}^{B} g(\hat{\tau}_{\text{env}}^{(b)}) \tag{4.7}$$

as suggested by Efron (2014, Section 4). The individual summands in (4.7) are estimates of

1. Fit the aster model to the data and obtain $\hat{\upsilon}$ and $\widehat{\Sigma}_{\upsilon,\upsilon}$ from the aster model fit.

2. Compute the envelope estimator of υ in the original sample, given as $\hat{\upsilon}_{\text{env}} = P_{\hat{\mathcal{E}}}\hat{\upsilon}$ where $P_{\hat{\mathcal{E}}}$ is computed by the 1D algorithm. The 1D algorithm takes $M = \widehat{\Sigma}_{\upsilon,\upsilon}$, $U = \hat{\upsilon}\hat{\upsilon}^T$, and dimension u as inputs. The dimension is selected using a model selection criterion of choice.

3. Perform a parametric bootstrap by generating resamples from the distribution of the aster model evaluated at $\hat{\tau}_{\text{env}} = (\widehat{\gamma}^T, \hat{\upsilon}_{\text{env}}^T)^T$. For iteration $b = 1, ..., B$ of the procedure:

   (3a) Compute $\hat{\tau}^{(b)}$ and $\widehat{\Sigma}^{(b)}_{\upsilon,\upsilon}$ from the aster model fit to the resampled data.

   (3b) Obtain $P^{(b)}_{\hat{\mathcal{E}}}$ from the 1D algorithm as done in Step 2 using $M = \widehat{\Sigma}^{(b)}_{\upsilon,\upsilon}$ and $U = \hat{\upsilon}^{(b)}\hat{\upsilon}^{(b)^T}$ as inputs where the dimension of the envelope is selected using the same model selection criterion as Step 2.

   (3c) Compute $\hat{\upsilon}^{(b)}_{\text{env}} = P^{(b)}_{\hat{\mathcal{E}}}\hat{\upsilon}^{(b)}$ and $\hat{\tau}^{(b)}_{\text{env}} = \left(\widehat{\gamma}^{(b)^T}, \hat{\upsilon}^{(b)^T}_{\text{env}}\right)^T$

   (3d) Store $\hat{\tau}_{\text{env}^{(b)}}$ and $g\left(\hat{\tau}^{(b)}_{\text{env}}\right)$ where g maps τ to the parameterization of Darwinian fitness.

4. After B steps, the bootstrap estimator of expected Darwinian fitness is the average of the envelope estimators stored in Step 3d. This completes the first part of the bootstrap procedure.

5. We now proceed with the second level of bootstrapping at the b-th stored envelope estimator $\hat{\tau}^{(b)}_{\text{env}}$. For iteration $k = 1, ..., K$ of the procedure:

   (5a) Generate data from the distribution of the aster model evaluated at $\hat{\tau}^{(b)}_{\text{env}}$.

   (5b) Perform Steps 3a through 3c with respect to the dataset obtained in Step 5a.

   (5c) Store $\hat{\tau}^{(b)^{(k)}}_{\text{env}}$ and $g\left(\hat{\tau}^{(b)^{(k)}}_{\text{env}}\right)$.

Figure 4.3: Algorithm 1. Parametric bootstrap envelope estimation of υ using the 1D algorithm.

expected Darwinian fitness obtained after model selection. The averaging in (4.7) smooths out erratic jumpiness that may occur from model selection (Efron, 2014). The envelope estimator (4.7), obtained from the parametric bootstrap in Algorithm 1, has variability analogous to that in Efron (2014, equation (4.15)). As in Efron (2014), we define the matrix $\mathbf{B}^{(b)} \in \mathbb{R}^{K\times p}$ which has rows $\hat{\tau}_{\text{env}}^{(b)(k)} - \sum_{k=1}^{K} \hat{\tau}_{\text{env}}^{(b)(k)}/K$ and the matrix $C^{(b)} \in \mathbb{R}^{K\times d}$ which has columns $g\left(\hat{\tau}_{\text{env}}^{(b)(k)}\right) - g\left(\hat{\tau}_{\text{env}}^{(b)}\right)$. We now estimate Δ_2 with

$$\widehat{\Delta}_2 = \frac{1}{B}\sum_{b=1}^{B}\left(\widehat{\text{cov}}^{(b)}\right)^T \widehat{V}^{(b)^{-1}}\widehat{\text{cov}}^{(b)} \tag{4.8}$$

where

$$\widehat{\text{cov}}^{(b)} = \left(\mathbf{B}^{(b)}\right)^T C^{(b)}/K \tag{4.9}$$

and

$$\widehat{V}^{(b)} = \left(\mathbf{B}^{(b)}\right)^T \mathbf{B}^{(b)}/K. \tag{4.10}$$

The estimator (4.8) of Δ_2 takes into account the volatility of model selection when estimating the variability of estimated expected Darwinian fitness using envelope methodology. The method of maximum likelihood estimation does not have the added model selection step that envelope estimation has. The bootstrap procedure outlined in Figure 4.3 efficiently estimates expected Darwinian fitness and accounts for variability associated with model selection volatility.

4.5 A novel alternative to general envelope estimation using reducing subspaces

We propose a new way of constructing envelope estimators provided that the eigenvalues of $\Sigma_{v,v}$ are unique. Envelope estimators are constructed directly from the reducing subspaces

of $\widehat{\Sigma}_{\upsilon,\upsilon}$. This new envelope estimator of υ is $\hat{\upsilon}_{\text{env}} = P_{\widehat{G}}\hat{\upsilon}$ where G is the smallest reducing subspace of $\Sigma_{\upsilon,\upsilon}$ such that $P_G\upsilon = \upsilon$. The reducing subspaces of $\widehat{\Sigma}_{\upsilon,\upsilon}$ are $\sqrt{n}$ consistent estimators of the reducing subspaces of $\Sigma_{\upsilon,\upsilon}$. Therefore $P_{\widehat{G}}$, and the corresponding estimator $P_{\widehat{G}}\hat{\upsilon}$ are $\sqrt{n}$ estimators of P_G and $P_G\upsilon$ respectively. Our envelope estimator of τ becomes $\hat{\tau}_{\text{env}} = \left(\widehat{\gamma}^T, \hat{\upsilon}_{\text{env}}^T\right)^T$ where $\hat{\gamma}$ is the MLE of the nuisance parameters obtained from the original aster model fit.

There is a close connection between envelope estimation using reducing subspaces and envelope estimation using the 1D algorithm. In the population, the envelope estimator of υ using reducing subspaces is the same as the envelope estimator obtained from the 1D algorithm. The connection between both estimation methods exists in applications as well. Suppose that the envelope space is the reducing subspace G with dimension u and let $\widehat{\Gamma}_u$ and $\Gamma_{\widehat{G}}$ be the estimated basis matrices for the envelope space using the 1D algorithm and reducing subspaces respectively. Let $\widehat{O} = \widehat{\Gamma}_u\Gamma_{\widehat{G}}^T$ be the matrix that changes from the coordinates of $\Gamma_{\widehat{G}}$ to the coordinates of $\widehat{\Gamma}_u$. The matrix $\widehat{O}$ is a $\sqrt{n}$-consistent estimator of the identity matrix of dimension k. Let $\widehat{M} = \widehat{O}^T\widehat{\Sigma}_{\upsilon,\upsilon}\widehat{O}$ and $\widehat{U} = \widehat{O}^T\hat{\upsilon}\hat{\upsilon}^T\widehat{O}$. Then the 1D algorithm returns $\Gamma_{\widehat{G}}$ as an estimated basis matrix for the envelope space when using $\widehat{M}$ and $\widehat{U}$ as inputs. Asymptotic normality of $\hat{P}_{\widehat{G}}$ follows from (Cook and Zhang, 2015b, Propositions 5 and 6) since $\widehat{M}$ and $\widehat{U}$ are both $\sqrt{n}$-consistent estimators of $\Sigma_{\upsilon,\upsilon}$ and U respectively.

In applications, envelope estimators obtained from reducing subspaces of $\widehat{\Sigma}_{\upsilon,\upsilon}$ are compared using AIC, BIC, or the LRT. Our procedure for envelope estimation of expected Darwinian fitness using reducing subspaces of $\widehat{\Sigma}_{\upsilon,\upsilon}$ is as follows:

1. Start with $u = 1$ and compute $\hat{\upsilon}_{\text{env}} = P_{\widehat{G}}\hat{\upsilon}$ for all u dimensional reducing subspaces $\widehat{G}$.

2. Compare all envelope estimators constructed in step 1 to $\hat{\upsilon}$ using a selection criterion like AIC, BIC, or the LRT. If the envelope estimator is preferred, then stop and proceed with the analysis using the envelope estimator. If $\hat{\upsilon}$ is preferred, then return to Step 1 and iterate u when $u < k$. If $\hat{\upsilon}$ is preferred and $u = k$ then stop and proceed

with the analysis using the MLE.

3. Perform the parametric bootstrap procedure outlined in Algorithm 2.

If the dimension of the problem is small enough, one can simply bypass the above procedure and compute all reducing subspaces at once. We bypass this procedure in both of our examples since the dimension of the problem is small enough to do so. The envelope estimators with respect to all of the reducing subspaces can then be compared using AIC, BIC, and LRT in one step. In either scenario, the reducing subspace approach considers $2^k - k$ more candidate envelope estimators than the 1D algorithm does. For this reason the researcher must use the 1D algorithm when k is large.

Once a decision is made on which reducing subspace $\widehat{G}$ to use, we need to estimate the variability of the envelope estimator $\hat{\upsilon}_{\text{env}} = P_{\widehat{G}}\hat{\upsilon}$ using a parametric bootstrap. The steps for the parametric bootstrap employed are presented in Algorithm 2. Note that the reducing subspace $\widehat{G}$ is not used to build envelope estimators at each iteration of the parametric bootstrap procedure. The indices of the eigenvectors of $\widehat{\Sigma}_{\upsilon,\upsilon}$ that comprise the reducing subspace $\widehat{G}$ are used instead. At each iteration of the parametric bootstrap the estimate of $\Sigma_{\upsilon,\upsilon}$ changes which implies that the estimate of the reducing subspace G changes. The parametric bootstrap procedure outlined in Algorithm 2, seen in Figure 4.4, takes into account model selection volatility by implementing a double bootstrap procedure analogous to that in Efron (2014).

When our bootstrap procedure has run for a total of B iterations, we obtain the envelope estimator of expected Darwinian fitness given by (4.7) with covariance matrix Δ_2 estimated by (4.8).

Envelope estimators constructed using reducing subspaces are different than those constructed using the 1D algorithm. At any iteration of the 1D algorithm, minimizers of the objective function stated in (Cook and Zhang, 2015a, Algorithm 2) are pulled towards reducing subspaces of $\widehat{\Sigma}_{\upsilon,\upsilon}$. This objective function is non-convex and contains potentially many local minima. The optimizations conducted within the 1D algorithm are sensitive to starting values and can get stuck at these local minima. This undermines the 1D al-

1. Fit the aster model to the data and obtain $\hat{\upsilon}$ and $\widehat{\Sigma}_{\upsilon,\upsilon}$ from the aster model fit.

2. Compute the envelope estimator of υ in the original sample, given as $\hat{\upsilon}_{\text{env}} = P_{\widehat{G}}\hat{\upsilon}$ where $P_{\widehat{G}}$ is computed using reducing subspaces and selected via a model selection criterion of choice.

3. Perform a parametric bootstrap by generating resamples from the distribution of the aster model evaluated at $\hat{\tau}_{\text{env}} = (\widehat{\gamma}^T, \hat{\upsilon}_{\text{env}}^T)^T$. For iteration $b = 1, ..., B$ of the procedure:

   (3a) Compute $\hat{\tau}^{(b)}$ and $\widehat{\Sigma}_{\upsilon,\upsilon}^{(b)}$ from the aster model fit to the resampled data.

   (3b) Build $P_{\widehat{G}}^{(b)}$ using the indices of $\widehat{\Sigma}_{\upsilon,\upsilon}^{(b)}$ that are selected using the same model selection criterion as Step 2 to build $\widehat{G}$.

   (3c) Compute $\hat{\upsilon}_{\text{env}}^{(b)} = P_{\hat{\mathcal{E}}}^{(b)}\hat{\upsilon}^{(b)}$ and $\hat{\tau}_{\text{env}}^{(b)} = \left(\widehat{\gamma}^{(b)^T}, \hat{\upsilon}_{\text{env}}^{(b)^T}\right)^T$.

   (3d) Store $\hat{\tau}_{\text{env}^{(b)}}$ and $g\left(\hat{\tau}_{\text{env}}^{(b)}\right)$ where g maps τ to the parameterization of Darwinian fitness.

4. After B steps, the bootstrap estimator of expected Darwinian fitness is the average of the envelope estimators stored in Step 3d. This completes the first part of the bootstrap procedure.

5. We now proceed with the second level of bootstrapping at the b-th stored envelope estimator $\hat{\tau}_{\text{env}}^{(b)}$. For iteration $k = 1, ..., K$ of the procedure:

   (5a) Generate data from the distribution of the aster model evaluated at $\hat{\tau}_{\text{env}}^{(b)}$.

   (5b) Perform Steps 3a through 3d with respect to the dataset obtained in Step 5a.

   (5c) Store $\hat{\tau}_{\text{env}}^{(b)^{(k)}}$ and $g\left(\hat{\tau}_{\text{env}}^{(b)^{(k)}}\right)$.

Figure 4.4: Algorithm 2. Parametric bootstrap envelope estimation of υ using reducing subspaces.

gorithm since it is required that users find global minima for its justification. Unlike the 1D algorithm, the reducing subspace approach does not involve any optimization routines necessary to the construction of envelope estimators and is preferred in settings when k is small.

4.6 Examples

We now provide two examples of our methods. In Example 1, there is a true envelope model incorporated in the simulation of the dataset. In Example 2, we show that our methods yield efficiency gains in a real data example.

4.6.1 Example 1

A population of 3000 organisms was simulated to form the dataset used in this aster analysis. We generated data according to a known reducing subspace and show that our methods recover the true indices of the reducing subspace that generated the data. These data are generated according to the graphical structure appearing in panel C of Figure 4.2. There are two covariates (z_1, z_2) associated with Darwinian fitness and the aster model selected by the LRT is a full quadratic model with respect to these covariates. A full aster analysis of data of the same kind and its construction can be seen in Geyer and Shaw (2009).

In our example we consider the partial envelope approach. We partition τ into $(\gamma^T, \upsilon^T)^T$ where $\gamma \in \mathbb{R}^4$ are nuisance parameters and $\upsilon \in \mathbb{R}^5$ are relevant to the estimation of expected Darwinian fitness. Here, $\upsilon \in \mathbb{R}^5$ because our model is full quadratic in z_1 and z_2. The true reducing subspace is the space spanned by the first and fourth eigenvectors of the covariance matrix of the parameters of interest estimated from the original data. We begin by considering envelope estimators constructed using the 1D algorithm. AIC, BIC, and the LRT at $\alpha = 0.05$ all select $u = 5$. This selection is equivalent to supposing that no non-trivial envelope structure would be present and one should proceed with the aster analysis using maximum likelihood estimation and conventional `aster` software. The parametric bootstrap procedure discussed in Figure 4.3 is not interesting in this case. We now consider

$g(\hat{\tau}_{\text{env}})$	$\hat{se}\left(g(\hat{\tau}_{\text{env}})\right)$	$g(\hat{\tau}_{\text{MLE}})$	$\hat{se}\left(g(\hat{\tau}_{\text{MLE}})\right)$	ratio
8.556	0.174	8.701	0.260	1.491
9.014	0.111	8.939	0.135	1.222
7.817	0.414	8.054	0.442	1.069
9.174	0.163	9.193	0.170	1.045
9.018	0.113	9.120	0.128	1.133
8.612	0.162	8.518	0.278	1.709
7.761	0.215	8.096	0.331	1.534

Table 4.1: Comparison of the MLE and the partial envelope estimator for components of interest in Example 1. We can see that the envelope estimator is providing useful variance reduction.

envelope estimators constructed from reducing subspaces.

AIC, BIC, and the LRT at $\alpha = 0.05$ all select a reducing subspace that is the sum of more eigenspaces than the true reducing subspace but fewer eigenspaces than the full space. There is also some disagreement between the model selection criteria. BIC and the LRT at $\alpha = 0.05$ select the reducing subspace that is the sum of the first, fourth, and fifth eigenspaces of $\widehat{\Sigma}_{v,v}$, denoted $\widehat{G}_1$. AIC selects the reducing subspace that is the sum of every eigenspace of $\widehat{\Sigma}_{v,v}$ except for the third eigenspace, denoted $\widehat{G}_2$. The parametric bootstrap algorithm discussed in Figure 4.4 is used to estimate the asymptotic variability of $g(\hat{\tau}_{\text{env}})$ using the reducing subspace $\widehat{G}_1$. The results are seen in Table 4.1 for selected output. Table 4.1 shows points that yield high values of estimated expected Darwinian fitness. The first two columns display the sample envelope estimator of expected Darwinian fitness and its bootstrapped standard error. The MLE of expected Darwinian fitness and its bootstrapped standard error are displayed in the third and fourth columns respectively. The ratios of bootstrapped standard errors for $g(\hat{\tau}_{\text{MLE}})$ to $g(\hat{\tau}_{\text{env}})$ are displayed in the final column. We can see that all of the ratios are greater than 1 which indicates that the envelope estimator of expected Darwinian fitness is less variable than the maximum likelihood estimator.

Contour plots of the ratios of estimated standard errors are displayed in Figure 4.5. These contour plots show that the envelope estimator of expected Darwinian fitness is less

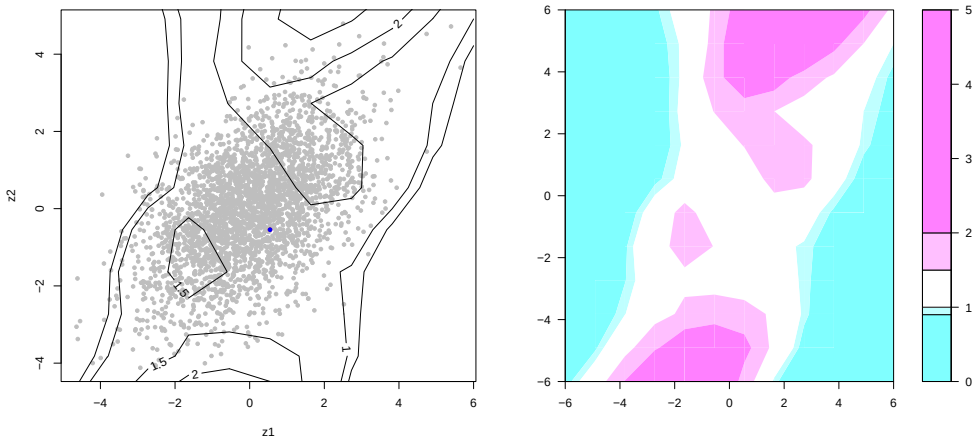

Figure 4.5: Contour plots for the ratios of $\mathrm{se}\,(h(\hat{\tau}))$ to $\mathrm{se}\,(h(\hat{\tau}_{\mathrm{env}}))$ in Example 1. Ratios greater than 1 indicate efficiency gains using envelope methodology.

variable than the maximum likelihood estimator for the majority of the observed data. The region where the envelope estimator is less variable includes the values of z_1 and z_2 that maximize estimated expected Darwinian fitness. Variance reduction is also obtained when we use the reducing subspace suggested by AIC. This is shown in Eck, et al. (2016a).

4.6.2 Example 2

In this example we apply our envelope methods to a real aster dataset. The data comes from Lowry and Willis (2010) and the study in which the data is obtained investigates the role of chromosomal inversions in adaptation and speciation. Phenotypic traits and covariates are recorded for 2313 yellow monkeyflowers, *Mimulus guttatus*. The lifecycle of the individual *M. guttatus* flowers is depicted in panel B of Figure 4.2. The covariates of interest include genetic background, field site, inversion orientation, and ecotype of the flower. All of the considered covariates are categorical. We fit the model with main effects only and find substantial gains with our methods. There are eight predictors in total and we partition τ into $(\gamma^T, \upsilon^T)^T$ where $\gamma \in \mathbb{R}^2$ are nuisance parameters and $\upsilon \in \mathbb{R}^6$ are relevant to the estimation of expected Darwinian fitness. AIC, BIC, and the LRT at $\alpha = 0.05$ all select a

$g(\hat{\tau}_{\text{env}})$	$\hat{se}\left(g(\hat{\tau}_{\text{env}})\right)$	$g(\hat{\tau}_{\text{MLE}})$	$\hat{se}\left(g(\hat{\tau}_{\text{MLE}})\right)$	ratio
9.646	0.326	9.171	0.642	1.973
8.640	0.300	8.887	0.369	1.230
7.659	0.315	7.603	0.361	1.144
7.517	0.539	7.010	0.649	1.205
10.943	0.607	10.475	0.896	1.476
7.329	0.707	6.618	1.038	1.469
7.498	0.521	7.522	0.658	1.263

Table 4.2: Comparison of the MLE and the partial envelope estimator for components of interest in Example 2. We can see that the envelope estimator is providing useful variance reduction.

reducing subspace that is the sum of all eigenspaces of $\widehat{\Sigma}_{\upsilon,\upsilon}$ with the exception of the fourth and fifth eigenspaces. The bootstrap procedure given in Figure 4.4 is used to estimate the variability of the envelope estimator of $\hat{\upsilon}$ accounting for uncertainty in model selection. Table 4.2 shows points that yield high values of estimated expected Darwinian fitness. We can see that all of the ratios are greater than 1 which indicates that the envelope estimator of expected Darwinian fitness is less variable than the maximum likelihood estimator. Contour plots are given in Figure 4.6.

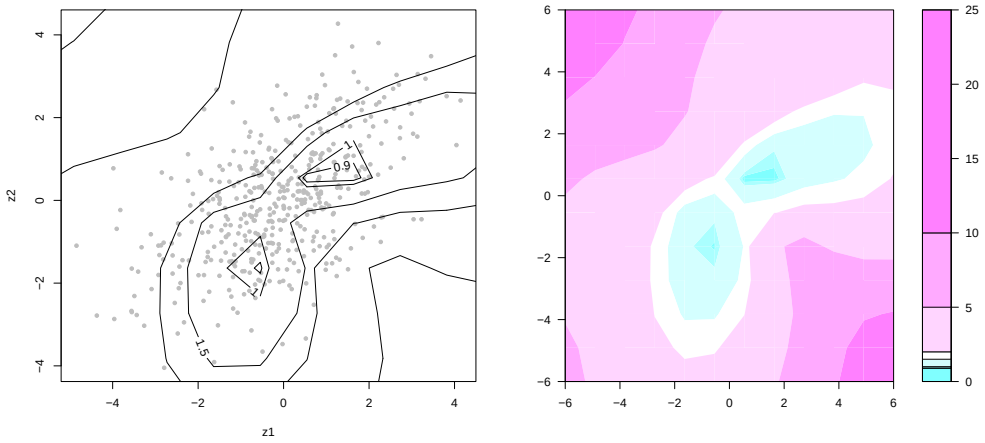

Figure 4.6: Contour plots for the ratios of $\text{se}\,(h(\hat{\tau}))$ to $\text{se}\,(h(\hat{\tau}_{\text{env}}))$ in Example 2. Ratios greater than 1 indicate efficiency gains using envelope methodology.

4.7 Envelope methods with respect to β

As already discussed, the aster model mean-value parameter τ is closely associated with mean-value parameter μ, see Figure 3.2 and consult Geyer (2010) for more details about the six aster model parameterizations. One could also perform envelope methodology to estimate model canonical parameter vector β, which possesses the same dimension as τ. In our experience, envelope methodology with respect to β is computationally faster.

The computational benefit of using envelope methodology with respect to β is countered by an important drawback. Aster model theory is developed to handle the relation between β and relevant predictors in the form of an affine model. Therefore, the canonical parameter vector β is not well-defined, one can shift β with an arbitrarily chosen offset vector without changing the value of the mean-value parameters τ and μ. Envelope methodology is not invariant to this form of arbitrary shifting. It is true that `aster` and `aster2` software have a default way of picking offsets. However, the conventions of `aster` and `aster2` differ and experienced users of this software can also change offsets as they see fit. It should be noted that τ can also be shifted via an arbitrarily chosen offset vector. However, when one changes

τ in this manner, one changes the definition of Darwinian fitness. Darwinian fitness, and surrogates to Darwinian fitness that are used in its place, are well-defined quantities.

4.8 Software

This chapter is accompanied by an `R` package `envlpaster` (Eck, 2015) and a technical report (Eck, et al., 2016a). This technical report reproduces the examples in this chapter and shows how functions in the `envlpaster` package are used.

4.9 Discussion

There are two types of errors that can be made when constructing envelope estimators and these two errors have very different consequences. The first error we could make is picking an envelope dimension smaller than the truth. Conditional on this dimension, the resulting envelope estimator is no longer consistent, and the first defining condition of the envelope space is violated. Alternatively, an envelope dimension larger than the truth can be chosen. Conditional on this type of dimension, the envelope estimator is consistent but it will have higher variability than the envelope estimator constructed from the true envelope dimension. Efficiency gains are still possible in this setting as seen in the first example.

The consequences of potential model selection errors served as the motivation for the implementation of the bootstrap procedure in Efron (2014). However, this particular choice of a bootstrap procedure is not without flaws. Hjort (2014) mentions that Efron does not derive the distribution of the final estimator, given by (4.7) in our context. The literature has not reached a consensus on the appropriate bootstrap procedure to be implemented when bootstrapping depends on data-driven model selection. Berk, et al. (2013) provides an estimation framework that is valid under all model selection criteria, but the degree of conservatism guaranteed in Berk, et al. (2013) is not required in our setting. Other applications of envelope methodology may require this degree of conservatism. As the literature currently stands, Efron (2014) provides a reasonable solution to the problem of potential model selection errors in the application of envelope methodology to aster models.

Our software also provides functions implementing bootstrap procedures not accounting for model selection.

The new envelope estimator constructed from reducing subspaces is seen to perform better than the envelope estimator constructed from the 1D algorithm in our first example. This new envelope estimator does not involve any non-convex optimization routines that are both sensitive to starting values and have potential problems with local minima. The underlying theory of the 1D algorithm justifies the consistency of our new envelope estimator. In envelope modeling problems with a small number of parameters of interest, possibly outside of our aster modeling context, the envelope estimator constructed from reducing subspaces has the potential to yield efficiency gains without the present worries of the current envelope estimation techniques.

In many life history analyses, specific trait values which are estimated to produce the highest expected Darwinian fitness are of interest. It is common practice to only report such trait values (Shaw and Geyer, 2010; Eck, et al., 2015a). Such reporting ignores the variability associated with the estimation of expected Darwinian fitness. There are likely many trait values having estimated expected Darwinian fitness that is statistically indistinguishable from the reported values. Our methodology addresses this concern directly. The potential set of candidate traits maximizing expected Darwinian fitness is smaller when the combination of envelope methodology into the aster modeling framework is utilized as seen in the accompanying technical report.

The aster model has been solely applied to problems in life history analysis. However, the aster model is a general statistical model which can analyze datasets outside of the life history context. The aster model itself is a generalization of the generalized linear model (Shaw, Geyer, Wagenius, Hangelbroek, and Etterson, 2008) and survival models (Geyer, Wagenius, and Shaw, 2007). The aster model is appropriate for any graphical modeling problem meeting the assumptions A1-A5 or the more general assumptions of Geyer, et al. (2007).

Our main emphasis is to show that expected Darwinian fitness can be estimated with lower variability through the incorporation of general envelope methodology with respect

to aster model parameters. A combination of the theories of aster and envelope models show that lower variability in estimation is obtainable. Our examples offer further support to our claims. The envelope estimator of expected Darwinian fitness is seen to be usefully less variable than the MLE. The variance reduction of estimated expected Darwinian fitness obtained through our methodology has the potential to be massive. Researchers using our methods will be able to draw strong inferences about expected Darwinian fitness through our variance reduction techniques.

Supplementary Materials

The accompanying technical report is available at the UMN Digital Conservancy (Eck, et al., 2016a). The calculations in the accompanying technical report are facilitated by the R package `envlpaster` (Eck, 2015).

Chapter 5

Weighted Envelope Methodology

5.1 Introduction

Envelope methodology was developed originally in the context of the multivariate linear regression model (Cook, et al., 2010),

$$Y = \alpha + \beta X + \varepsilon, \tag{5.1}$$

where $\alpha \in \mathbb{R}^r$, $\beta \in \mathbb{R}^{r\times p}$, the random response vector $Y \in \mathbb{R}^r$, the fixed predictor vector $X \in \mathbb{R}^p$ is centered to have mean zero, and the error vector $\varepsilon \sim N(0, \Sigma)$. Estimation is assumed to be based on n independent samples from model (5.1) where $n > p$. It was shown by Cook, et al. (2010) that the envelope estimator of the unknown coefficient matrix β in (5.1) has the potential to yield massive efficiency gains relative to the maximum likelihood estimator of β. These efficiency gains can arise when the dimension u of the envelope space, defined in the next section, is less than r. In most practical applications, u is unknown and has to be estimated. This estimation can be problematic since the estimated variance of the envelope estimator is typically calculated conditional on the estimated dimension $\hat{u}$. Variation associated with model selection is therefore not considered in the current envelope paradigm.

We propose a weighted envelope estimator of β that smooths out model selection volatility. The weighting is across all possible envelope models under (5.1). The weights corre-

sponding to each envelope estimator are functions of the Bayesian Information Criterion (BIC) value corresponding to that particular envelope model. Weighting in this manner is similar to the model averaging techniques discussed by Buckland, et al. (1997) and Burnham and Anderson (2004) who provided a philosophical justification for the use of such weighted estimators without giving any theoretical properties. Hjort and Claeskens (2003) and Liang, et al. (2011) built on the philosophical justification for weighted estimators by deriving their asymptotic properties. Claeskens and Hjort (2008) summarized extensions and applications of the theory of weighted estimators. However, these extensions do not include bootstrap techniques and do not encompass the framework of envelope models. Envelope models fit at dimensions greater than or equal to u are all true non-nested data generating models and are ordered in preference from dimension u to r. This context seems novel and is outside of the framework of Claeskens and Hjort (2008).

Candidate envelope estimators of β at dimension j, denoted $\hat{\beta}_j$, are found via maximum likelihood estimation of model (4.5) with $\hat{\beta}_j = \widehat{\Gamma}\hat{\eta}$. An estimator of u is found by using a model selection criterion such as BIC, Akaike Information Criterion (AIC), likelihood ratio tests, or cross-validation. The estimated dimension $\hat{u}$ obtained from any one of these selection criteria is a variable quantity dependent on the observed data. Current envelope methodology does not address this extra variability. In the next two sections, we develop properties of a weighted estimator that takes this extra variability into account.

5.2 bic Weighted Estimators

The weighted estimator that we consider is of the form

$$\hat{\beta}_w = \sum_{j=1}^{r} w_j \hat{\beta}_j, \tag{5.2}$$

where $\sum_{j=1}^{r} w_j = 1$ and $w_j \geq 0$, for $j = 1, ..., r$. The weights w_j depend on the BIC values for all of the candidate envelope models under consideration. Let the BIC value for the envelope model with dimension j be denoted by $b_j = -2l(\hat{\beta}_j) + k(j)\log(n)$, where $l(\hat{\beta}_j)$ is

the log likelihood evaluated at the envelope estimator $\hat{\beta}_j$ and $k(j) = r + pj + r(r+1)/2$ is the number of parameters of the envelope model of dimension j. The weight for envelope model j is constructed as

$$w_j = \frac{\exp(-b_j)}{\sum_{k=1}^{r} \exp(-b_k)}. \tag{5.3}$$

It follows from arguments in the Supplement that $\hat{\beta}_w$ is a $\sqrt{n}$-consistent estimator of β, but assessing the variance of $\hat{\beta}_w$ is not so straightforward. In the next section, we show that the residual bootstrap provides a consistent estimator of $\text{Var}(\hat{\beta}_u)$. We use BIC in (5.3) because, in ours and others' experiences, BIC performs well when selecting the dimension of an envelope model. AIC tends to overselect the true dimension of an envelope model, likelihood ratio testing is inconsistent, and cross-validation is primarily used in prediction problems. We do not claim that BIC is optimal in this application.

5.3 Bootstrap for $\hat{\beta}_w$

The envelope estimator $\hat{\beta}_u$ at the true dimension u is $\sqrt{n}$-consistent and asymptotically normal (Cook, et al., 2010; Cook and Zhang, 2015a). The residual bootstrap used to estimate the variability of $\hat{\beta}_u$ uses the starred responses,

$$Y^* = \mathbb{X}\hat{\beta}_u^T + \varepsilon^*, \tag{5.4}$$

to obtain $\hat{\beta}_u^*$, where $\mathbb{X} \in \mathbb{R}^{n\times p}$ is the fixed design matrix with rows X_i^T and the rows of $\varepsilon^* \in \mathbb{R}^{n\times r}$ are the realizations of n resamples of the residuals from the ordinary least squares fit of (5.1). This process is performed a total of B times with a new $\hat{\beta}_u^*$ computed from (5.4) at each iteration. The setup in Andrews (2002, Section 2, pgs. 122-124 and Theorem 2) confirms that the sample variance of the $\hat{\beta}_u^*$s provides a $\sqrt{n}$-consistent estimator of the asymptotic variability of $\hat{\beta}_u$. The problem with this approach, as it currently stands, is that u is unknown. The current implementation of the residual bootstrap implicitly assumes that $\hat{u} = u$. Therefore, variability introduced by model selection uncertainty is ignored.

This issue is resolved by using $\hat{\beta}_w$ in place of $\hat{\beta}_u$ in (5.4). The next theorem formalizes our asymptotic justification for the use of the weighted envelope estimator $\hat{\beta}_w$ in practical problems. Its proof is given in the Supplement.

Theorem 12

Assume regression model (5.1) and suppose that an envelope subspace of dimension $u = 1, ..., r$ exists. Assume that $\widehat{\Sigma}_X = n^{-1}\mathbb{X}^T\mathbb{X} \to \Sigma_X > 0$. Let $\hat{\beta}_w$ be the weighted envelope estimator of β defined in (5.2) and let $\hat{\beta}_w^*$ be the weighted envelope estimator of β obtained from resampled data. Then, as n tends to ∞,

$$\begin{aligned}\sqrt{n}\left\{\text{vec}(\hat{\beta}_w^*) - \text{vec}(\hat{\beta}_w)\right\} &= \sqrt{n}\left\{\text{vec}(\hat{\beta}_u^*) - \text{vec}(\hat{\beta}_u)\right\} \\ &+ O_p\left\{n^{(1/2-p)}\right\} + 2(u-1)O_p(1)\sqrt{n}e^{-n|O_p(1)|}.\end{aligned} \tag{5.5}$$

□

Proof: We go through the steps showing that (5.5) holds. Recall that $u = \dim(\mathcal{E})$. Define $l(\hat{\beta}_j)$ to be the log likelihood of the envelope model evaluated at the envelope estimator $\hat{\beta}_j$, fitting with $\dim(\mathcal{E}) = j$, and define $k(j)$ to be the number of parameters of the envelope model of dimension j. From the construction of b_j and the above calculations we see that

$$e^{b_u - b_j} = e^{-2\{l(\hat{\beta}_u) - l(\hat{\beta}_j)\}} n^{-\{k(j)-k(u)\}}.$$

Let b_j^* be the BIC value of the envelope model of dimension j fit to the starred data and define

$$w_j^* = \frac{e^{-b_j^*}}{\sum_{k=1}^r e^{-b_k^*}}.$$

Let $\|\cdot\|$ be the Euclidean norm. We show that $\sqrt{n}\left\{w_j^*\text{vec}(\hat{\beta}_j^*) - w_j\text{vec}(\hat{\beta}_j)\right\} \to 0$ for $j \neq u$ by showing that

$$\sqrt{n}\|w_j^*\text{vec}(\hat{\beta}_j^*) - w_j\text{vec}(\hat{\beta}_j)\| \;\leq\; \sqrt{n}\|w_j^*\text{vec}(\hat{\beta}_j^*)\| + \sqrt{n}\|w_j\text{vec}(\hat{\beta}_j)\| \;\to\; 0$$

as $n \to \infty$ for all $j \neq u$. Now,

$$\begin{aligned}\sqrt{n}w_j\|\text{vec}(\hat{\beta}_j)\| &\leq \sqrt{n} \mid O_p(1) \mid e^{b_u - b_j} \\ &= \mid O_p(1) \mid n^{\{k(u)-k(j)+1/2\}} e^{-2\left\{l(\hat{\beta}_u)-l(\hat{\beta}_j)\right\}} \\ &= \mid O_p(1) \mid n^{\{k(u)-k(j)+1/2\}} e^{2\left\{l(\hat{\beta}_r)-l(\hat{\beta}_u)\right\}-2\left\{l(\hat{\beta}_r)-l(\hat{\beta}_j)\right\}}.\end{aligned} \tag{5.6}$$

The first inequality in (5.6) follows from the fact that $\|\text{vec}(\hat{\beta}_j)\| \leq \|\text{vec}(\hat{\beta}_r)\|$ and $\|\text{vec}(\hat{\beta}_r)\| = O_p(1)$. We first consider the case where $j = u+1, ..., r$. In this setting, models with envelope dimensions u and j are both true and nested within the full model with envelope dimension r. Consequently, $-2\{l(\hat{\beta}_u) - l(\hat{\beta}_r)\}$ and $-2\{l(\hat{\beta}_j) - l(\hat{\beta}_r)\}$ are asymptotically distributed as $\chi^2_{p(r-u)}$ and $\chi^2_{p(r-j)}$ by Wilks' Theorem. Therefore $e^{-2\{l(\hat{\beta}_u)-l(\hat{\beta}_j)\}} = O_p(1)$ since it is the exponentiation of the difference between two χ^2 random variables. We see that

$$\sqrt{n}w_j\|\text{vec}(\hat{\beta}_j)\| \leq \mid O_p(1) \mid n^{\{k(u)-k(j)+1/2\}} = O_p\left[n^{\{k(u)-k(j)+1/2\}}\right].$$

Since $j > u$, we have that $k(u) - k(j) = p(u - j) \leq -p$. Thus,

$$\sqrt{n}w_j\|\text{vec}(\hat{\beta}_j)\| \leq O_p\left\{n^{(1/2-p)}\right\}$$

for $j = u + 1, ..., r$. Following the same steps as (5.6), applied to the starred data, yields

$$\sqrt{n}w_j^*\|\text{vec}(\hat{\beta}_j^*)\| \leq \mid O_p(1) \mid n^{\{k(u)-k(j)+1/2\}} e^{-2\left\{l^*(\hat{\beta}_u^*)-l^*(\hat{\beta}_r^*)\right\}+2\left\{l^*(\hat{\beta}_j^*)-l^*(\hat{\beta}_r^*)\right\}} \tag{5.7}$$

where $l^*(\cdot)$ is the log likelihood function corresponding to the starred data.

Both $-2\left\{l^*(\hat{\beta}_u^*) - l^*(\hat{\beta}_r^*)\right\}$ and $2\left\{l^*(\hat{\beta}_j^*) - l^*(\hat{\beta}_r^*)\right\}$ in (5.7) are $O_p(1)$. Thus,

$$\sqrt{n}w_j\|\text{vec}(\hat{\beta}_j^*)\| \leq \mid O_p(1) \mid n^{\{k(u)-k(j)+1/2\}} = O_p\left[n^{\{k(u)-k(j)+1/2\}}\right],$$

and, $\sqrt{n}w_j\|\text{vec}(\hat{\beta}_j^*)\| \leq O_p\left\{n^{(1/2-p)}\right\}$ for all $j = u + 1, ..., r$. This establishes that

$$\sqrt{n}\|w_j^*\text{vec}(\hat{\beta}_j^*) - w_j\text{vec}(\hat{\beta}_j)\| \leq O_p\left\{n^{(1/2-p)}\right\},$$

for $j = u+1, ..., r$.

Turning to the case when $j = 1, ..., u-1$, consider the exponent $e^{-\lambda_j}$, with $\lambda_j = 2\left\{l(\hat{\beta}_r) - l(\hat{\beta}_j)\right\}$. This is a log likelihood ratio although, unlike the case when $j = u+1, ..., r$, it does not follow a χ^2 distribution asymptotically. Let $\widehat{G}$ and $\widehat{G}_o$ be the estimated bases for the envelope space and its orthogonal complement fitting with dimension $j = 1, ..., u-1$, so $\widehat{G} \in \mathbb{R}^{r\times j}$ and $\widehat{G}_o \in \mathbb{R}^{r\times(r-j)}$. We write

$$\begin{aligned}
\lambda_j &= 2\left\{l(\hat{\beta}_r) - l(\hat{\beta}_j)\right\} \\
&= n\log \mid \widehat{G}^T\widehat{\Sigma}_{\text{res}}\widehat{G} \mid + n\log \mid \widehat{G}_o^T\widehat{\Sigma}_Y\widehat{G}_o \mid - n\log \mid \widehat{\Sigma}_{\text{res}} \mid \\
&= n\log \mid \widehat{G}^T\widehat{\Sigma}_{\text{res}}\widehat{G} \mid + n\log \mid \widehat{G}_o^T\widehat{\Sigma}_{\text{res}}\widehat{G}_o \mid - n\log \mid \widehat{\Sigma}_{\text{res}} \mid \\
&\qquad + n\log \mid I_p + \widehat{\Sigma}_X^{1/2}\hat{\beta}_r^T\widehat{G}_o\left(\widehat{G}_o^T\widehat{\Sigma}_{\text{res}}\widehat{G}_o\right)^{-1}\widehat{G}_o^T\hat{\beta}_r\widehat{\Sigma}_X^{1/2} \mid
\end{aligned} \tag{5.8}$$

where $\widehat{\Sigma}_Y = n^{-1}\mathbb{Y}^T\mathbb{Y}$. The second equation in (5.8) follows by applying the usual expansion of the determinant of a sum of the form $A + BB^T$. To see this,

$$\begin{aligned}
\mid \widehat{G}_o^T\widehat{\Sigma}_Y\widehat{G}_o \mid &= \mid \widehat{G}_o^T\widehat{\Sigma}_{\text{res}}\widehat{G}_o + \widehat{G}_o^T\mathbb{Y}^T\mathbb{X}(\mathbb{X}^T\mathbb{X})^{-1}\mathbb{X}^T\mathbb{Y}\widehat{G}_o \mid \\
&= \mid \widehat{G}_o^T\widehat{\Sigma}_{\text{res}}\widehat{G}_o + \widehat{G}_o^T\hat{\beta}_r\widehat{\Sigma}_X\hat{\beta}_r^T\widehat{G}_o \mid \\
&= \mid \widehat{G}_o^T\widehat{\Sigma}_{\text{res}}\widehat{G}_o \mid \times \mid I_p + \widehat{\Sigma}_X^{1/2}\hat{\beta}_r^T\widehat{G}_o\left(\widehat{G}_o^T\widehat{\Sigma}_{\text{res}}\widehat{G}_o\right)^{-1}\widehat{G}_o^T\hat{\beta}_r\widehat{\Sigma}_X^{1/2} \mid,
\end{aligned}$$

where

$$\widehat{G}_o^T\hat{\beta}_r\widehat{\Sigma}_X\hat{\beta}_r^T\widehat{G}_o = \widehat{G}_o^T\mathbb{Y}^T\mathbb{X}(\mathbb{X}^T\mathbb{X})^{-1}\mathbb{X}^T\mathbb{Y}\widehat{G}_o$$

because of the definition of $\hat{\beta}_r = \mathbb{Y}^T\mathbb{X}(\mathbb{X}^T\mathbb{X})^{-1}$.

We bound λ_j from below by further minimizing the first three addends in (5.8) over $(\widehat{G}, \widehat{G}_o)$. These are minimized globally when the columns of $\widehat{G}$ span any reducing subspace

of $\widehat{\Sigma}_{\text{res}}$ and is 0 at the minimum. Thus

$$\begin{aligned}\lambda_j &\geq n \log \mid I_p + \widehat{\Sigma}_X^{1/2} \hat{\beta}_r^T \widehat{G}_o \left(\widehat{G}_o^T \widehat{\Sigma}_{\text{res}} \widehat{G}_o \right)^{-1} \widehat{G}_o^T \hat{\beta}_r \widehat{\Sigma}_X^{1/2} \mid \\ &= n \log \mid I_p + \widehat{\Sigma}_X^{1/2} \hat{\beta}_r^T \widehat{\Sigma}_{\text{res}}^{-1/2} \left\{ \widehat{\Sigma}_{\text{res}}^{1/2} \widehat{G}_o \left(\widehat{G}_o^T \widehat{\Sigma}_{\text{res}} \widehat{G}_o \right)^{-1} \widehat{G}_o^T \widehat{\Sigma}_{\text{res}}^{1/2} \right\} \widehat{\Sigma}_{\text{res}}^{-1/2} \hat{\beta}_r \widehat{\Sigma}_X^{1/2} \mid \quad (5.9) \\ &= n \log(\widehat{A}_{j,n}),\end{aligned}$$

where $\widehat{A}_{j,n}$ is defined implicitly. The quantity $\widehat{\Sigma}_{\text{res}}^{1/2} \widehat{G}_o \left(\widehat{G}_o^T \widehat{\Sigma}_{\text{res}} \widehat{G}_o \right)^{-1} \widehat{G}_o^T \widehat{\Sigma}_{\text{res}}^{1/2}$ in (5.9) is the projection into the column space of $\widehat{\Sigma}_{\text{res}}^{1/2} \widehat{G}_o$. The quantity $\widehat{G}_o^T \hat{\beta}_r \neq 0$ almost surely since $j = 1, ..., u-1$. As a result, the column space of $\widehat{\Sigma}_{\text{res}}^{-1/2} \hat{\beta}_r \widehat{\Sigma}_X^{1/2}$ in (5.9) has a nontrivial intersection with the column space of $\widehat{\Sigma}_{\text{res}}^{1/2} \widehat{G}_o$ almost surely. Therefore $\widehat{A}_{j,n} > 1$ almost surely. We can write $n \log(\widehat{A}_{j,n}) = n \mid O_p(1) \mid$ and we have the bound

$$e^{-\lambda_j} = e^{-2\{l(\hat{\beta}_j) - l(\hat{\beta}_r)\}} \leq e^{-n \log(\widehat{A}_{j,n})} = e^{-n|O_p(1)|}.$$

Therefore,

$$\begin{aligned}\log(w_j) &\leq b_u - b_j \\ &= -2\{l(\hat{\beta}_u) - l(\hat{\beta}_r)\} + 2\{l(\hat{\beta}_j) - l(\hat{\beta}_r)\} + \{k(u) - k(j)\} \log(n) \\ &= |O_p(1)| - \lambda_j + \{k(u) - k(j)\} \log(n) \\ &\leq |O_p(1)| - n \mid O_p(1) \mid + \{k(u) - k(j)\} \log(n) = -n \mid O_p(1) \mid\end{aligned} \quad (5.10)$$

and we see that $\sqrt{n} w_j \leq \sqrt{n} e^{-n|O_p(1)|}$ for $j = 1, ..., u-1$.

Define $\widehat{G}_o^*$ to be the estimate of G_o obtained from the starred data and let

$$\begin{aligned}A_{j,n}^* =& \mid I_p + \widehat{\Sigma}_X^{1/2} \hat{\beta}_r^{*T} \widehat{G}_o^* \left(\widehat{G}_o^{*T} \widehat{\Sigma}_{\text{res}}^* \widehat{G}_o^* \right)^{-1} \widehat{G}_o^{*T} \hat{\beta}_r^* \widehat{\Sigma}_X^{1/2} \mid \\ =& \mid I_p + \widehat{\Sigma}_X^{1/2} \hat{\beta}_r^{*T} \widehat{\Sigma}^{*-1/2} \left\{ \widehat{\Sigma}^{*1/2} \widehat{G}_o^* \left(\widehat{G}_o^{*T} \widehat{\Sigma}_{\text{res}}^* \widehat{G}_o^* \right)^{-1} \widehat{G}_o^{*T} \widehat{\Sigma}^{*1/2} \right\} \times \\ & \widehat{\Sigma}^{*-1/2} \hat{\beta}_r^* \widehat{\Sigma}_X^{1/2} \mid\end{aligned} \quad (5.11)$$

The same logic that applied to $\widehat{A}_{j,n}$ applies to $A^*_{j,n}$. The quantity

$$\widehat{\Sigma}^{*1/2}\widehat{G}^*_o\left(\widehat{G}^{*T}_o\widehat{\Sigma}^*_{\text{res}}\widehat{G}^*_o\right)^{-1}\widehat{G}^{*T}_o\widehat{\Sigma}^{*1/2}$$

in (5.11) is the projection onto the column space of $\widehat{\Sigma}^{*1/2}\widehat{G}^*_o$. The quantity $\widehat{G}^{*T}_o\hat{\beta}^*_r \neq 0$ almost surely since $j = 1, ..., u-1$. As a result, the column space of $\widehat{\Sigma}^{*-1/2}\hat{\beta}^*_r\widehat{\Sigma}^{1/2}_X$ in (5.11) has a nontrivial intersection with the column space of $\widehat{\Sigma}^{*1/2}\widehat{G}^*_o$ almost surely. Therefore $A^*_{j,n} > 1$ almost surely. The steps in (5.10), applied to the starred data, yields

$$\sqrt{n}w^*_j \leq \sqrt{n}e^{-n|O_p(1)|}. \tag{5.12}$$

Thus,

$$\begin{aligned}\sqrt{n}\|w^*_j\text{vec}(\hat{\beta}^*_j) - w_j\text{vec}(\hat{\beta}_j)\| &\leq \sqrt{n}\|w^*_j\text{vec}(\hat{\beta}^*_j)\| + \sqrt{n}\|w_j\text{vec}(\hat{\beta}_j)\| \\ &\leq \sqrt{n}e^{-n|O_p(1)|}\|\text{vec}(\hat{\beta}^*_j)\| + \sqrt{n}e^{-n|O_p(1)|}\|\text{vec}(\hat{\beta}_j)\| \\ &= 2O_p(1)\sqrt{n}e^{-n|O_p(1)|}\end{aligned}$$

for $j = 1, ..., u-1$ where $\|\text{vec}(\hat{\beta}_j)\|$ and $\|\text{vec}(\hat{\beta}^*_j)\|$ are both $O_p(1)$ just as in the $j = u+1, ..., r$ case. Combining all of these term yields the $2(u-1)O_p(1)\sqrt{n}e^{-n|O_p(1)|}$ order in (5.5). This completes the proof when $j = 1, ..., u-1$.

The final case is when $j = u$. Let $E_n = \sum_{i\neq u}^r e^{b_u - b_i}$. We can write $w_u = \frac{1}{1+E_n} = 1 - \frac{E_n}{1+E_n}$. The term $E_n = O_p\left(n^{-p}\right)$ since $e^{-n|O_p(1)|} = O_p\left(n^{-p}\right)$. Therefore

$$\begin{aligned}\sqrt{n}w^*_u\text{vec}(\hat{\beta}^*_u) &= \sqrt{n}\left(1 - \frac{E_n}{1+E_n}\right)\text{vec}(\hat{\beta}^*_u) \\ &= \sqrt{n}\text{vec}(\hat{\beta}^*_u) + O_p\left\{n^{(1/2-p)}\right\}, \\ \sqrt{n}w_u\text{vec}(\hat{\beta}_u) &= \sqrt{n}\left(1 - \frac{E_n}{1+E_n}\right)\text{vec}(\hat{\beta}_u) \\ &= \sqrt{n}\text{vec}(\hat{\beta}_u) + O_p\left\{n^{(1/2-p)}\right\}.\end{aligned}$$

Adding the previous results over j to form $\sqrt{n}\left\{\text{vec}(\hat{\beta}_w^*) - \text{vec}(\hat{\beta}_w)\right\}$ yields the result given in (5.5) This completes the proof. □

Theorem 12 shows the utility of the weighted envelope estimator $\hat{\beta}_w$. In (5.5), we see that the asymptotic distribution of the residual bootstrap at $\hat{\beta}_w$ is the same as the asymptotic distribution of the residual bootstrap at $\hat{\beta}_u$. The difference between the two bootstrap procedures is that the bootstrap given in Theorem 12 does not require the conditioning on $\hat{u}$ as a prerequisite for its implementation.

The orders in (5.5) result from model selection variability that arises from four sources. The $O_p\left\{n^{(1/2-p)}\right\}$ term corresponds to the rate at which $\sqrt{n}w_j$ and $\sqrt{n}w_j^*$ vanish for $j = u+1, ...r$. This rate is a cost of overestimation of the envelope space. It decreases quite fast, particularly when p is not small, because models with $j > u$ are true and thus have no systematic bias due to choosing the wrong dimension.

The $2(u-1)\sqrt{n}e^{-n|O_p(1)|}$ term corresponds to the rate at which $\sqrt{n}w_j$ and $\sqrt{n}w_j^*$ vanish for $j = 1, ..., u-1$. This rate arises from under estimating the envelope space and it is affected by systematic bias arising from choosing the wrong dimension. To gain intuition about this rate, let $B_j = \left(G_o^T\Sigma G_o\right)^{-1/2} G_o^T\beta\Sigma_X^{1/2}$, where $G_o \in \mathbb{R}^{r\times(r-j)}$ is the population basis matrix for the complement of the envelope space of dimension j. This quantity is a standardized version of $G_o^T\beta$ that reflects bias, since $G_o^T\beta \neq 0$ when $j < u$, but $G_o^T\beta = 0$ when $j \geq u$. Let $\widehat{B}_{j,n}$ denote the $\sqrt{n}$-consistent estimator of B_j obtained by plugging in the sample version of Σ_X and the estimators of G_o, Σ and β that arise by maximizing the likelihood with dimension $j < u$. Then the $-n \mid O_p(1) \mid$ term appearing in the exponent of $2(u-1)\sqrt{n}e^{-n|O_p(1)|}$ is the rate at which $-n\log(\mid I_p + \widehat{B}_{j,n}^T\widehat{B}_{j,n} \mid)$ approaches $-\infty$. Additionally, this term is 0 when $u = 1$. That arises because we consider only regressions in which $\beta \neq 0$ and thus $u \geq 1$. When $u = 1$ underestimation is not possible in our context and thus $2(u-1)\sqrt{n}e^{-n|O_p(1)|}$ vanishes.

The weights in (5.3) differ from those mentioned in Burnham and Anderson (2004) which were also advocated by Kass and Raftery (1995) and Tsague (2014). These weights

are of the form

$$\tilde{w}_j = \frac{\exp(-b_j/2)}{\sum_{k=1}^{r} \exp(-b_k/2)} \tag{5.13}$$

and they correspond to an approximation of the posterior probability for model j given the observed data under the prior that places equal weight for all candidate models. Weights of the form (5.13) do not have the same asymptotic properties as the weights given by (5.3). When $p = 1$, the term $\sqrt{n}\tilde{w}_{j=u+1}$ defined by (5.13) does not vanish as $n \to \infty$. We therefore would not have the same asymptotic result given by (5.5) in Theorem 12. Instead, there would be non-zero weight placed on the envelope model with dimension $j = u + 1$ asymptotically. This weighting scheme would therefore lead to higher estimated variability than is necessary in practice. However, this issue is no longer problematic when $p > 1$. When $p > 1$ and weights (5.13) are used, the $O_p\left\{n^{(1/2-p)}\right\}$ term in (5.5) becomes $O_p\left\{n^{(1-p)/2}\right\}$, resulting in a slower rate of convergence.

Constructing $\hat{\beta}_w$ with respect to BIC may not be the only weighting scheme that satisfies

$$\sqrt{n}\left\{\text{vec}(\hat{\beta}_w^*) - \text{vec}(\hat{\beta}_w)\right\} = \sqrt{n}\left\{\text{vec}(\hat{\beta}_u^*) - \text{vec}(\hat{\beta}_u)\right\} + O_p\left\{f(p,n)\right\} \tag{5.14}$$

where $f(p, n)$ is a function that depends on how the weights are constructed. Any weighting scheme such that, for all $j \neq u$,

$$\sqrt{n}\left\{\text{vec}(\hat{\beta}_j^*) - \text{vec}(\hat{\beta}_j)\right\} \to 0 \tag{5.15}$$

as $n \to \infty$ satisfies (5.14). Weighting schemes that violate (5.15) will not result in a bootstrap that is consistent.

Similar weights with AIC in place of BIC do not satisfy (5.15). Interchanging BIC with AIC in the proof of Theorem 12 produces weights of the form $w_j =\mid O_p(1) \mid e^{2\{k(u)-k(j)\}}$ for all $j = u + 1, ..., r$ which do not vanish as $n \to \infty$.

5.4 Examples

We now provide three examples which show the utility of Theorem 12. The first two are simulated examples in which we know β, Σ, u, and $\mathcal{P}_{\mathcal{E}_\Sigma(\mathcal{B})}$. The third is based on real data.

5.4.1 Simulated examples

Example 1: For this example we create a setting in which $Y \in \mathbb{R}^3$ is generated according to the model

$$Y_i = \beta X_i + \varepsilon_i, \qquad \varepsilon_i \overset{ind}{\sim} N(0, \Sigma), \tag{5.16}$$

$(i = 1, ..., n)$, where $X_i \in \mathbb{R}^2$ is a continuous predictor with entries generated independently from a normal distribution with mean 4 and variance 1. The covariance matrix Σ was generated using three orthonormal vectors and has eigenvalues of 50, 10, and 0.01. The matrix $\beta \in \mathbb{R}^{3\times 2}$ is an element in the space spanned by the second and third eigenvectors of Σ. We know that the dimension of $\mathcal{E}_\Sigma(\mathcal{B})$ is $u = 2$.

	$n = 50$	$n = 100$	$n = 500$	$n = 2000$
$\|\text{vec}(\hat{\beta}_w) - \text{vec}(\hat{\beta}_{u=2})\|_2$	2.3	0.016	≈ 0	≈ 0
$\|\widehat{\text{Var}}(\hat{\beta}_w^* - \hat{\beta}_{u=2})\|$	0.18	0.12	0.021	0.0051

Table 5.1: Comparison of $\hat{\beta}_w$ and $\hat{\beta}_{u=2}$. The first row is the Euclidean difference between $\text{vec}(\hat{\beta}_w)$ and $\text{vec}(\hat{\beta}_{u=2})$ from the original dataset. The second row is the spectral norm of the estimated variance of the difference of all bootstrap realizations of $\hat{\beta}_w^*$ and $\hat{\beta}_{u=2}$ with bootstrap sample size $B = n$.

Four datasets were simulated under model (5.16) at different sample sizes. The multivariate residual bootstrap was used to compare the weighted envelope estimator $\hat{\beta}_w$ with the oracle envelope estimator $\hat{\beta}_{u=2}$ across the simulated datasets. In Table 5.1, we see that the Euclidean difference of $\text{vec}(\hat{\beta}_{u=2})$ and $\text{vec}(\hat{\beta}_w)$ shrinks as n increases, and that the spectral norm of the variance of differences also shrinks as n increases. Taken together, these findings support the conclusions of Theorem 12.

Example 2: For this example we illustrate the effect that p has on the performance of the

weighted envelope estimator. We generated data according to model (5.16) with $Y \in \mathbb{R}^5$. In this example $u = 1$ and Σ is compound symmetric with diagonal entries set to 1 and off-diagonal entries set to 0.5, $\beta = 1_r c_p^T$, where 1_r is the $r \times 1$ vector of ones, and c_p is a $p \times 1$ vector where every entry is 10. We generate the predictors according to $X \sim N(0, I_p)$, where I_p is the p-dimensional identity matrix. We set $n = 250$.

We then perform a residual bootstrap with sample size $B = 250$ and, for each p considered, we report the number of times each dimension was selected by BIC, denoted by $n(\hat{u})$. From Table 5.2, we see that the distribution of $\hat{u}$, across the B resamples, approaches a point mass at the truth as p increases with u fixed. This implies that our bootstrap procedure improves as p increases with u fixed, as indicated by Theorem 12.

	$n(\hat{u}=1)$	$n(\hat{u}=2)$	$n(\hat{u}=3)$
$p=2$	128	111	11
$p=5$	214	34	2
$p=10$	249	1	0
$p=25$	250	0	0

Table 5.2: The bootstrap distribution of $\hat{u}$ as p increases, where $\hat{u}$ is selected by BIC and $n(\hat{u} = j)$ is the number of times BIC selected envelope dimension j.

5.4.2 Cattle data

The data in this example, analyzed in Kenward (1987) and Cook and Zhang (2015a), came from an experiment that compared two treatments for the control of a parasite in cattle. The experimenters were interested in finding if the treatments had differential effects on weight and, if so, about when they first occurred. There were sixty animals in this experiment and thirty animals were randomly assigned to the two treatments. Their weights (in kilograms) were then recorded at weeks 2, 4,..., 18 and 19 after treatment (Kenward, 1987). In our analysis, we considered the multivariate linear model (5.1), where $Y_i \in \mathbb{R}^{10}$ is the vector of cattle weights from week 2 to week 19, and predictor X_i is either 0 or 1 indicating which of the two treatments was assigned. In this model, α is the mean profile for one treatment and β is the mean difference between the two treatments.

Since the two treatments were not expected to have an immediate measurable effect on weight, some linear combinations of the response vector are not expected to depend on the treatment. Therefore the envelope model (4.5) is expected to perform well in this application because of our belief that (4.4) holds with $\mathcal{E}_{\Sigma}^{\perp}(\mathcal{B})$ at least as large as the span of the linear combinations that isolate the first few elements of the response vector.

Envelope models were fitted at each dimension from 1 to 10. The likelihood ratio test selected $\hat{u} = 1$ and BIC selected $\hat{u} = 3$ as the dimension of the envelope model. Further complicating matters, when BIC is used to determine u at every resample of the multivariate residual bootstrap with sample size $B = 60$, we see high variability in the models selected. Specifically, $n(\hat{u} = 1) = 10$, $n(\hat{u} = 2) = 10$, $n(\hat{u} = 3) = 24$, $n(\hat{u} = 4) = 12$, and $n(\hat{u} = 5) = 4$. Model selection variability of this variety is precisely the reason why the weighted envelope estimator is advocated.

In Table 5.3, we see the ratios of bootstrapped estimated standard errors for envelope estimators to those of the maximum likelihood estimator of the β from the full model (5.1), $\text{se}^*(\hat{\beta}_r)/\text{se}^*(\hat{\beta}_w)$, averaged across 25 replications. Standard errors of the averaged ratios across replications are all less than 7% of the reported ratios and the average standard error is 2.6% of the reported ratio. A complete table that includes standard errors for all of the averaged ratios is included in the Supplementary Materials. Ratios greater than 1 indicate that the envelope estimator is more efficient than the standard estimator. We see that $\hat{\beta}_w$ is comparable to $\hat{\beta}_{u=3}$. Similar conclusions are drawn from the other elements of estimates of β. The findings displayed in Table 5.3 illustrate that the weighted envelope estimator can provide useful efficiency gains while properly accounting for model selection variability.

B	$\hat{\beta}_w$	$\hat{\beta}_{u=1}$	$\hat{\beta}_{u=2}$	$\hat{\beta}_{u=3}$	$\hat{\beta}_{u=4}$	$\hat{\beta}_{u=5}$
60	1.98	5.54	3.05	1.69	1.31	1.23
100	1.97	5.54	2.55	1.54	1.32	1.21
500	1.82	5.47	2.78	1.57	1.31	1.16
2000	1.81	5.37	2.60	1.53	1.29	1.16

Table 5.3: Averaged ratios of estimated standard errors across 25 replications of the multivariate residual bootstrap at different numbers of resamples B for the fifth element of estimates of β.

We next report results of a simulation study using the cattle data to show further support for Theorem 12. We generate data according to the model

$$Y_i = \alpha + \beta X_i + \varepsilon_i, \qquad \varepsilon_i \overset{ind}{\sim} N(0, \Sigma),$$

$(i = 1, ..., n)$ where α, β, and Σ were set to the estimates obtained from the envelope model fit to the cattle data at dimension $u = 3$, and X_i is the binary indicator that specified treatment. Cows are split evenly between the two treatment groups and the assignment was random.

In Table 5.4, we see that the Euclidean differences between $\text{vec}(\hat{\beta}_{u=3})$ and $\text{vec}(\hat{\beta}_w)$ shrink as n increases. The same is true for the differences between $\text{vec}(\hat{\beta}_{u=4})$ and $\text{vec}(\hat{\beta}_w)$. This was expected since the envelope model fit with $u = 4$ is a true data generating model. However, we see that the Euclidean distance between $\text{vec}(\hat{\beta}_{u=2})$ and $\text{vec}(\hat{\beta}_w)$ does not shrink as n increases. Again, this was expected since the envelope model fit with $u = 2$ is not a true data generating model. These simulation results are in alignment with the conclusions of Theorem 12.

	$n = 60$	$n = 100$	$n = 500$	$n = 2000$
$\|\text{vec}(\hat{\beta}_w) - \text{vec}(\hat{\beta}_{u=2})\|_2$	9.36	0.83	0.91	4.2
$\|\text{vec}(\hat{\beta}_w) - \text{vec}(\hat{\beta}_{u=3})\|_2$	9.37	0.54	0.070	0.00028
$\|\text{vec}(\hat{\beta}_w) - \text{vec}(\hat{\beta}_{u=4})\|_2$	9.37	0.69	0.34	0.090

Table 5.4: Comparison of $\hat{\beta}_w$ and $\hat{\beta}_{u=2}$, $\hat{\beta}_{u=3}$, and $\hat{\beta}_{u=4}$. The rows are the Euclidean difference between $\text{vec}(\hat{\beta}_w)$ and the indicated envelope estimator from the original dataset.

5.5 Discussion

Efron (2014) proposed an estimator motivated by bagging (Breimen, 1996) that aims to reduce variability and smooth out discontinuities resulting from model selection volatility. Variability of the model averaged estimator of Efron (2014) is assessed via a double bootstrap. These techniques have been applied to envelope methodology in Eck, et al. (2017)

and useful variance reduction was found empirically. The problem of interest in Eck, et al. (2017) falls outside the scope of the multivariate linear regression model, and general envelope methodology (Cook and Zhang, 2015a) was required to obtain efficiency gains. n the context of the multivariate linear regression model, we showed that only a single level of bootstrapping is necessary.

The idea of weighting envelope estimators across all candidate dimensions extends to partial least squares (Cook, et al., 2013), predictor envelopes (Cook and Su, 2016), and sparse response envelopes (Su, et al., 2016).

Chapter 6

Bootstraping for Multivariate Linear Regression Models

6.1 Introduction

The linear regression model is an important and useful tool in many statistical analyses for studying the relationship among variables. Regression analysis is primarily used for predicting values of the response variable at interesting values of the predictor variables, discovering the predictors that are associated with the response variable, and estimating how changes in the predictor variables affects the response variable (Weisberg, 2005). The standard linear regression methodology assumes that the response variable is a scalar. However, it may be the case that one is interested in investigating multiple response variables simultaneously. One could perform a regression analysis on each response separately in this setting. Such an analysis would fail to detect associations between responses. Regression settings where associations of multiple responses is of interest require a multivariate linear regression model for analysis.

Bootstrapping techniques are well understood for the linear regression model with a univariate response (Bickel and Freedman, 1981; Freedman, 1981). In particular, theoretical justification for the residual bootstrap as a way to estimate the variability of the ordinary least squares (OLS) estimator of the regression coefficient vector in this model has been developed (Freedman, 1981). Theoretical extensions of residual bootstrap techniques appropriate for the multivariate linear regression model have not been formally introduced.

The existence of such an extension is stated without proof and rather implicitly in subsequent works (Freedman and Peters, 1984; Diaconis and Efron, 1983). In this article we show that the bootstrap procedures in Freedman (1981) provide consistent estimates of the variability of the OLS estimator of the regression coefficient matrix in the multivariate linear regression model. Our proof technique follows similar logic as Freedman (1981). The generality of the bootstrap theory developed in Bickel and Freedman (1981) provide the tools required for our extension to the multivariate linear regression model.

6.2 Bootstrap for the multivariate linear regression model

The multivariate linear regression is

$$Y_i = \beta X_i + \varepsilon_i, \quad (i = 1, ..., n), \tag{6.1}$$

where $Y_i \in \mathbb{R}^r$ and $r > 1$ in order to have an interesting problem, $\beta \in \mathbb{R}^{r \times p}$, $X_i \in \mathbb{R}^p$, and the ε_i's are errors having mean zero and variance Σ where $\Sigma > 0$. It is assumed that separate realizations from the model (6.1) are independent. We further define $\mathbb{X} \in \mathbb{R}^{n \times p}$ as the design matrix with rows X_i^T, $\mathbb{Y} \in \mathbb{R}^{n \times r}$ is the matrix of responses with rows Y_i^T, and $\varepsilon \in \mathbb{R}^{n \times r}$ is the matrix of all errors with rows ε_i^T. The OLS estimator of β in model (6.1) is $\hat{\beta} = \mathbb{Y}^T\mathbb{X}(\mathbb{X}^T\mathbb{X})^{-1}$. We let $\widehat{\varepsilon} \in \mathbb{R}^{n \times r}$ denote the matrix of residuals consisting of rows $\widehat{\varepsilon}_i^T = (Y_i - \hat{\beta}X_i)^T$. The multivariate linear regression model assumed here is slightly different than the traditional multivariate linear regression model. The traditional model makes the additional assumptions that the errors are normally distributed and the design matrix $\mathbb{X}$ is fixed.

We consider two bootstrap procedures that consistently estimate the asymptotic variability of $\text{vec}(\hat{\beta})$ under different assumptions placed upon the model (6.1). The first bootstrap procedure is appropriate when the design matrix $\mathbb{X}$ is assumed to be fixed and the errors are homoscedastic. In this setup, residuals are resampled. The second bootstrap procedure is appropriate when $(X_i^T, \varepsilon_i^T)^T$ are realizations from a joint distribution. In this setup, cases $(X_i^T, Y_i^T)^T$ are resampled. It is known that bootstrapping under these setups

provides a consistent estimator of the variability of $\mathrm{Var}(\hat{\beta})$ in model (6.1) when $r = 1$ (Freedman, 1981). We now provide the needed extensions.

6.2.1 Fixed design

We first establish the residual bootstrap of Freedman (1981) when $\mathbb{X}$ is assumed to be a fixed design matrix. Resampled, starred, data is generated by the model

$$\mathbb{Y}^* = \mathbb{X}\hat{\beta}^T + \varepsilon^*, \tag{6.2}$$

where $\varepsilon^* \in \mathbb{R}^{n\times r}$ is the matrix of errors with rows being independent with common distribution $\widehat{F}_n$, the empirical distribution of the residuals, centered at their mean, from the original dataset. Now $\hat{\beta}^* = {\mathbb{Y}^*}^T \mathbb{X}(\mathbb{X}^T\mathbb{X})^{-1}$ is the OLS estimator of β from the starred data. This process is performed a total of B times with a new estimator $\hat{\beta}^*$ computed from (6.2) at each iteration. We then estimate the variability of $\mathrm{vec}(\hat{\beta})$ with

$$\mathrm{Var}^*\left\{\mathrm{vec}(\hat{\beta})\right\} = (B-1)^{-1}\sum_{b=1}^{B}\left\{\mathrm{vec}(\hat{\beta}_b^*) - \mathrm{vec}(\bar{\beta}^*)\right\}\left\{\mathrm{vec}(\hat{\beta}_b^*) - \mathrm{vec}(\bar{\beta}^*)\right\}^T$$

where $\hat{\beta}_b^*$ is the residual bootstrap estimator of β at iteration b and $\bar{\beta}^* = B^{-1}\sum_{b=1}^{B}\hat{\beta}_b^*$.

Before the theoretical justification of the residual bootstrap is formally given, some important quantities are stated. The residuals from the regression (6.2) are $\varepsilon^* = \mathbb{Y}^* - \mathbb{X}{\hat{\beta}^*}^T$. The variance-covariance matrix Σ in model (6.1) is then estimated by

$$\widehat{\Sigma} = n^{-1}\sum_{i=1}^{n}\widehat{\varepsilon}_i\widehat{\varepsilon}_i^T - \hat{\mu}^2, \qquad \hat{\mu}^2 = \left(n^{-1}\sum_{i=1}^{n}\widehat{\varepsilon}_i\right)\left(n^{-1}\sum_{i=1}^{n}\widehat{\varepsilon}_i\right)^T.$$

Likewise, the variance-covariance estimate from the starred data is

$$\widehat{\Sigma}^* = n^{-1}\sum_{i=1}^{n}\widehat{\varepsilon}_i^*\widehat{\varepsilon}_i^{*T} - {\hat{\mu}^*}^2, \qquad {\hat{\mu}^*}^2 = \left(n^{-1}\sum_{i=1}^{n}\widehat{\varepsilon}_i^*\right)\left(n^{-1}\sum_{i=1}^{n}\widehat{\varepsilon}_i^*\right)^T.$$

Theorem 1 provides bootstrap asymptotics for the regression model (6.1). It extends The-

orem 2.2 of Freedman (1981) to the multivariate setting.

Theorem 13

Assume the regression model (6.1) where the errors have finite fourth moments. Suppose that $n^{-1}\mathbb{X}^T\mathbb{X} \to \Sigma_X > 0$. Along almost all sample paths $Y_1, ..., Y_n$, as n tends to ∞,

a) the distribution of $\sqrt{n}\left\{\text{vec}(\hat{\beta}^*) - \text{vec}(\hat{\beta})\right\}$ converges weakly to a normal distribution with mean 0 and variance-covariance matrix given by $\Sigma_X^{-1} \otimes \Sigma$.

b) the sequence $\widehat{\Sigma}^*$ converges to Σ in probability.

c) the distribution of $\left\{(\mathbb{X}^T\mathbb{X})^{1/2} \otimes \widehat{\Sigma}^{*^{-1/2}}\right\}\left\{\text{vec}(\hat{\beta}^*) - \text{vec}(\hat{\beta})\right\}$ converges to a standard normal distribution in $\mathbb{R}^{rp}$. □

The proof of Theorem 13, along with the details of several necessary lemmas and theorems, are included in the theoretical details section. Theorem 13 establishes the multivariate analogue for the residual bootstrap. This theorem shows that standard error estimation of the estimated β matrix obtained through bootstrapping, is $\sqrt{n}$-consistent. Now let $f : \mathbb{R}^{rp} \to \mathbb{R}^k$ be a differentiable function. Then the conclusions of Theorem 13 can be applied to establish a multivariate delta method based on estimates obtained via the residual bootstrap. This immediately follows from a first order Taylor expansion and some algebra arriving at

$$\begin{aligned}&\sqrt{n}\left[f\left\{\text{vec}(\hat{\beta}^*)\right\} - f\left\{\text{vec}(\hat{\beta})\right\}\right] \\ &\quad = \nabla f\left\{\text{vec}(\hat{\beta})\right\}\sqrt{n}\left\{\text{vec}(\hat{\beta}^*) - \text{vec}(\hat{\beta})\right\} + O_p(n^{-1/2})\end{aligned} \tag{6.3}$$

Therefore (6.3) converges to a normal distribution with mean zero and variance given by

$$\nabla f\left\{\text{vec}\left(\beta\right)\right\}\left(\Sigma_X^{-1} \otimes \Sigma\right)\nabla^T f\left\{\text{vec}\left(\beta\right)\right\}$$

as $n \to \infty$.

6.2.2 Random design and heteroskedasticity

In this section we assume that the X_is in model (6.1) are realizations of a random variable X. The regression coefficient matrix β now takes the form $\beta = \mathrm{E}(YX^T)\Sigma_X^{-1}$ where $\Sigma_X = \mathrm{E}(XX^T)$ and it is assumed that Σ_X is positive definite. Now that X is stochastic, there may be some association between X and the errors ε. The possibility of heteroskedasticity means that we need to alter the bootstrap procedure outlined in the previous section in order to consistently estimate the variability of $\mathrm{vec}(\hat{\beta})$.

It is assumed that the data vectors $(X_i^T, Y_i^T)^T \in \mathbb{R}^{p+r}$ are independent, with a common distribution μ and $\mathrm{E}(\|(X_i^T, Y_i^T)^T\|^4) < \infty$ where $\|\cdot\|$ is the Euclidean norm. Unlike the fixed design setting, data pairs $(X_i^T, Y_i^T)^T$ are resampled with replacement to form the starred data $(X_i^{*T}, Y_i^{*T})^T$, for $i = 1, ..., n$. Given the original sample, $(X_i^T, Y_i^T)^T$, $i = 1, ..., n$, the resampled vectors are independent, with distribution μ_n. Denote $\mathbb{X}^* \in \mathbb{R}^{n\times p}$ and $\mathbb{Y}^* \in \mathbb{R}^{n\times r}$ as the matrix with rows X_i^{*T} and Y_i^{*T} respectively. The starred estimator of β obtained from resampling is then $\hat{\beta}^* = \mathbb{Y}^{*T}\mathbb{X}^*\left(\mathbb{X}^{*T}\mathbb{X}^*\right)^{-1}$. For every n there is positive probability, albeit low, that $\mathbb{X}^{*T}\mathbb{X}^*$ is singular, and the probability of singularity decreases exponentially in n. We assume that displayed equation (1.17) in Chatterjee and Bose (2000) holds in order to circumvent singularity in our bootstrap procedure.

The bootstrap is performed a total of B times with a new estimator $\hat{\beta}^*$ computed at each iteration. We then estimate the variability of $\mathrm{vec}(\hat{\beta})$ with

$$\mathrm{Var}^*\left\{\mathrm{vec}(\hat{\beta})\right\} = (B-1)^{-1}\sum_{b=1}^{B}\left\{\mathrm{vec}(\hat{\beta}_b^*) - \mathrm{vec}(\bar{\beta}^*)\right\}\left\{\mathrm{vec}(\hat{\beta}_b^*) - \mathrm{vec}(\bar{\beta}^*)\right\}^T$$

where $\hat{\beta}_b^*$ is the bootstrap estimator of β at iteration b and $\bar{\beta}^* = B^{-1}\sum_{b=1}^{B}\hat{\beta}_b^*$.

We now show that the variability of $\mathrm{vec}(\hat{\beta})$ is estimated consistently by our multivariate bootstrap procedure which resamples cases. Let M be a non-negative definite matrix with entries $M_{jk} = \mathrm{E}\left\{\mathrm{vec}(X_i\varepsilon_i^T)_j\mathrm{vec}(X_i\varepsilon_i^T)_k\right\}$ for $j, k = 1, ..., rp$ and define $\Delta =$

$\left(\Sigma_X^{-1} \otimes I_r\right) M \left(\Sigma_X^{-1} \otimes I_r\right)$. where $n^{-1}\mathbb{X}^T\mathbb{X} \to \Sigma_X$ a.e. as $n \to \infty$. Then

$$\begin{aligned} \sqrt{n}\text{vec}\left(\hat{\beta} - \beta\right) &= \text{vec}\left\{n^{-1/2}\varepsilon^T\mathbb{X}(n^{-1}\mathbb{X}^T\mathbb{X})^{-1}\right\} \\ &= \left\{(n^{-1}\mathbb{X}^T\mathbb{X})^{-1} \otimes I_r\right\} \text{vec}\left(n^{-1/2}\varepsilon^T\mathbb{X}\right) \to N(0, \Delta). \end{aligned} \tag{6.4}$$

The next theorem states that $\sqrt{n}\text{vec}\left(\hat{\beta}^* - \hat{\beta}\right)$ is the same as (6.4). This is an extension of Theorems 3.1 and 3.2 of Freedman (1981) to the multivariate linear regression setting.

Theorem 14

Assume that $(X_i^T, Y_i^T)^T \in \mathbb{R}^{p+r}$ are independent, with a common distribution μ, $\text{E}(\|(X_i^T, Y_i^T)^T\|^4) < \infty$, and $\Sigma_X = \text{E}(XX^T)$ is positive definite. Along almost all sample sequences, given $(X_i^T, Y_i^T)^T$, for $i = 1, ..., n$, as $n \to \infty$,

a) $n^{-1}\left(\mathbb{X}^{*T}\mathbb{X}^*\right)$ converges to Σ_X in conditional probability,

b) the conditional law of $\sqrt{n}\left\{\text{vec}(\hat{\beta}^*) - \text{vec}(\hat{\beta})\right\}$ converges weakly to a Normal random variable that is mean 0 and has variance-covariance matrix Δ,

c) the sequence $\widehat{\Sigma}^*$ converges to Σ in probability. □

The proof of Theorem 14, along with necessary lemmas, are included in the theoretical details section.

6.3 Examples

In this section we provide two simulated examples which show support for our multivariate bootstrap procedures.

6.3.1 Example 1: fixed design

This example illustrates Theorem 13. We generated data according to the multivariate linear regression model (6.1) where $Y_i \in \mathbb{R}^3$, $X_i \in \mathbb{R}^2$, and both β and Σ are prespecified. Our goal is to make inference about $\text{vec}(\beta)$ using the residual bootstrap. Bootstrapped

standard errors are compared to the true standard deviations, which are the square root of the diagonal elements of $n^{-1}(\mathbb{X}^T\mathbb{X})^{-1} \otimes \Sigma$. Three data sets were generated at different sample sizes and the performance of the multivariate residual bootstrap is assessed. The bootstrap sample size is taken to be $B = 4n$ in each dataset. The results are displayed in Table 6.1. We see that the standard errors of $\text{vec}(\hat{\beta})$ obtained from the residual bootstrap are close to the true standard errors and that the distance between the two shrinks as n increases.

$n = 100$		$n = 500$		$n = 1000$	
$\text{se}^*\{\text{vec}(\hat{\beta})\}$	$\text{se}_{\text{true}}\{\text{vec}(\hat{\beta})\}$	$\text{se}^*\{\text{vec}(\hat{\beta})\}$	$\text{se}_{\text{true}}\{\text{vec}(\hat{\beta})\}$	$\text{se}^*\{\text{vec}(\hat{\beta})\}$	$\text{se}_{\text{true}}\{\text{vec}(\hat{\beta})\}$
0.249	0.281	0.144	0.140	0.091	0.097
0.317	0.336	0.146	0.141	0.093	0.100
0.237	0.251	0.129	0.125	0.080	0.087
0.270	0.301	0.133	0.126	0.082	0.089
0.140	0.154	0.077	0.077	0.050	0.053
0.168	0.184	0.079	0.077	0.054	0.055

Table 6.1: Comparison of bootstrapped standard errors to the true standard errors across three sample sizes in the fixed design case. The bootstrap sample size is set at $B = 4n$ for each dataset.

6.3.2 Example 2: random design and heteroskedasticity

This example aims to show support for Theorem 14. We generated data according to the multivariate linear regression model (6.1) where $Y_i \in \mathbb{R}^3$, $X_i \in \mathbb{R}^2$, and both β and Σ are prespecified. The predictors and errors are generated according to

$$\begin{pmatrix} X_i \\ \varepsilon_i \end{pmatrix} \sim N\left\{ \begin{pmatrix} 0 \\ 0 \end{pmatrix}, \begin{pmatrix} \Sigma_X & \Sigma_{X\varepsilon} \\ \Sigma_{\varepsilon X} & \Sigma \end{pmatrix} \right\},$$

for $i = 1, ..., n$. Our goal is to make inference about $\text{vec}(\beta)$ using the multivariate bootstrap procedure in the random design case. Bootstrapped standard errors are compared to the true standard deviations, which are the square root of the diagonal elements of $(n-1)^{-1}\Sigma_X^{-1} \otimes \left(\Sigma - \Sigma_{\varepsilon X}\Sigma_X^{-1}\Sigma_{X\varepsilon}\right)$. Three data sets were generated at different sample

sizes and the performance of the multivariate bootstrap is assessed. The bootstrap sample size is taken to be $B = 4n$ in each dataset. The results are displayed in Table 6.2. We see that the standard errors of $\text{vec}(\hat{\beta})$ obtained from the bootstrap are close to the true standard errors.

$n = 100$		$n = 500$		$n = 1000$	
$\text{se}^*\{\text{vec}(\hat{\beta})\}$	$\text{se}_{\text{true}}\{\text{vec}(\hat{\beta})\}$	$\text{se}^*\{\text{vec}(\hat{\beta})\}$	$\text{se}_{\text{true}}\{\text{vec}(\hat{\beta})\}$	$\text{se}^*\{\text{vec}(\hat{\beta})\}$	$\text{se}_{\text{true}}\{\text{vec}(\hat{\beta})\}$
0.340	0.310	0.131	0.138	0.101	0.098
0.257	0.275	0.106	0.123	0.082	0.087
0.146	0.159	0.068	0.071	0.046	0.050
0.333	0.310	0.138	0.138	0.104	0.098
0.225	0.275	0.124	0.123	0.086	0.087
0.135	0.159	0.071	0.071	0.051	0.050

Table 6.2: Comparison of bootstrapped standard errors to the true standard errors across three sample sizes in the random design case with heteroskedasticity. The bootstrap sample size is set at $B = 4n$ for each dataset.

6.4 Theoretical details

Before we present our proof of Theorems 13 and 14, we motivate the Mallows metric as a central tool for our proof technique. The Mallows metric for probabilities in $\mathbb{R}^p$, relative to the Euclidean norm was the driving force needed to establish the validity of the residual bootstrap approximation in the context of univariate regression (Bickel and Freedman, 1981; Freedman, 1981). The Mallows metric, relative to the Euclidean norm, for two probability measures μ, ν in $\mathbb{R}^p$, denoted $d_l^p(\mu, \nu)$, is the infimum of $\text{E}^{1/l}\left(\|U - V\|^l\right)$ over all joint distributions of random vectors U and V, where U has law μ and V has law ν. Properties of the Mallows metric are developed for random variables on separable Banach spaces of finite dimension (Bickel and Freedman, 1981). Therefore the machinery is already in place for our multivariate extension of the residual bootstrap. We use the Mallows metric when $r > 1$ to prove that the residual bootstrap can be used to estimate the variability of $\text{vec}(\hat{\beta})$ consistently.

6.4.1 Fixed design

Let $\Psi_n(F)$ be the distribution function of $\sqrt{n}\left\{\text{vec}(\hat{\beta}) - \text{vec}(\beta)\right\}$ where F is the law of the errors ε so that $\Psi_n(F)$ is a probability measure on $\mathbb{R}^{rp}$. Let G be an alternate law of the errors, where it is assumed that G is mean-zero with finite variance $\Sigma_G > 0$. In applications, G will be the centered empirical distribution of the residuals.

Theorem 15

$[d_2^{rp}\{\Psi_n(F), \Psi_n(G)\}]^2 \leq nr \,\text{tr}\left\{(\mathbb{X}^T\mathbb{X})^{-1}\right\}\{d_2^r(F,G)\}^2$. □

Proof: Let $B = \mathbb{X}(\mathbb{X}^T\mathbb{X})^{-1}$. Then $\Psi_n(F)$ is the law of $\sqrt{n}\varepsilon_n^T(F)B$ where $\varepsilon_n(F)$ is the matrix with n rows of independent random variables ε, having common law F. $\Psi_n(G)$ can be thought of similarly. Observe that $B^TB = (\mathbb{X}^T\mathbb{X})^{-1}$. Then, from Lemma 8.9 in Bickel and Freedman (1981), we see that

$$\begin{aligned}
[d_2^{rp}\{\Psi_n(F), \Psi_n(G)\}]^2 &= \left(d_2^{rp}\left[\text{vec}\{\varepsilon_n^T(F)B\}, \text{vec}\{\varepsilon_n^T(G)B\}\right]\right)^2 \\
&= \left(d_2^{rp}\left[(B^T \otimes I_r)\text{vec}\{\varepsilon_n^T(F)\}, (B^T \otimes I_r)\text{vec}\{\varepsilon_n^T(G)\}\right]\right)^2 \\
&\leq n \,\text{tr}\left\{(B^T \otimes I_r)(B^T \otimes I_r)^T\right\}\{d_2^r(F,G)\}^2 = n \,\text{tr}\left\{(B^T \otimes I_r)(B \otimes I_r)\right\}\{d_2^r(F,G)\}^2 \\
&= n \,\text{tr}\left(B^TB \otimes I_r\right)\{d_2^r(F,G)\}^2 = n \,\text{tr}\left\{(\mathbb{X}^T\mathbb{X})^{-1} \otimes I_r\right\}\{d_2^r(F,G)\}^2 \\
&= nr \,\text{tr}\left\{(\mathbb{X}^T\mathbb{X})^{-1}\right\}\{d_2^r(F,G)\}^2,
\end{aligned}$$

which is our desired conclusion. □

With Theorem 15 we can bound the distance between the sample dependent distribution functions $\Psi_n(F)$ and $\Psi_n(G)$ by the distance between their underlying laws. As in Freedman (1981), we proceed with F_n as the empirical distribution function of $\varepsilon_1, ..., \varepsilon_n$. Let $\widetilde{F}_n$ be the empirical distribution of the residuals $\widehat{\varepsilon}_1, ..., \widehat{\varepsilon}_n$ from the original regression, and let $\widehat{F}_n$ be $\widetilde{F}_n$ centered at its mean $\hat{\mu} = n^{-1}\sum_{i=1}^n \widehat{\varepsilon}_i$. Since $\widehat{\varepsilon} = \mathbb{Y} - \mathbb{X}\hat{\beta}^T$, we have $\widehat{\varepsilon} - \varepsilon = -\mathcal{P}\varepsilon$ where $\mathcal{P}$ is the projection into the column space of $\mathbb{X}$.

Lemma 2
$\mathrm{E}^2\left\{d_2^r(\widetilde{F}_n, F_n)\right\} \leq p\,\mathrm{tr}(\Sigma)/n.$ □

Proof: From the definition of the Mallows metric we have

$$\begin{aligned}\left\{d_2^r(\widetilde{F}_n, F_n)\right\}^2 &\leq n^{-1}\sum_{i=1}^{n}\|\widehat{\varepsilon}_i - \varepsilon_i\|^2 = n^{-1}\,\mathrm{tr}\left\{(\widehat{\varepsilon}-\varepsilon)^T(\widehat{\varepsilon}-\varepsilon)\right\} \\ &= n^{-1}\,\mathrm{tr}\left(\varepsilon^T\mathcal{P}\varepsilon\right).\end{aligned}$$

From linearity of the expectation with respect to the trace operator,

$$\mathrm{E}\left\{\mathrm{tr}\left(\varepsilon^T\mathcal{P}\varepsilon\right)\right\} = \mathrm{tr}\left\{\mathrm{E}\left(\varepsilon^T\mathcal{P}\varepsilon\right)\right\} = \mathrm{tr}\left\{\mathcal{P}\,\mathrm{E}\left(\varepsilon\varepsilon^T\right)\right\} \leq \mathrm{tr}\left(\mathcal{P}\right)\mathrm{tr}\left(\Sigma\right) = p\,\mathrm{tr}\left(\Sigma\right)$$

and this completes the proof. □

Lemma 3
$\mathrm{E}^2\left\{d_2^r(\widehat{F}_n, F_n)\right\} \leq (p+1)\,\mathrm{tr}(\Sigma)/n.$ □

Proof: From Lemma 8.8 in Bickel and Freedman (1981) we have

$$\begin{aligned}d_2^r(\widehat{F}_n, F_n)^2 &= d_2^r\{\widetilde{F}_n - \mathrm{E}(\widetilde{F}_n), F_n - \mathrm{E}(F_n)\}^2 + \|\,\mathrm{E}(F_n)\|^2 \\ &= d_2^r(\widetilde{F}_n, F_n)^2 - \|\,\mathrm{E}(\widetilde{F}_n) - \mathrm{E}(F_n)\|^2 + \|\,\mathrm{E}(F_n)\|^2 \\ &\leq d_2^r(\widetilde{F}_n, F_n)^2 + \|n^{-1}\sum_{i=1}^{n}\varepsilon_i\|^2\end{aligned}$$

with the empirical distribution functions F_n,$\widetilde{F}_n$, and $\widehat{F}_n$ used as random variables in the application of Lemma 8.8 in Bickel and Freedman (1981). We see that

$$\mathrm{E}\left(\|n^{-1}\sum_{i=1}^{n}\varepsilon_i\|^2\right) = n^{-2}\left\{\mathrm{E}\left(\sum_{i=1}^{n}\varepsilon_i^T\varepsilon_i + \sum_{i\neq j}\varepsilon_i^T\varepsilon_j\right)\right\} = n^{-1}\left\{\mathrm{E}(\varepsilon_1^T\varepsilon_1)\right\} = n^{-1}\,\mathrm{tr}\left(\Sigma\right).$$

Our conclusion follows from Lemma 2. □

These results imply the validity of the bootstrap approximation, in probability, for the model (6.1) if we assume that $n^{-1}\mathbb{X}^T\mathbb{X} \to \Sigma_X > 0$. From Theorem 15,

$$\mathrm{E}\left[d_2^{rp}\{\Psi_n(\widehat{F}_n), \Psi_n(F)\}\right] \leq nr \,\mathrm{tr}\left\{(\mathbb{X}^T\mathbb{X})^{-1}\right\} d_2^r(\widehat{F}_n, F)$$

and because of the metric properties of $d_2^r(\cdot,\cdot)$

$$\frac{1}{2}d_2^r(\widehat{F}_n, F)^2 \leq d_2^r(\widehat{F}_n, F_n)^2 + d_2^r(F_n, F)^2$$

where Lemma 3 shows that the first term on the right hand side converges in probability to 0; the second term on the right hand side converges to 0 in probability by Lemma 8.4 of (Bickel and Freedman, 1981) where the separable Banach space is taken to be $\mathbb{R}^r$. The next results are special cases of Lai et. al. (1979) which are adapted from Freedman (1981) to the multivariate setting. We let ε_j, $j = 1, ..., r$, be the column of ε corresponding to the errors of response Y_j.

Lemma 4

$n^{-1}\mathbb{X}^T\varepsilon \to 0$ almost everywhere and $\hat{\beta} \to \beta$ almost everywhere. □

Proof: Let B_j be the jth column of ε. Then $n^{-1}\mathbb{X}^T\varepsilon \in \mathbb{R}^{p\times r}$ with columns $n^{-1}\mathbb{X}^T\varepsilon$. Lemma 2.3 of Freedman (1981) state that $n^{-1}\mathbb{X}^T B_j \to 0$ almost everywhere for any particular $j = 1, ..., r$. Therefore $n^{-1}\mathbb{X}^T\varepsilon \to 0$ almost everywhere. A similar argument verifies our second result. □

Lemma 5

$n^{-1}\,\mathrm{tr}\left\{(\widehat{\varepsilon} - \varepsilon)^T(\widehat{\varepsilon} - \varepsilon)\right\} \to 0$ almost everywhere. □

Proof: A similar argument to that of Lemma 2.4 in Freedman (1981) gives

$$\begin{aligned} n^{-1}\,\mathrm{tr}\left\{(\widehat{\varepsilon} - \varepsilon)^T(\widehat{\varepsilon} - \varepsilon)\right\} &= n^{-1}\,\mathrm{tr}\left\{\varepsilon^T\mathbb{X}(\mathbb{X}^T\mathbb{X})^{-1}\mathbb{X}^T\varepsilon\right\} \\ &= \mathrm{tr}\left\{\left(n^{-1}\varepsilon^T\mathbb{X}\right)\left(n^{-1}\mathbb{X}^T\mathbb{X}\right)^{-1}\left(n^{-1}\mathbb{X}^T\varepsilon\right)\right\}. \end{aligned}$$

The center term converges to $\Sigma_X > 0$ and the left and right terms converge to 0 almost everywhere by Lemma 4. Our result follows. □

Lemma 6

$d_2^r(\widehat{F}_n, F_n) \to 0$ almost everywhere and $d_2^r(\widehat{F}_n, F) \to 0$ almost everywhere. □

Proof: From the arguments in the proofs of Lemmas 2 and 3 we have that

$$\begin{aligned} d_2^r(\widehat{F}_n, F_n) &= d_2^r(\widetilde{F}_n, F_n)^2 - \| \mathrm{E}(\widetilde{F}_n) - \mathrm{E}(F_n)\|^2 + \| \mathrm{E}(F_n)\|^2 \\ &= \|n^{-1} \sum_{i=1}^n \varepsilon_i\|^2 - \|n^{-1} \sum_{i=1}^n (\widehat{\varepsilon}_i - \varepsilon_i)\|^2 + d_2^r(\widetilde{F}_n, F_n) \\ &\leq \|n^{-1} \sum_{i=1}^n \varepsilon_i\|^2 + n^{-1} \operatorname{tr}\left\{(\widehat{\varepsilon} - \varepsilon)^T (\widehat{\varepsilon} - \varepsilon)\right\} \end{aligned}$$

which converges to 0 almost everywhere by Lemma 5. Therefore the first convergence result holds. From the metric properties of the Mallows metric we have that

$$\frac{1}{2} d_2^r(\widehat{F}_n, F)^2 \leq d_2^r(\widehat{F}_n, F_n)^2 + d_2^r(F_n, F)^2.$$

Our second convergence result follows from the first convergence result and Lemma 8.4 of Bickel and Freedman (1981). □

Lemma 7

Let u_i and v_i, $i = 1, ..., n$, be $r \times 1$ vectors. Let

$$\bar{u} = n^{-1} \sum_{i=1}^n u_i, \quad \text{and} \quad s_u^2 = n^{-1} \sum_{i=1}^n (u_i - \bar{u})(u_i - \bar{u})^T$$

and similarly for v. Then

$$\|s_u^2 - s_v^2\|_F^2 \leq \|n^{-1} \sum_{i=1}^n (u_i - v_i)(u_i - v_i)^T\|_F^2$$

where $\|\cdot\|_F$ is the Frobenius norm. □

Proof: We have

$$\begin{aligned}\|s_u^2 - s_v^2\|_F^2 &= \sum_{j=1}^{n}\sum_{k=1}^{n} |n^{-1}\sum_{i=1}^{n}(u_i-\bar{u})_j(u_i-\bar{u})_k^T - n^{-1}\sum_{i=1}^{n}(v_i-\bar{v})_j(v_i-\bar{v})_k^T|^2 \\ &\leq \sum_{j=1}^{n}\sum_{k=1}^{n} |n^{-1}\sum_{i=1}^{n}(u_i-v_i)_j(u_i-v_i)_k|^2 \\ &= \|n^{-1}\sum_{i=1}^{n}(u_i-v_i)(u_i-v_i)^T\|_F^2,\end{aligned}$$

where the inequality follows from (Freedman, 1981, Lemma 2.7). □

The proof of Theorem 13 is now given.

Proof: Exchange $\widehat{F}_n$ for G in Theorem 15 and observe that

$$d_2^{rp}\left\{\Psi_n(F), \Psi_n(\widehat{F}_n)\right\} \leq nr \operatorname{tr}\left\{(\mathbb{X}^T\mathbb{X})^{-1}\right\} d_2^r(F, \widehat{F}_n)^2.$$

From Lemma 6 we know that $d_2^r(F, \widehat{F}_n)^2 \to 0$ almost everywhere. Our result for part a) follows since F is mean-zero normal with variance $\Sigma_X^{-1} \otimes \Sigma$. We now show that part b) holds. First, we need to establish that $\widehat{\Sigma} \to \Sigma$ almost everywhere. To see this, introduce

$$\Sigma_n = n^{-1}\sum_{i=1}^{n}\varepsilon_i\varepsilon_i^T - \left(n^{-1}\sum_{i=1}^{n}\varepsilon_i\right)\left(n^{-1}\sum_{i=1}^{n}\varepsilon_i\right)^T.$$

Clearly, $\Sigma_n \to \Sigma$ almost everywhere. Let $C_n = n^{-1}\sum_{i=1}^{n}(\hat{\varepsilon}_i - \varepsilon_i)(\hat{\varepsilon}_i - \varepsilon_i)^T$. We have,

$$\begin{aligned}\|\widehat{\Sigma} - \Sigma_n\|_F^2 \leq \|C_n\|_F^2 &= \operatorname{tr}(C_nC_n) \leq \operatorname{tr}^2(C_n) \\ &= \operatorname{tr}^2\left\{n^{-1}\sum_{i=1}^{n}(\widehat{\varepsilon}_i - \varepsilon_i)^T(\widehat{\varepsilon}_i - \varepsilon_i)\right\} \\ &= \operatorname{tr}^2\left\{n^{-1}(\widehat{\varepsilon} - \varepsilon)^T(\widehat{\varepsilon} - \varepsilon)\right\} \to 0\end{aligned}$$

almost everywhere where the first inequality follows from Lemma 7 with $\widehat{\Sigma}_n$ and Σ_n taking the place of s_u^2 and s_v^2 respectively, the second inequality follows from the fact that C_n is

positive definite almost everywhere, and the convergence follows from Lemma 5.

Let $D_n = \mathrm{E}\left(\|\widehat{\Sigma}_n^* - \Sigma_n^*\|_F \mid Y_1, ..., Y_n\right)$. From Lemma 7 and the proof of Lemma 2 we see that,

$$\begin{aligned} D_n &\leq \mathrm{E}\left\{\|n^{-1}\sum_{i=1}^{n}\left(\widehat{\varepsilon}_i^* - \varepsilon_i^*\right)\left(\widehat{\varepsilon}_i^* - \varepsilon_i^*\right)^T\|_F \mid Y_1, ..., Y_n\right\} \\ &\leq \mathrm{E}\left[\mathrm{tr}\left\{n^{-1}(\widehat{\varepsilon}^* - \varepsilon^*)^T(\widehat{\varepsilon}^* - \varepsilon^*)\right\} \mid Y_1, ..., Y_n\right] \\ &\leq p\,\mathrm{tr}\left(\widehat{\Sigma}\right)/n \end{aligned}$$

where the last inequality follows from the argument that proves Lemma 2 applied to the starred data, and $p\,\mathrm{tr}\left(\widehat{\Sigma}\right)/n \to 0$ almost everywhere. It remains to show that $\widehat{\Sigma}_n^*$ converges to Σ. Conditional on $Y_1, ..., Y_n$,

$$\begin{aligned} &d_2^{r(r+1)/2}\left\{n^{-1}\sum_{i=1}^{n}\mathrm{vech}(\varepsilon_i^*\varepsilon_i^{*T}), n^{-1}\sum_{i=1}^{n}\mathrm{vech}(\varepsilon_i\varepsilon_i^T)\right\} \\ &\quad\leq d_2^{r(r+1)/2}\left\{\mathrm{vech}(\varepsilon_1^*\varepsilon_1^{*T}), \mathrm{vech}(\varepsilon_1\varepsilon_1^T)\right\} \end{aligned} \tag{6.5}$$

by Lemma 8.6 in Bickel and Freedman (1981). Now ε^* has conditional distribution $\widehat{F}_n$ and ε has law F and Lemma 6 gives $d_2^r\left(\widehat{F}_n, F\right) \to 0$ almost everywhere. We now show that $d_1\left\{\mathrm{vech}(\varepsilon_1^*\varepsilon_1^{*T}), \mathrm{vech}(\varepsilon_1\varepsilon_1^T)\right\} \to 0$ almost everywhere by Lemma 8.5 of Bickel and Freedman (1981) with $\phi(x) = \mathrm{vech}\left(xx^T\right)$ where $x \in \mathbb{R}^r$. To do this, we show that K can be chosen so that $\|\phi(x)\|_1 \leq K(1 + \|x\|_2^2)$ where $\|\cdot\|_1$ and $\|\cdot\|_2$ are the $\mathcal{L}^1$ and $\mathcal{L}^2$ norms respectively. From the definition of the Euclidean norm, we have $\|x\|_2^2 = \sum_{i=1}^r x_i^2$. It is clear that $x_i^2 + x_j^2 \geq 2|x_i x_j|$ for all $i, j = 1, ..., r$. Now, pick $K = \binom{r}{2} + 1$. We see that

$$\begin{aligned} K(1 + \|x\|_2^2) &\geq \left|\sum_{i=1}^{r} x_i^2 + \binom{r}{2}\sum_{i=1}^{r} x_i^2\right| \geq \left|\sum_{i=1}^{r} x_i^2 + \sum_{i\neq j}^{r}|x_i x_j|\right| \\ &\geq \left|\sum_{i\geq j}^{r}|x_i x_j|\right| \geq \|\mathrm{vech}\left(xx^T\right)\|_1 = \|\phi(x)\|_1 \end{aligned}$$

A similar argument shows that $1/n \sum_{i=1}^{n} \varepsilon_i^*$ converges to 0. Part c) follows from both a) and b). □

6.4.2 Random design and heteroskedasticity

In this section we provide the proof of Theorem 14. Several quantities and lemmas are introduced in order to prove Theorem 14. The logic follows that of (Freedman, 1981, Section 3). Define,

$$\begin{aligned} \Sigma(\mu) &= \int xx^T \mu(dx), \\ \beta(\mu) &= \int yx^T \mu(dx, dy) \Sigma(\mu)^{-1}, \\ \varepsilon(\mu, x, y) &= y - \beta(\mu) x^T. \end{aligned}$$

The next two lemmas are needed to prove Theorem 14.

Lemma 8

If $d_4^{p+r}(\mu_n, \mu) \to 0$ as $n \to \infty$, then

a) $\Sigma(\mu_n) \to \Sigma(\mu)$ and $\beta(\mu_n) \to \beta(\mu)$,

b) the μ_n-law of $\text{vec}\{\varepsilon(\mu_n, x, y)x^T\}$ converges to the μ-law of $\text{vec}\{\varepsilon(\mu, x, y)x^T\}$ in d_2^{rp},

c) the μ_n-law of $\|\varepsilon(\mu_n, x, y)\|^2$ converges to the μ-law of $\|\varepsilon(\mu, x, y)\|^2$ in d_1. □

Proof: Part a) immediately follows from (Bickel and Freedman, 1981, Lemma 8.3c).

We use (Bickel and Freedman, 1981, Lemma 8.3a) to verify part b). The weak convergence step is trivial. Now,

$$\begin{aligned} \|\text{vec}\{\varepsilon(\mu_n, x, y)x^T\}\|^2 &= \|\text{vec}\{yx^T - \beta(\mu_n)xx^T\}\|^2 \\ &= \|\text{vec}(yx^T)\|^2 + \|\text{vec}(\beta(\mu_n)xx^T)\|^2 - 2\text{vec}(yx^T)^T \text{vec}\{\beta(\mu_n)xx^T\}. \end{aligned}$$

Let $z = (x^T, y^T)^T$. Part b) follows from, integration with respect to μ_n, part a), and (Bickel and Freedman, 1981, Lemma 8.5) with $\phi(z) = \text{vech}(zz^T)$. The steps involving (Bickel and Freedman, 1981, Lemma 8.5) are similar to those in the proof of Theorem 13.

Part c) follows from the same argument used to prove part b). □

Lemma 9

$d_4^{p+r}(\mu_n, \mu) \to 0$ a.e. as $n \to \infty$. □

Proof: The steps are the same as those in (Freedman, 1981, Lemma 3.2). □

The proof of Theorem 14 is now given.

Proof: We can write

$$\begin{aligned}
\text{vec}\left\{\sqrt{n}\left(\hat{\beta}^* - \hat{\beta}\right)\right\} &= \text{vec}\left[\sqrt{n}\left\{\mathbb{Y}^{*T}\mathbb{X}^*(\mathbb{X}^{*T}\mathbb{X}^*)^{-1} - \hat{\beta}\right\}\right] \\
&= \text{vec}\left[\sqrt{n}\left\{(\varepsilon^* + \mathbb{X}^*\hat{\beta}^T)^T\mathbb{X}^*(\mathbb{X}^{*T}\mathbb{X}^*)^{-1} - \hat{\beta}\right\}\right] \\
&= \text{vec}\left\{n^{-1/2}\varepsilon^{*T}\mathbb{X}^*(n^{-1}\mathbb{X}^{*T}\mathbb{X}^*)^{-1}\right\} \\
&= \text{vec}\left(Z^*W^{*-1}\right) = \left(W^{*-1} \otimes I_r\right)\text{vec}(Z^*)
\end{aligned}$$

where $Z^* = n^{-1/2}\varepsilon^{*T}\mathbb{X}^*$ and $W^* = n^{-1}\mathbb{X}^{*T}\mathbb{X}^*$. (Freedman, 1981, Theorem 3.1) shows that the conditional law of W^* converges to Σ_X in probability. This verifies part a).

We now verify part b). From (Bickel and Freedman, 1981, Lemma 8.7), we have

$$d_2^{rp}\left\{\text{vec}(Z^*), \text{vec}(Z)\right\}^2 \leq d_2^{rp}\left\{\text{vec}(X_i^*\varepsilon_i^{*T}), \text{vec}(X_i\varepsilon_i^T)\right\}^2$$

where the right side goes to 0 a.e. as $n \to \infty$. Lemma 9 states that $\mu_n \to \mu$ a.e. in d_4^{r+p} as $n \to \infty$ and part b) of Lemma 8 implies that the distribution of $\text{vec}(Z^*)$, conditional on (X_i, Y_i), $i = 1, ..., n$, converges to $\text{vec}(Z)$. The random variable $\text{vec}(Z)$ is normally distributed with mean 0 and variance matrix M. Combining this with part a) verifies that the conditional distribution of $\left(W^{*-1} \otimes I_r\right)\text{vec}(Z^*)$ converges to $\left(\Sigma_X^{-1} \otimes I_r\right)\text{vec}(Z)$

as $n \to \infty$. This completes the proof of part b).

Part c) follows from the same argument in the proof of Theorem 13 where Lemmas 9 and 8c combine to show that (6.5) converges to 0 as $n \to \infty$. Note that $\varepsilon_1^* = Y_1^* - \hat{\beta} X_1^*$ in this argument. This completes the proof. □

Chapter 7

Dimensional Analysis in Multivariate Experimental Design

7.1 Introduction

Dimensional analysis (DA) is a methodology developed in physics for reducing the number and complexity of experimental factors so that the relationship between the factors and the response can be determined efficiently and effectively. If a response appears to depend on m physical predictors or factors, dimensional analysis can reduce the number of factors required to k *dimensionless* factors, where the reduction $m-k$ is typically between one and four, and is given by the number of *fundamental dimensions* in the problem.

White (2009) gives a compelling example in which the experimenter wished to determine the force (F) exerted on a body submerged in water, as a function of the body length L, stream velocity V, fluid density ρ, and fluid viscosity, μ. Ignoring experimental error, we have:

$$F = g(L, V, \rho, \mu) \tag{7.1}$$

where g is an unknown vector-valued function that we wish to characterize at least approximately. White suggests that a full factorial experiment involving $10^4 = 10{,}000$ runs would be required to fully characterize g, assuming that "it takes about 10 points to define a curve" (White, 2009, p.294). He then notes that the technique of dimensional analysis

can be used to reduce the number of experimental factors to 4 - 3 = 1, because there are three fundamental dimensions—mass, length, and time–involved in the relationship. The solution to the DA problem is:

$$\frac{F}{\rho V^2 L^2} = h\left(\frac{\rho V L}{\mu}\right)$$

The result is that the *dimensionless force coefficient*, $F/(\rho V^2 L^2)$, is a function of only one factor, the *dimensionless Reynolds number*, $\rho V L/\mu$. Thus, the required experimental design has been reduced from 10,000 runs to 10 runs (maintaining White's 10-points per variable assumption). In addition, because the variables are dimensionless, the experimental results will be completely scalable. That is, if we run our experiment in a lab with a small submerged body, e.g., a model, the results will be valid when applied to a much larger body of interest. The DA model is frequently written:

$$\pi_0 = h(\pi_1, \pi_2, ..., \pi_{m-k}) \tag{7.2}$$

and the dimensionless variables $\{\pi_i\}$ are referred to as the "pi-groups." The validity of the DA process is established by the well-known Buckingham Π-Theorem (Buckingham (1914)).

Of course, most statisticians might question both the need for a full factorial design and the 10-runs-per-factor assumption. Surprisingly, although DA has been a well-established technique in the sciences since the early part of the 20th century, the design of experiments for engineering dimensional analysis (DA) has received scant attention in the statistics literature. Perhaps the first paper to treat this topic in the statistical literature was Albrecht, et. al., (2013). They give a description of the DA method, tailored for statisticians, and then make recommendations for designing DA experiments. An example using classical designs in the hydrodynamics literature is given by Islam and Lye (2009).

The benefits of the DA process do not come without some attendant complications. First, the DA model can be highly non-linear. For this reason, an experimental design must be capable of estimating models models of higher order than those typically assumed in

screening or response surface studies. Second, omission of a key explanatory variable can be fatal to the DA process. In an effort to alleviate this concern, Albrecht, et al. (2013), proposed "robust-DA" designs that permit simultaneous estimation of the DA model and a standard empirical model in the original m factors. The robust-DA approach maximizes the efficiency of the DA design in the dimensionless factors, subject to lower-bound constraint on the efficiency of the design for the original factors.

Although multiple responses are frequently present in DA experiments, design for multivariate responses in DA experiments has not been considered. In this paper, we extend the Buckingham Π-Theorem to the multivariate response case, give strategies for design of DA experiments for multiple responses, and illustrate results through a standard example. A brief outline of the paper is as follows. In Section 2, we provide a brief overview of the DA process. The extension of the Buckingham Π-Theorem to multivariate responses is given in Section 3, and the design of experiments for multivariate DA problems is considered in Section 4. An illustration is provided in Section 4 that involves the design of water pump, and we conclude with a discussion in Section 5.

7.2 Overview of DA

In this section, we provide a brief overview of the DA process. For more detail, see, for example, Sonin (2001) and/or Albrecht, et al. (2013).

When implementing DA, physical quantities are classified as either base quantities or derived quantities. Base quantities are composed of a single fundamental dimension. In physics, the system international (SI) states that length, mass, time, electrical current, temperature, amount, and luminous intensity are all base quantities. In economics or operations research the base quantity of cost is also of importance. A base quantity can be measured using different measurement systems. For example, one can use meters, feet, or inches to measure length. A derived quantity of the first kind is a physical quantity that is comprised of a power-law combination of base quantities.

It has been shown that not all formulas can be used to represent physical quantities.

Because base quantities all have a physical origin, the ratio of the measurements of any two base quantities does not change if the base unit changes. This is known as the *principle of absolute significance* (Bridgman, 1931). The principle of absolute significance will hold for a physical quantity π having a monomial formula only if it assumes the power-law form:

$$x = \gamma \prod_{i=1}^{k} Z_i^{b_i},$$

where Z_i is the numerical value of the ith base quantity and the coefficients $\gamma, b_1, ..., b_k$ are real numbers. Thus, all physical quantities have power-law form and no other form represents a physical quantity. A generalized form recognizes that any given base quantity may appear more than once in the expression. For example, length may be used to represent both a radius and a height of a cylinder. Letting n_i denote the number of times that the ith base quantity appears in the formula, letting Z_{ij} denote the jth instance of the ith base quantity Z_i and, letting b_{ij} denote the power to which the jth instance of that base quantity is raised, the generalized form is

$$x = \gamma \prod_{i=1}^{k} \prod_{j=1}^{n_i} Z_{ij}^{b_{ij}}.$$

Denote by L_{ij} the fundamental dimension of Z_{ij}. That is, $[Z_{ij}] = L_{ij} = L_i$. It follows that the dimension of x is

$$[x] \;=\; \prod_{i=1}^{k} L_i^{\sum_{j=1}^{n_i} b_{ij}} \;=\; \prod_{i=1}^{k} L_i^{b_{i\cdot}},$$

where $\mathbf{b}_{i\cdot} = \sum_{j=1}^{n_i} b_{ij}$. If the units chosen for the ith dimension are changed by a factor c_i, for $i = 1, ..., k$, it follows that the value of x becomes $x' = c^{-1}x$, where $c = \prod_{i=1}^{k} c_i^{b_{i\cdot}}$. Finally, we say that a derived quantity is dimensionless if its value does not change when the units of the base quantities change.

Albrecht, et al. (2013) describe the DA process using four steps.

1. Identify the dependent and independent variables. In the example of the Introduction, (7.1) gives the dependent variable, F, and the dependent variables, L, V, ρ, and μ.

2. Identify a complete, dimensionally independent subset of the dependent variables. A subset is dimensionally independent if none of the dimensions of any of the variables not in the subset can be written as dimensions of products of powers of omitted variables. The subset is complete if the dimensions of each of the variables in the omitted set can be written as the products of powers of the dimensions of the variables in the subset. Albrecht, et al. (2013) refer to this subset as the *basis set*.

3. Identify the dimensionless forms of the variables not in the basis set. (Not sure how much to provide here—need to make this consistent with the statement of the new theorem). See Albrecht, et al. (2013) for details.

4. Apply Buckingham's Π-Theorem to obtain a DA model. In practice this simply means that we can now employ (7.2), where π_0 is the dimensionless response, and $\pi_1, \ldots, \pi_{m-k}$ are the dimensionless forms of the omitted variables.

7.3 Buckingham Π-Theorem for multivariate responses

The examples in Albrecht, Nachtsheim, Albrecht, and Cook (2013) show that DA is a valuable tool that provides dimension reduction of the predictors when the response is a scalar. The same ideas apply to any regression or design of experiments problem with a vector-valued response. In this setting, the Buckingham Π-Theorem has a multivariate analog where $\mathbf{Y} \in \mathbb{R}^r$ is the vector of responses and $\mathbf{x} \in \mathbb{R}^p$ is the vector of predictors. Both types of variables can be expressed as power-law combinations of m fundamental dimensions that are measured with respect to a particular system of units. Let $\mathbf{b}_i = (b_{1i}, b_{2i}, ..., b_{mi})'$ be the dimension vector of x_i, $i = 1, ..., p$, and let

$$\mathbf{B} = \begin{pmatrix} b_{11} & b_{12} & \cdots & b_{1p} \\ b_{21} & b_{22} & \cdots & b_{2p} \\ \vdots & \vdots & & \vdots \\ b_{m1} & b_{m2} & \cdots & b_{mp} \end{pmatrix}$$

be the $m \times p$ dimension matrix for the predictors in a given problem. Let $\mathbf{a}_i = (a_{1i}, a_{2i}, ..., a_{mi})'$ be the dimension vector of Y_i, $i = 1, ..., r$, and let

$$\mathbf{A} = \begin{pmatrix} a_{11} & a_{12} & \cdots & a_{1r} \\ a_{21} & a_{22} & \cdots & a_{2r} \\ \vdots & \vdots & & \vdots \\ a_{m1} & a_{m2} & \cdots & a_{mr} \end{pmatrix}$$

be the $m \times r$ dimension matrix for the response variables in a given problem. Define

$$L_{\mathbf{Y}} = \{L_i : a_{ij} \neq 0, \text{ some } j = 1, ..., r\},$$
$$L_{\mathbf{X}} = \{L_i : b_{ij} \neq 0, \text{ some } j = 1, ..., p\}.$$

The Multivariate Buckingham Π−Theorem assumes the following where the assumptions and some of the theoretical details follow from Bluman and Kumei (1989, p. 5-9).

Theorem 16

Assume the following:

(i) A vector $\mathbf{Y} \in \mathbb{R}^r$ has a functional relationship with p predictors $(x_1, ..., x_p)$:

$$\mathbf{Y} = \mathbf{f}(x_1, ..., x_p), \tag{7.3}$$

where $\mathbf{f}$ is an unknown function of the predictors.

(ii) The quantities $(Y_1, ..., Y_r, x_1, ..., x_p)$ involve m fundamental dimensions labeled by $L_1, ..., L_m$ where $m < p$ is assumed to ensure a meaningful problem. Then it is assumed that $\text{span}(\mathbf{A}) \subseteq \text{span}(\mathbf{B})$ where $L_{\mathbf{x}}$ contains all m fundamental dimensions.

(iii) Let Z represent any of $(Y_1, ..., Y_r, x_1, ..., x_p)$. Then,

$$[Z] = \prod_{i=1}^{m} L_i^{\alpha_i}$$

for some $\alpha_i \in \mathbb{R}, i = 1, .., m$ which are the dimension exponents of Z.

(iv) For any set of fundamental dimensions one can choose a system of units for measuring the value of any quantity Z. A change from one system of units to another involves a positive scaling of each fundamental dimension which in turn induces a scaling of each quantity Z. Under a change of system of units the value of a dimensionless quantity is unchanged, i.e. its value is invariant under an arbitrary scaling of fundamental dimension.

Assumptions (i)-(iv) give:

(i) Formula (7.3) can be written in terms of dimensionless quantities.

(ii) The number of dimensionless predictors is $k = p - \text{rank}(\mathbf{B})$ where $\text{rank}(\mathbf{B})$ is the rank of the matrix $\mathbf{B}$.

(iii) Let $x_i = (\pi_{1i}, \pi_{2i}, ..., \pi_{pi})'$, $i = 1, ..., k$ represent the $k = p - \text{rank}(\mathbf{B})$ linearly independent solutions of the system $\mathbf{B}x_i = 0$. Let $\mathbf{a}_i = (a_{1i}, a_{2i}, ..., a_{mi})'$ be the dimension vector for response $Y_i, i = 1, ..., r$ and let $\mathbf{y}_i = (\rho_{1i}, \rho_{2i}, ..., \rho_{pi})$ represent a solution to the system $\mathbf{B}\mathbf{y}_i = -\mathbf{a}_i$. Then formula (7.3) simplifies to $\tilde{\boldsymbol{\pi}} = \mathbf{h}(\pi_1, ..., \pi_k)$ where $\tilde{\boldsymbol{\pi}} \in \mathbb{R}^r$. All elements of $\tilde{\boldsymbol{\pi}}$ and π_i are dimensionless quantities for all $i = 1, ..., k$. □

The proof of the Multivariate Buckingham Π-Theorem is included in the Appendix. To see why $\text{span}(\mathbf{A}) \subseteq \text{span}(\mathbf{B})$ is needed, consider a design problem with two responses and three predictors where each variable has fundamental dimensions given by $[Y_1] = ML$, $[Y_2] = MT$, $[x_1] = ML$, $[x_2] = MT^2$, $[x_3] = MT^2$. In this setup, $L_{\mathbf{Y}} = L_{\mathbf{X}}$ and

$$\mathbf{A} = \begin{pmatrix} 1 & 1 \\ 1 & 0 \\ 0 & 1 \end{pmatrix}, \qquad \mathbf{B} = \begin{pmatrix} 1 & 1 & 1 \\ 1 & 0 & 0 \\ 0 & 2 & 2 \end{pmatrix}.$$

We can use DA to create a single dimensionless predictor x_2/x_3 and a dimensionless response Y_1/x_1. However, no combination of predictors can combine with Y_2 to yield a second dimensionless response. This is a result of violating $\text{span}(\mathbf{A}) \subseteq \text{span}(\mathbf{B})$.

When $\text{span}(\mathbf{A}) \subset \text{span}(\mathbf{B})$ the Multivariate Buckingham Π-Theorem holds and Dimensional Analysis is applicable for multivariate models. However, all is not lost when $\text{span}(\mathbf{A}) \setminus \text{span}(\mathbf{B}) \neq \emptyset$ but care is needed in this setting. When $\text{span}(\mathbf{A}) \setminus \text{span}(\mathbf{B}) \neq \emptyset$, it may be the case that certain responses need to be excluded from the DA model. For $j = 1, ..., r$ let $\mathbf{A}_j$ denote the j^{th} column of $\mathbf{A}$ and let $\mathbf{A}_{-j}$ be the matrix $\mathbf{A}$ with $\mathbf{A}_j$ removed. Suppose that $\mathbf{A}_j \notin \text{span}(\mathbf{A}_{-j}) \cup \text{span}(\mathbf{B})$ then the response $\mathbf{Y}_j$ cannot be made to be dimensionless and cannot be used to make other responses dimensionless. Therefore Y_j must be excluded from consideration in the DA model. With such cases in mind we proceed with the a corollary to the Multivariate Buckingham Π-Theorem that accounts for when $\text{span}(\mathbf{A}) \setminus \text{span}(\mathbf{B}) \neq \emptyset$.

Corollary 2

Multivariate Buckingham Π-Theorem II. Suppose that $\text{span}(\mathbf{A}) \setminus \text{span}(\mathbf{B}) \neq \emptyset$ and exclude responses such that $\mathbf{A}_j \notin \text{span}(\mathbf{A}_{-j}) \cup \text{span}(\mathbf{B})$ from consideration. Suppose that $0 < r_1 \leq r$ responses remain. Let r_2 be the number of responses not belonging to $\text{span}(\mathbf{B})$, let $\mathbf{A}^*$ be the dimension matrix corresponding to these responses and put $\mathbf{C} = \begin{bmatrix}\mathbf{A}^* & \mathbf{B}\end{bmatrix}$. Assume the following:

(i) A vector $\mathbf{Y} \in \mathbb{R}^{r_1}$ has a functional relationship with p predictors $(x_1, ..., x_p)$ given by $\mathbf{Y} = \mathbf{f}(x_1, ..., x_p)$ where $\mathbf{f}$ is an unknown function of the predictors.

(ii) The quantities $(Y_1, ..., Y_r, x_1, ..., x_p)$ involve m fundamental dimensions labeled by $L_1, ..., L_m$ where $m < p$ is assumed to ensure a meaningful problem.

(iii) Let conditions (iii)-(iv) be as in the Multivariate Buckingham Π-Theorem.

These assumptions give:

(i) The number of dimensionless predictors is $k = p - \text{rank}(\mathbf{B})$.

(ii) The number of dimensionless response variables is $r_3 = r_1 - \text{rank}(\mathbf{C}) + \text{rank}(\mathbf{B})$.

(iii) There exists a function $\mathbf{g} : \mathbb{R}^{r_1} \to \mathbb{R}^{r_3}$ such that

$$\mathbf{Y}' = \mathbf{g}(\mathbf{Y}) = \mathbf{g} \circ \mathbf{f}(x_1, ..., x_p) \tag{7.4}$$

can be written in dimensionless quantities. □

The proof of this Corollary is included in the Appendix. We now outline a four step procedure necessary for implementation of the DA model. The steps outlined here are similar to those in Albrecht, et al. (2013, section 2.4). However, our procedure differs from that in Albrecht, et al. (2013, section 2.4) because we need to account for when $\text{span}(\mathbf{A}) \setminus \text{span}(\mathbf{B}) \neq \emptyset$ occurs. Care is needed in identifying the functional form that describes the experiment when the response is multivariate.

Step 1. Identify which variables are responses and which are predictors. Before the DA model can take its form, the experimenter needs to identify the roles of the variables considered. The response variables $\{Y_1, ..., Y_r\}$ and the predictors $\{x_1, ..., x_p\}$ require specification. The set of variables $\{x_1, ..., x_p\}$ is complete if no other quantity has an effect on the response vector, and is independent if each quantity can be changed without altering the other $p-1$ quantities. This is to say that the predictors are defined on a product space. It is of utmost importance for the validity of the DA approach that the set of predictors is complete and independent. This rules out the consideration of simplex designs where uniform designs over all predictors do not produce marginal uniform designs for each predictor.

Step 2. Identify the dimensionless forms of the variables not in the basis set. The dimensionless forms must keep the role of the response variables intact.

Step 3. Identify a complete and dimensionally independent subset of variables. When the roles of variables are identified we then find a basis subset of variables in the context of base quantities and fundamental dimensions. In the case where $\text{span}(\mathbf{A}) \setminus \text{span}(\mathbf{B}) \neq \emptyset$ the functional form of interest may need changing. Also, new predictors may need to be considered and/or some response variables may need to be removed from consideration.

Step 4. Apply the Multivariate Buckingham Π*-Theorem to build the DA model.* Whether or not $\text{span}(\mathbf{A}) \subseteq \text{span}(\mathbf{B})$ holds with respect to the original variables under consideration,

the Multivariate Buckingham Π-Theorem preserves a functional relationship between dimensionless response variables and predictors.

We consult White (1999, p. 722) for an example of dimensional analysis in the presence of multiple responses. For a given pump design, the output variables gH and brake horsepower (bhp) should be dependent upon discharge Q, impeller diameter D, and shaft speed n, at least. Other possible parameters include fluid density ρ, viscosity μ, and surface roughness ϵ. Thus, we have a functional relation where $\mathbf{f} : \mathbb{R}^6 \to \mathbb{R}^2$ given by

$$\begin{pmatrix} gH \\ bhp \end{pmatrix} = \mathbf{f}(Q, D, n, \rho, \mu, \epsilon) \tag{7.5}$$

where the variables are comprised of dimensions as seen in the table below:

variable	dimensions
gH	$\left[L^2T^{-2}\right]$
bhp	$\left[ML^2T^{-3}\right]$
Q	$\left[L^3T^{-1}\right]$
D	$[L]$
n	$\left[T^{-1}\right]$
ρ	$\left[ML^{-3}\right]$
μ	$\left[ML^{-1}T^{-1}\right]$
ϵ	$[L]$

There are eight variables in this model and a total of three fundamental dimensions, length (L), mass (M) and time (T). In this example we see that $\text{span}(\mathbf{A}) \subseteq \text{span}(\mathbf{B})$. Therefore we can express the functional relationship (7.5) in terms of three dimensionless quantities as a result of the Multivariate Buckingham Π-Theorem. Implementation with respect to this example is continued in Section 5.

7.4 Design for DA with multiple responses

In this section, we consider the design of DA experiments for multiple responses. We assume that the DA model has been formulated, that there are r responses, $\mathbf{Y} = (Y_1, ..., Y_r)'$, p dimensionless factors, $\mathbf{x} = (x_1, \ldots, x_p)'$, so that our DA model can be written:

$$\mathrm{E}(\mathbf{y}|\mathbf{x}) = \mathbf{h}(\mathbf{x}) = \begin{pmatrix} h_1(\mathbf{x}) \\ \vdots \\ h_r(\mathbf{x}) \end{pmatrix}$$

In the univariate setting, when the form of the DA model h is unknown and potentially complex, Albrecht et al. (2013) identified the use of a nonparametric *uniform* design as one alternative. In a uniform design, the design points are distributed in such a way that the empirical cumulative distribution is as close as possible to the cumulative distribution of a uniform probability measure on the design space. We note that for nonparametric designs, the multivariate design will be the same as the univariate design for any one of the responses provided that predictors are defined on a product space. Thus, given the multivariate DA model, there are no new design issues.

The alternative approach suggested by Albrecht, et al. (2013) is to design for estimation of third- or higher-order polynomials in the dimensionless factors, and they advocated the use of D-optimal designs in that context. They also suggested that the integrated variance might be more appropriate for design of dimensional analysis experiments, since the objective is to predict the expected response over the design space. In this paper, V-optimality will be of primary design criterion of interest when polynomial models are to be estimated.

We will assume for simplicity that the design, denoted ξ_n, is exact and concentrated on the n design points $\mathbf{x}_1, \ldots, \mathbf{x}_n \in \mathbb{R}^p$. The value of the jth response variable for the ith run of the experiment can be modeled as:

$$y_j(\mathbf{x}_i) = \mathbf{g}_j'(\mathbf{x}_i)\boldsymbol{\beta}_j + \varepsilon_{ij}, \text{ for } i = 1, \ldots, n \text{ and } j = 1, \ldots, r \tag{7.6}$$

where the model vectors $\mathbf{g}_j(\mathbf{x})$, $j = 1, \ldots, r$, are known and the coefficient vectors $\boldsymbol{\beta}$ are unknown. The multivariate formulation of model (7.6) is constructed with

$$\boldsymbol{\beta} = \begin{pmatrix} \boldsymbol{\beta}_1 \\ \vdots \\ \boldsymbol{\beta}_r \end{pmatrix} \quad \mathbf{f}_j = \begin{pmatrix} \mathbf{0}_{j,1} \\ \mathbf{g}_j(\mathbf{x}) \\ \mathbf{0}_{j,2} \end{pmatrix}$$

for $j = 1, \ldots, r$ where $\mathbf{0}_{j,1} \in \mathbb{R}^{m_1+\cdots+m_{j-1}}$, $\mathbf{0}_{j,2} \in \mathbb{R}^{m_{j+1}+\cdots+m_r}$, $\boldsymbol{\beta}_j \in \mathbb{R}^{m_j}$ and $\mathbf{g}_j(\mathbf{x}) \in \mathbb{R}^{m_j}$ and $m_\cdot = m_1 + \cdots m_r$, and $\boldsymbol{\beta}_i$ and $\boldsymbol{\beta}_j$, $i \neq j$, do not have terms in common. Here it is possible that $\mathbf{f}_i$ and $\mathbf{f}_j$, $i \neq j$, may have terms in common, but there is no reason to expect the regression coefficients of the common terms to be the same. The covariance matrix of the response vector is also assumed known and denoted

$$\mathrm{Var}(\mathbf{y}|\mathbf{x}) = \mathbf{W}^{-1}(\mathbf{x})$$

where $\mathbf{W}(\mathbf{x})$ is the weight matrix for at $\mathbf{x}$. We assume that the weight matrix $\mathbf{W}(\mathbf{x})$ is known. This assumption is reasonable since variability of engineering measurement instruments is known. Let $\mathbf{F}(\mathbf{x})$ denote the $m \times r$ matrix $[\mathbf{f}_1(\mathbf{x}), \mathbf{f}_2(\mathbf{x}), \ldots, \mathbf{f}_k(\mathbf{x})]$. **Theorem 1.7.1 (Federov, 1972)**. The best linear estimator for $\boldsymbol{\beta}$ is

$$\hat{\boldsymbol{\beta}} = \mathbf{M}^{-1}(\xi_n)\mathbf{Y}$$

where

$$\mathbf{M}(\xi_n) = \sum_{i=1}^{n} \mathbf{F}(\mathbf{x}_i)\mathbf{W}(\mathbf{x}_i)\mathbf{F}'(\mathbf{x}_i) \qquad \text{and} \qquad \mathbf{Y} = \sum_{i=1}^{n} \mathbf{F}(\mathbf{x}_i)\mathbf{W}(\mathbf{x}_i)\mathbf{y}_i$$

The variance-covariance matrix of the estimator is

$$\mathbf{D}(\hat{\boldsymbol{\beta}}) = \mathbf{M}^{-1}(\xi_n)$$

Corollary 1. The best linear unbiased estimate of $\mathbf{f}_l'(\mathbf{x})\boldsymbol{\beta}$, for $l = 1, \ldots, r$ is the function

$$\hat{\eta}_l(\mathbf{x}) = \mathbf{f}_l'(\mathbf{x})\hat{\boldsymbol{\beta}}, \tag{7.7}$$

Let $\hat{\boldsymbol{\eta}}(\mathbf{x}) = [\hat{\boldsymbol{\eta}}_1(\mathbf{x}), \hat{\boldsymbol{\eta}}_2(\mathbf{x}), \ldots, \hat{\boldsymbol{\eta}}_k(\mathbf{x})]'$. The dispersion matrix of $\hat{\boldsymbol{\eta}}(\mathbf{x})$ is

$$\mathbf{d}(\mathbf{x}, \xi_n) = \mathbf{F}'(\mathbf{x})\mathbf{M}^{-1}(\xi_n)\mathbf{F}(\mathbf{x}).$$

We make two simplifying assumptions concerning $\text{Var}(\mathbf{y}|\mathbf{x})$:

1. The error variance matrix is constant over the design space. That is $\text{Var}(\mathbf{y}|\mathbf{x}) = \mathbf{W}^{-1}$.

2. The covariances of the errors are zero, that is:

$$\text{Var}(\mathbf{y}|\mathbf{x}) = \begin{bmatrix} \sigma_1^2 & & \\ & \ddots & \\ & & \sigma_r^2 \end{bmatrix} \text{ so that } \mathbf{W} = \begin{bmatrix} w_1 & & \\ & \ddots & \\ & & w_r \end{bmatrix}$$

   where $w_i = \sigma_i^{-2}$ for $i = 1, \ldots, r$.

For a discussion of multivariate design in the presence of correlated errors, see Cook and Nachtsheim (2017). Given these assumptions, we have:

$$\mathbf{M}(\xi_n) = \sum \mathbf{F}(\mathbf{x}_i)\mathbf{W}\mathbf{F}'(\mathbf{x}_i) \tag{7.8}$$

$$= \begin{bmatrix} w_1\mathbf{M}_1(\xi_n) & & \\ & \ddots & \\ & & w_r\mathbf{M}_r(\xi_n) \end{bmatrix} \tag{7.9}$$

where $\mathbf{M}_i(\xi_n) = \sum_{j=1}^{n} \mathbf{f}_i(\mathbf{x}_j)\mathbf{f}_i'(\mathbf{x}_j)$. One measure of the "goodness" of the design ξ is given by the D criterion:

$$|\mathbf{M}(\xi_n)| = \prod_{i=1}^{r} w_i|\mathbf{M}_i(\xi_n)| \tag{7.10}$$

If the r approximating models are identical such that $\mathbf{f}_1 = \cdots = \mathbf{f}_r$, the D criterion simplifies to:

$$|\mathbf{M}(\xi_n)| = (\prod_{i=1}^{r} w_i)|\mathbf{M}_1(\xi_n)|^r$$

Thus, the D-optimal design maximizes $|\mathbf{M}_1(\xi_n)|$. As noted, our emphasis herein will be on the minimization of the integrated variance of prediction, that is, the V criterion. We have from (7.9)

$$\mathbf{M}^{-1}(\xi_n) = \mathbf{D}^{-1}(\xi_n) = \begin{bmatrix} w_1^{-1}\mathbf{D}_1(\xi_n) & & \\ & \ddots & \\ & & w_r^{-1}\mathbf{D}_r(\xi_n) \end{bmatrix} \tag{7.11}$$

where $\mathbf{D}_i(\xi_n) = \mathbf{M}_i^{-1}(\xi_n)$, for $i = 1, \ldots, r$. Let $v_\chi = \int_\chi d\mathbf{x}$ denote the volume of the design space χ. Then the average value of the dispersion matrix $\hat{\boldsymbol{\eta}}(\mathbf{x})$ over the design space is:

$$\begin{aligned} v_\chi^{-1} \int_\chi \mathbf{d}(\mathbf{x}, \xi_n) d\mathbf{x} &= v_\chi^{-1} \int_\chi \mathbf{F}'(\mathbf{x})\mathbf{D}(\xi_n)\mathbf{F}(\mathbf{x}) d\mathbf{x} \\ &= v_\chi^{-1} \begin{bmatrix} w_1^{-1} \int_\chi \mathbf{f}_1(\mathbf{x})\mathbf{D}_1(\xi_n)\mathbf{f}_1(\mathbf{x}) d\mathbf{x} & & \\ & \ddots & \\ & & w_r^{-1} \int_\chi \mathbf{f}_r(\mathbf{x})\mathbf{D}_r(\xi_n)\mathbf{f}_r(\mathbf{x}) d\mathbf{x} \end{bmatrix} \end{aligned}$$

Since $\int_\chi \mathbf{f}_r(\mathbf{x})\mathbf{D}_r(\xi_n)\mathbf{f}_r(\mathbf{x})d\mathbf{x} = \text{Trace}[\mathbf{D}_i(\xi_n) \int_\chi \mathbf{f}_i(\mathbf{x})\mathbf{f}_1'(\mathbf{x})d\mathbf{x}] = \text{Trace}[\mathbf{D}_i\mathbf{M}_\chi]$, where $\mathbf{M}_\chi = \int_\chi \mathbf{f}_i(\mathbf{x})\mathbf{f}_1'(\mathbf{x})d\mathbf{x}$, we have:

$$v_\chi^{-1} \int_\chi \mathbf{d}(\mathbf{x}, \xi_n) d\mathbf{x} = v_\chi^{-1} \begin{bmatrix} w_1^{-1}\text{Trace}[\mathbf{D}_1\mathbf{M}_\chi] & & \\ & \ddots & \\ & & w_r^{-1}\text{Trace}[\mathbf{D}_r\mathbf{M}_\chi] \end{bmatrix}$$

At this point the criterion is multivariate. One natural way to reduce the criterion to a scalar is obtained by averaging. Let

$$V_{MV}(\xi_n) = r^{-1}v_\chi^{-1} \sum_{i=1}^{r} \text{Trace}[\mathbf{D}_i\mathbf{M}_\chi] \tag{7.12}$$

Similar to the determinant case, if the forms of the r approximating polynomials are identical, the criterion reduces to the minimization of the Trace$[\mathbf{D}_1\mathbf{M}_\chi]$.

7.5 Illustrations: Multivariate DA designs for pump design

We now continue with the pump design that is mentioned at the end of Section 3. In this section, we show how the Multivariate Buckingham Π-Theorem leads to a cheaper pump design with dimensionless variables. We can rewrite (7.5) as

$$\begin{pmatrix} \frac{gH}{n^2D^2} \\ \\ \frac{bhp}{\rho n^3 D^5} \end{pmatrix} = \mathbf{g}\left(\frac{Q}{nD^3}, \frac{\rho n D^2}{\mu}, \frac{\epsilon}{D}\right) \tag{7.13}$$

where $\frac{\rho n D^2}{\mu}$ and $\frac{\epsilon}{D}$ are recognized as the Reynolds number and roughness ratio respectively. Three new pump parameters have arisen:

$$\begin{aligned} \text{Capacity coefficient } C_Q &= \frac{Q}{nD^3} \\ \text{Head coefficient } C_H &= \frac{gH}{n^2D^2} \\ \text{Power coefficient } C_P &= \frac{bhp}{\rho n^3 D^5} \end{aligned}$$

For purposes of illustration, we make the simplifying assumption that the pump is being designed for use in one fluid only (e.g., water) and that roughness ratio is constant. Thus ϵ, μ, and ρ are constant. The response models become:

$$\begin{pmatrix} \frac{gH}{n^2D^2} \\ \\ \frac{bhp}{\rho n^3 D^5} \end{pmatrix} = \mathbf{g}\left(\frac{Q}{nD^3}, \frac{\rho n D^2}{\mu}\right) \tag{7.14}$$

where $\mathbf{g} : \mathbb{R}^3 \to \mathbb{R}^2$. Expression (7.14) is a valid dimensionless functional form by the

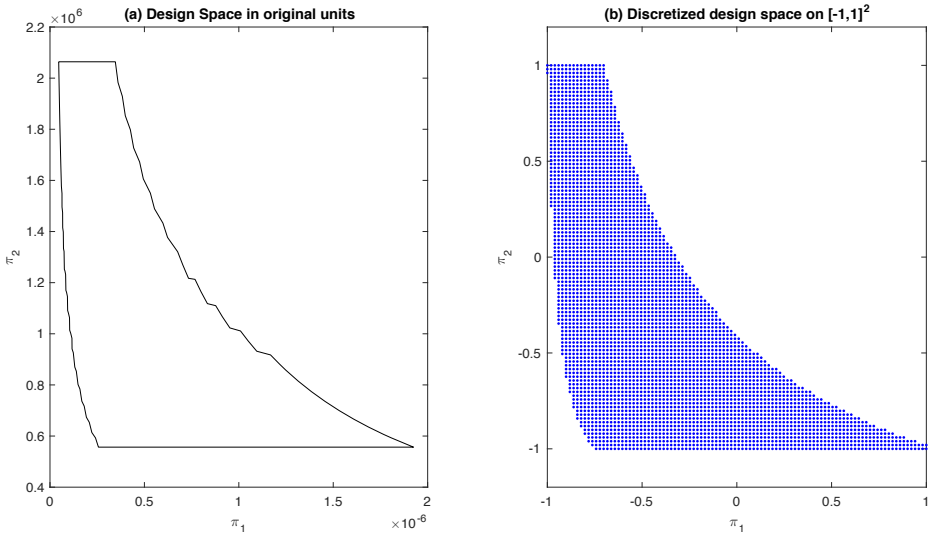

Figure 7.1: Design space for π_1 and π_2 in original units (a) and discretized and scaled to $[-1, 1]^2$

Multivariate Buckingham Π-Theorem since the set of fundamental dimensions present in the response variables is equal to the set of fundamental dimensions present in the predictors. The design region for the original variables variables Q, n, and D is

$$\chi = \{\, (Q, n, D) : 4 \leq Q \leq 30,\ 710 \leq n \leq 1170,\ 28 \leq D \leq 42 \,\}.$$

The dimensionless variables are $\pi_1 = \frac{Q}{nD^3}$ and $\pi_2 = nD^2$. The design region corresponding to the dimensionless π-variables is given by

$$\chi_\pi = \{\, (\pi_1, \pi_2) : \pi_1 = Q/(nD^3), \pi_2 = nD^2 \text{ where } (Q, n, D) \in \chi \,\}.$$

χ_π is shown in Figure 7.1(a), and a discretized version, scaled to $[-1, 1]^2$ is shown in Figure 7.1(b).

We now construct a series of alternative designs for this problem, assuming that $n = 16$. Albrecht et al., (2013) considered two alternatives: (1) the use of D-optimal designs for a full third-order (approximating) model; and (2) the use of nonparametric, uniform designs. They also suggested in Note that eight support points are in evidence, although two could easily be combined to provide an additional degree of freedom for pure error. For the third-

order approximation, a minimum of 10 support points and four levels for each factor are required. For π_1, there are many levels, for π_2 there are roughly four. Finally, the fourth-order approximation requires a minimum of 15 support points; the design has 16 distinct points spread somewhat uniformly through the design space.

7.5.1 Parametric design: $\mathbf{g}_1(\boldsymbol{\pi}) \neq \mathbf{g}_2(\boldsymbol{\pi})$

We now consider the case where the two approximating polynomials do not have the same form. In this case the design criteria will not reduce to familiar univariate criteria. For simplicity, we will assume that the first response requires a third-order approximating polynomial in both π_1 and π_1, and that the second response is cubic in π_2 only. The V-optimal design for the first response was previously computed and is shown in Figure 7.2(c). Optimal design theory tells us that the optimal approximate design for the second model will place 50% of the observations near zero, with the other 50% split evenly at the ± 1 boundaries. The V-Optimal multivariate design, as indicated by (7.12) will attempt to optimize both of these criteria simultaneously. Thus we expect to see a shifting of the points in Figure 7.2(c) toward $\pi_2 = 0$ and toward $\pi_2 = \pm 1$. The optimal multivariate design, shown in Figure 7.3, confirms this expectation.

7.5.2 Parametric design: $\bar{\mathbf{V}}$-optimal design for $\mathbf{g}_1(\boldsymbol{\pi}) = \mathbf{g}_2(\boldsymbol{\pi})$

Since we do not know in advance of the experiment what level of approximating polynomial will be required, a compromise approach is to use a $\bar{V}$-optimal design as suggested by Albrecht et al;.(2013). The $\bar{V}$-optimal design maximizes the average efficiency of the design for the alternative approximating polynomials considered. Here the experimenter would give the set of approximating polynomials that might be effective and assigns weights to each of the posited orders. As an example, we will assume that the models being considered are the first- through fourth-order models as previously considered in Figure 7.2. For simplicity and for purposes of illustration, we assign each model weight equal to 0.25. The $\bar{V}$-optimal design is shown in Figure 7.4.

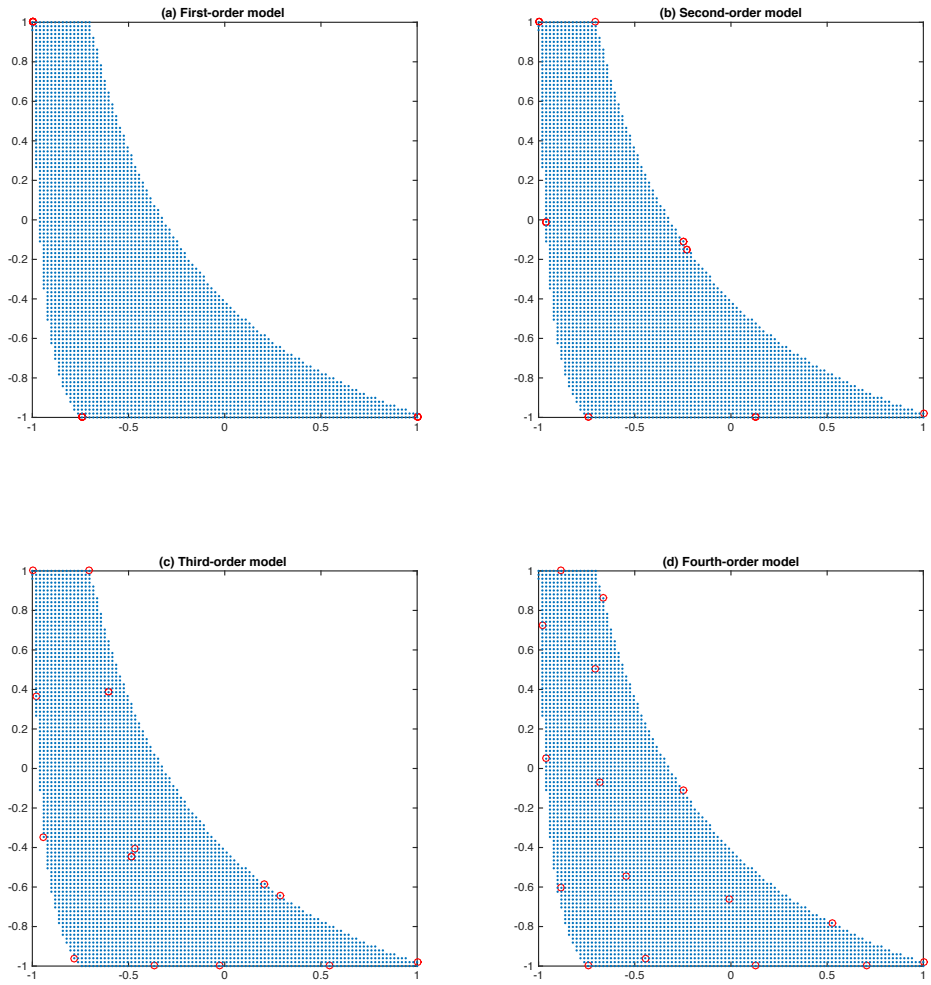

Figure 7.2: V-optimal designs for first- through fourth-order approximating polynomials for $n = 16$

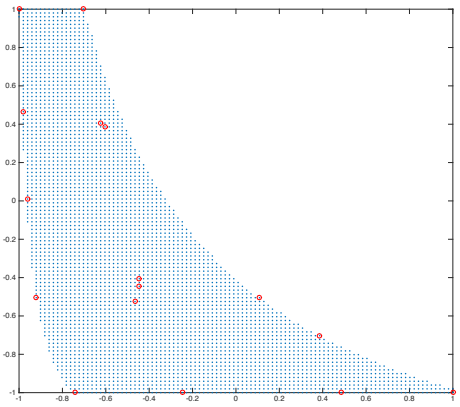

Figure 7.3: The multivariate design: $\mathbf{g}_1$ is a full third-order polynomial in π_1 and π_2; $\mathbf{g}_1$ is a quadratic in π_2 only.

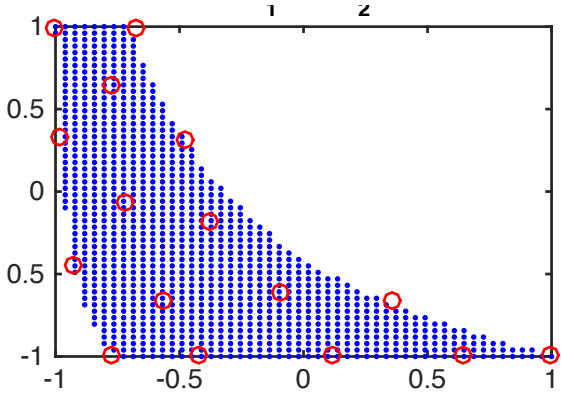

Figure 7.4: $\bar{V}$-optimal design given equal weighting of the first- through fourth-order approximating polynomials for $n = 16$

7.5.3 Robust-DA design

From a statistician's perspective, the traditional choice is the design space is χ, the design space in the base factors, $x_1, \ldots, x_n$. The traditional statistical approach is then to design an experiment that will permit efficient estimation of first- or second-order *empirical* models in those factors. From the engineer's perspective, a more economical and powerful design can be constructed in the lower-dimensional π-space. But any design setting in the π factors requires choosing specific values for each of the base factors. For example, the first dimensionless factor in the current example is $\pi_1 = \frac{Q}{nD^3}$. Recall that the design region in the original factors is $\chi = \{\, (Q, n, D) : 4 \leq Q \leq 30,\ 710 \leq n \leq 1170,\ 28 \leq D \leq 42 \,\}$. Suppose the DA design specified that in a particular run $\pi_1 = 0.5 \times 10^{-6}$. Referring to Figure 7.1, this refers to a value of π_1 that is just left of center. Various combinations of values of Q, n, and D can be employed to produce the desired result. Figure 7.5 shows values of Q, n, and D that lead to $\pi_1 = 0.5 \times 10^{-6}$. While all of these combinations lead to the desired value of π, some will be better than others as design points for the empirical design. This motivated the development of "Robust-DA" designs in Albrecht, et al. (2013). The basic idea is to construct highly efficient DA designs that are also efficient for the estimation of empirical models in χ. In this way, if a variable is omitted from the DA model, so that the DA model fails, a good design in the χ will have been fielded, and the empirical model can still be estimated efficiently.

Albrecht, et al. (2013) construct robust-DA designs using a compound design criterion. Let $E_{\mathrm{EMP}}(\xi)$ denote the V-efficiency of the empirical design ξ_n for estimation of full quadratic model in the base factors, and let $E_{\mathrm{DA}}(\xi)$ denote the efficiency of the DA design. For $0 \leq w \leq 1$, let E^w_{RDA} denote the weighted average of the empirical design efficiency and the DA design efficiency:

$$E^w_{\mathrm{RDA}} = (1 - w)E^w_{\mathrm{DA}} + wE_{\mathrm{EMP}}(\xi) \tag{7.15}$$

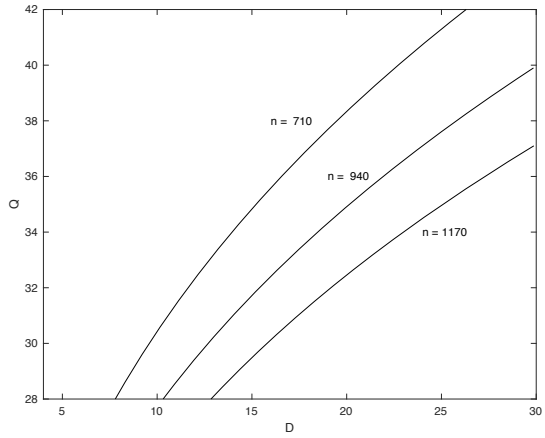

Figure 7.5: Combinations of Q, n, and D that yield $\pi_1 = 0.5 \times 10^{-6}$

We can now define the robust-DA design as follows:

$$E_{\text{RDA}} = \underset{w}{\text{argmax}} E^w_{\text{RDA}}$$

In practice, to find a robust-DA design, we compute E^w_{RDA} for a grid of w values between zero and one and then choose the design that maximizes (7.15). Albrecht, et al. (2013) recommend the use of a "w-trace", that is, a plot of E^w_{RDA}, E_{DA}, and $E^w_{\text{EMP}}(\xi)$ against w, as an aid to choosing a design.

We constructed a robust-DA design using $\bar{V}$-optimality as the criterion for the DA design with equal weights for first through fourth-order polynomial models, and V-optimality for the second-order empirical model in the base factors. For ease of exposition, we have chosen a sparse w-grid based on seven values. For ease of exposition we only consider seven values in order to communicate efficiency trade-offs. We recommend searching through a finer grid of possible w values in actual design problems. The w-trace is shown in Figure 7.6. From the figure, we see that E^w_{RDA} is maximized for $w = 0.4$ For this design the V-efficiency of the empirical design is 0.68 and the $\bar{V}$-efficiency of the DA design is 0.95. This yields $E^{0.4}_{\text{RDA}} = 0.84$.

The progression of empirical and DA designs as w varies from zero to one is shown in Figure 7.7. For $w = 0$, the empirical design places most of the observations at the

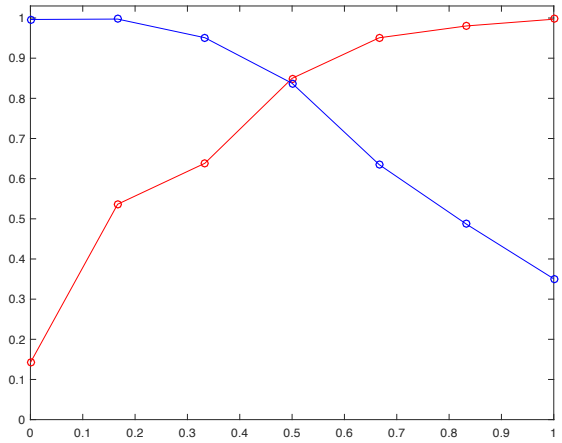

Figure 7.6: Trade-off (w-trace) plot for robust DA designs

boundaries of the design space with just a few points at the corners or near the center. As w increases, the design points gravitate (as much as possible) toward the corners, the edge centers and the center of the design space. These locations, of course, comprise the support of the empirical V-optimal design. On the negative side, as w increases, the near uniform spread through the design space, clearly in evidence for $w = 0$, degrades as w increases.

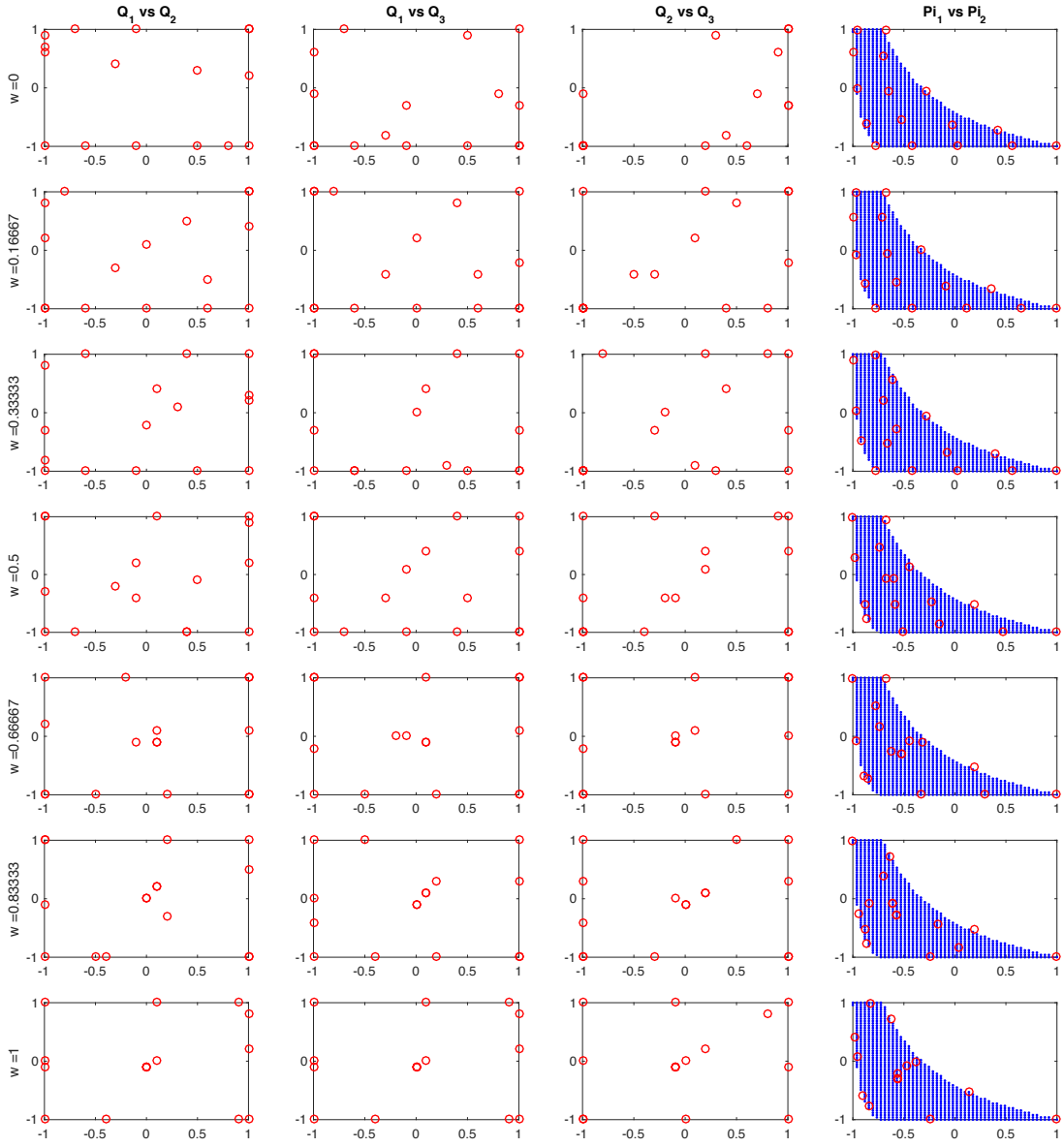

Figure 7.7: DA designs for the χ-space and for χ_π-space for varying w

7.6 Discussion

In this paper, we have developed new methodology for designing DA experiments when there is more than one response. We began by extending the Buckingham Pi-Theorem has been extended to the multivariate case. We then developed basic criteria for multivariate design of experiments and we illustrated various approaches for a DA problem involving mechanical pump design.

Our multivariate extension of DA design techniques allow for scalable experiments and have the potential to reduce the dimensions of the design problem when multiple responses are of interest. This methodology provides an appropriate design context when response variables are of incomparable fundamental dimensions (eg, one is length and one is mass). After the DA procedure is applied, the previously incomparable responses are then dimensionally homogeneous. The multivariate DA experiment design allows for reduction of design costs in two ways. There is the potential to run smaller experiments since the DA model is of lower dimension than the original model. Then the experiment can be run on much smaller units because results obtained from the DA model are scalable. This methodology works when that the span of dimension matrix for the response variables A is contained in the span of dimension matrix for the explanatory variables B and no relevant fundamental dimensions are missing in the functional form (3). Absence of a key fundamental dimension is fatal but such a design flaw can be mitigated through the robust DA design or the addition of more predictors. Adding more variables to the experiment can seem prohibitively costly but this cost can be largely offset or completely recovered through scalability of the DA experiment.

Other points:

Algorithms: Can search in the Q space and project to the π-space or can search directly in the π-space. The latter will generally involve irregular designs spaces, so that the space should first be discretized and then a candidate-set-based row-exchange algorithm, such as the modified Fedorov algorithm (Cook and Nachtsheim (1980)) can be used. Alternatively, searching in the often regular Q-space (this notation has to change because we have an

actual Q in the example). requires a higher-dimensional search, and the projections of the points into the π-space will not be uniform, which can negatively affect the search. Examples showing what can be an extreme lack of uniformity are given in Albrecht, et al. (2013). For robust-DA designs, the search *must* be carried out in the Q-space so that the empirical design in the Q space can be optimized.

7.7 Appendix

In this Appendix, we provide the proofs of the Multivariate Buckingham Π-Theorem and then its Corollary. The following is the proof of the Multivariate Buckingham Π-Theorem.

Proof: We have $\mathbf{Y} \in \mathbb{R}^r$ as our response vector, $\mathbf{x} \in \mathbb{R}^p$ as our vector of predictors, and m fundamental dimensions where assumption (ii) states that all fundamental dimensions are represented by elements in the vector of predictors. The dimensions of elements in either the response vector or the vector of predictors can be written as

$$[Y_j] = \prod_{i=1}^{m} L_i^{a_{ij}}, \quad j = 1, ..., r$$
$$[x_j] = \prod_{i=1}^{m} L_i^{b_{ij}}, \quad j = 1, ..., p$$

Now, for the first dimension L_1, consider invariance under arbitrary scaling. Let $L_1^* = e^{\varepsilon} L_1$ where $\varepsilon \in \mathbb{R}$ and according to this scaling define

$$Y_i^* = e^{a_{1i}\varepsilon} Y_i, \quad i = 1, ..., r, \tag{7.16}$$

$$x_j^* = e^{b_{1j}\varepsilon} x_j, \quad j = 1, ..., p. \tag{7.17}$$

These equations define a one-parameter Lie group of the $p+r$ quantities $(x_1, ..., x_p, Y_1, ..., Y_r)$. This group is induced by the one-parameter group of scalings of the fundamental dimension

L_1. Assumption (iv) says that equation (7.3) holds iff

$$(Y_1^*, ..., Y_r^*)' = \mathbf{f}(x_1^*, ..., x_p^*)$$

holds for all $\varepsilon \in \mathbb{R}$. Consider the following three cases that occur when trivialities exist in our original problem.

(i) : $b_{11} = \cdots = b_{1p} = 0$ and/or at least one $a_{1j} \neq 0$ for some $j = 1, ..., r$ which implies that L_1 is not a fundamental dimension for the problem and $\mathbf{Y}_j = 0$ whenever $a_{1j} \neq 0$.

(ii) : If in case (i) we have $a_{1j} \neq 0$ for all $j = 1, ..., r$ then $\mathbf{Y} = \mathbf{0}_r$ where $\mathbf{0}_r$ is the 0's vector in $\mathbb{R}^r$.

(iii) : If only one $b_{1j} \neq 0$ for some $j = 1, ..., p$ and $a_{1i} = 0$ for all $i = 1, ..., r$, then either $\mathbf{Y} = \mathbf{0}_r$ and L_1 is a fundamental dimension for the problem or $\mathbf{Y}$ is independent of x_j and L_1 is not a fundamental dimension for the problem.

Suppose the problem is set up so that cases (i)-(iii) do not occur. It follows that $b_{1j} \neq 0$ for some $j = 1, ..., p$. Without loss of generality, assume that $b_{11} \neq 0$. Define new measurable quantities

$$\begin{aligned} W_{i-1} &= x_i x_1^{-b_{1i}/b_{11}} \quad i = 2, ..., p, \\ W_p &= x_1, \end{aligned}$$

and

$$\mathbf{V} = (Y_1 W_1^{-a_{11}/b_{11}}, ..., Y_r W_1^{-a_{1r}/b_{11}})'.$$

Then formula (7.3) is equivalent to

$$\mathbf{V} = \mathbf{F}(W_1, ..., W_p)$$

where $\mathbf{F}$ is an unknown function and the group of transformations seen in (7.16) and (7.17) yields

$$\begin{aligned}
&\mathbf{V}^* = \mathbf{V},\\
&W_i^* = W_i, \quad i = 1, ..., p-1,\\
&W_p^* = e^{b_{11}\varepsilon} W_p,
\end{aligned}$$

so that $(V_1, ..., V_r, W_1, ..., W_{p-1})$ are invariants of (7.16) and (7.17). These quantities satisfy assumption (iii) and

$$\mathbf{V}^* = \mathbf{F}(W_1, ..., W_p)$$

holds as a result of assumption (iv). Hence,

$$\mathbf{V}^* = \mathbf{F}(W_1, ..., W_{p-1}, e^{\varepsilon b_{11}} W_p)$$

for all $\varepsilon \in \mathbb{R}$. Consequently, $\mathbf{F}$, is independent of W_p. Moreover, the measurable quantities $(W_1, ..., W_{p-1})$ and the elements of $\mathbf{V}$ are power-law combinations of the original $(x_1, ..., x_p)$. Formula (7.3) reduces to

$$\mathbf{V} = \mathbf{H}(W_1, ..., W_{p-1}),$$

where all variables are dimensionless with respect to L_1 and $\mathbf{H}$ is an unknown function. This argument is repeated for the other $m-1$ fundamental dimensions. The repetition of this argument reduces (7.3) to a dimensionless formula one fundamental dimension at a time. We arrive at the functional form

$$\tilde{\boldsymbol{\pi}} = \mathbf{h}(\pi_1, ..., \pi_k),$$

where

$$\tilde{\boldsymbol{\pi}} = \begin{pmatrix} \tilde{\pi}_1 \\ \vdots \\ \tilde{\pi}_r \end{pmatrix} = \operatorname{diag}\left(\prod_{i=1}^{p} \mathbf{x}_i^{y_{i1}}, ..., \prod_{i=1}^{p} \mathbf{x}_i^{y_{ir}} \right) \begin{pmatrix} Y_1 \\ \vdots \\ Y_r \end{pmatrix}.$$

Next it is shown that the number of measurable dimensionless predictors is in fact $p - \text{rank}(\mathbf{B})$. This follows immediately since

$$\left[\prod_{j=1}^{p} x_i^{\pi_{ij}}\right] = 1 \quad \text{if and only if} \quad \mathbf{B}x_i = 0$$

and $\mathbf{Bx} = 0$ has $p - \text{rank}(\mathbf{B})$ linearly independent solutions. The vectors $\mathbf{y}_i$ are chosen such that

$$\left[Y_i \prod_{j=1}^{r} x_j^{\rho_{ji}}\right] = 1.$$

This choice is valid because of assumption (ii). Therefore $\mathbf{By}_i = -\mathbf{a}_i$ for $i = 1, ..., r$ and this completes the proof. □

The following is the proof of the Corollary to the Multivariate Buckingham Π-Theorem.

Proof: Conclusion (i) follows using the same techniques in the proof of the Multivariate Buckingham Π-Theorem. Now to show that conclusion (ii) holds. The argument used to show that conclusion (i) holds shows that variables corresponding to the dimension matrix $\mathbf{C}$ can be made into $k' = p + r_2 - \text{rank}(\mathbf{C})$ dimensionless quantities. $k' - k$ of these dimensionless quantities are responses. A little algebra shows that there are r_3 dimensionless responses in total. We can see that a function $\mathbf{g}$ exists (satisfying (7.4)) by combining what has already been proved, assumption (i), and the Multivariate Buckingham Π-Theorem. The other assumptions are necessary for these manipulations to hold. This completes the proof. □

Chapter 8

Central Limit Theory under Additive Deformations

8.1 Introduction

The classical central limit theorem (CLT) is a cornerstones of statistics. We generalize this classical result to settings in which standard addition on the real line is replaced by a binary operation that satisfies Lie group properties. Additional mild smoothness assumptions are also imposed, allowing us to obtain explicit limiting distributions.

Our principal motivation comes from physics. As explained by Tempesta (2011), different Lie group operations on the real line are associated with distinctive forms of entropy that extend Boltzmann–Gibbs entropy, which corresponds to standard addition and classical central limit theory. Tsallis entropy applies to statistical systems exhibiting the features of long range dependence (Tsallis, 1988), and has been successfully applied, for example, in image thresholding (Portes de Albuquerque et al., 2004), modeling debris flow (Singh and Cui, 2015), analyzing electromagnetic pre-seismic emissions (Potirakis et al., 2012), and modeling the distribution of momenta of cold atoms in optical lattices (Douglas et al., 2006). Kaniadakis entropy arises when combining momenta in special relativity (Kaniadakis, 2006, 2013), and its associated central limit theory has recently been developed by McKeague (2015), who showed that the limiting distributions take the form of hyperbolic functions of standard normals.

There is a general formulation of the CLT on locally compact Lie groups due to Wehn

(1962), but conditions are placed on the random elements after they are logarithmically mapped into the Lie algebra (tangent space at the identity). The limit distribution is described in terms of the infinitesimal generator of a semi-group of probability measures on the Lie group, but in general it does not have an explicit form. In our setting of Lie groups on the real line, however, we are able to provide an explicit CLT using only classical conditions on the random summands and a mild smoothness condition on the associated logarithmic map. Our main result generalizes the classical CLT to this setting, and addresses an open problem raised by (Tempesta, 2011, Section VIII) as to whether under suitable conditions an analogue of the CLT holds for "universality classes" related to generalized types of entropy, including those mentioned above.

We also establish an extension of our main result to more severe deformations that arise when the smoothness condition on the logarithmic map is relaxed (for which a slower than $\sqrt{n}$-normalization is required). We then discuss in detail all the Lie group examples mentioned above, as well as the operation for combining velocities in special relativity, and more severe additive deformations defined via exponentiation.

Both the Tsallis and Kaniadakis universality classes involve fitting parameters, so the question naturally arises as to the effect of a random specification of such parameters on the central limit behavior of the system. We investigate this question by Monte Carlo simulation studies, and reach the somewhat surprising conclusion that there is a universal limit law in the sense that it is determined solely by the form of the deformation and the expected value of the fitting parameter.

8.2 CLTs under additive deformations

Our results extend the classical CLT on the real line to allow additive deformations of the following form. Standard addition is replaced by a group operation $\oplus$ defined on an open and possibly infinite interval G, with $(G, \oplus)$ assumed to be a Lie group under the usual topology on the real line. Since all Lie groups on the real line are isomorphic to their Lie algebra $(\mathbb{R}, +)$, there exists an isomorphism $g : G \to \mathbb{R}$ (that is unique up to scalar

multiples) such that

$$g(x \oplus y) = g(x) + g(y) \tag{8.1}$$

for all $x, y \in G$. In Lie group terminology, g is called the "logarithmic" map, and its inverse $f = g^{-1}$ the "exponential" map. Let $e \in G$ be the identity, and denote $G_e = G - e$. We now give our main result showing that if g has a second order Taylor expansion around e, in which the leading term is linear, then the CLT extends to $\oplus$-addition.

Theorem 17

Let $\{X_i\}$ be a sequence of iid G_e-valued mean-zero random variables with finite variance σ^2, and let $X_{n,i} = e + X_i/\sqrt{n}$. Suppose there exists a function $\rho : G_e \to \mathbb{R}^+$ such that

$$\rho(x) \to 0 \text{ as } x \to 0, \qquad \rho(x/s) \leq M \text{ for } x \in G_e,\ s \geq s_0 \tag{8.2}$$

$$|g(e + x) - x - ax^2| \leq x^2 \rho(x) \quad \text{for } x \in G_e, \tag{8.3}$$

where a, $s_0 > 1$ and $M > 0$ are prespecified constants. Also suppose there exist constants c_1, c_2, c_3, and $s_1 > 0$, such that for all $x \in G_e$ and $s \geq s_1$,

$$s|g(e + x/s)| \leq c_1|x|1(|x| \geq c_2) + c_3. \tag{8.4}$$

Then

$$X_{n,1} \oplus X_{n,2} \oplus ... \oplus X_{n,n} \xrightarrow{d} f(Z) \tag{8.5}$$

□

where $Z \sim N(a\sigma^2, \sigma^2)$.

Remarks:

1. The key smoothness condition (8.3) in Theorem 17 is that g has a parabolic local approximation at the identity e. The parabola can take the general form $x \mapsto a(x -$

$e)^2 + b(x-e)$, the only requirements being that it go through $(e,0)$, since $g(e)=0$, and that $b \neq 0$ (so the leading term is linear). The coefficients a and b, along with σ^2, determine the "bias" of the normal r.v. Z that appears in the limit; for simplicity we stated the result just for the case $b=1$ (giving bias $a\sigma^2$), but the result extends to the general case, where the limit is $f(bZ_b)$ with $Z_b \sim N(a\sigma^2/b, \sigma^2)$. This follows from Theorem 17 with a changed to a/b, and the maps g and f changed to $x \mapsto g(x)/b$ and $x \mapsto f(bx)$, respectively. When g is locally approximated by a straight line $x \mapsto b(x-e)$ (i.e., $a=0$), there is no bias.

2. In Section 3 we will examine various examples in which we can find the logarithmic map g, along with its local parabolic approximation, leading to an explicit limit distribution. A classical and well-known instance arises in connection with the CLT for products of positive r.v.s, in which case $G=(0,\infty)$, $x \oplus y = xy$ for $x,y \in G$, $e=1$, $g=\log$, $f=\exp$, and the limit distribution is log-normal. Specifically, our result gives $\prod_{i=1}^n X_{n,i} \xrightarrow{d} \exp(Z)$, where $Z \sim N(-\sigma^2/2, \sigma^2)$, where $X_i > -1$ is assumed to have mean zero and finite variance σ^2. Condition (8.3) holds in this case by a Taylor series expansion of $x \mapsto \log(1+x)$ around $0 \in G_e = (-1,\infty)$, namely

$$|\log(1+x) - x + x^2/2| \leq x^2\rho(x), \quad x > -1, \tag{8.6}$$

where $\rho(x) = |x/(1+x)|$ satisfies (8.2) with $M = 1/(s_0-1)$ for any $s_0 > 1$. This expansion is verified in Section Section 8.3.2.

3. Condition (8.4) was only used in the proof to allow dominated convergence arguments to be applied to $\sqrt{n}g(X_1/\sqrt{n})$ and $ng(X_1/\sqrt{n})^2$. However, if X_1 is assumed to have a finite *fourth* moment then (8.4) is not needed and the theorem continues to hold, as shown in Lemma 10.

Proof: For simplicity we assume that the identity $e = 0$, so $G_e = G$, but the proof easily extends to the general case. By the definition of isomorphism, we have

$$\begin{aligned} X_{n,1} \oplus X_{n,2} \oplus ... \oplus X_{n,n} &= f\left[g(X_{n,1}) + g(X_{n,2}) + ... + g(X_{n,n})\right] \\ &= f\left[\sum_{i=1}^{n} \left(g(X_{n,i}) - \mathrm{E}\, g(X_{n,i})\right) + n\,\mathrm{E}\, g(X_{n,1})\right]. \end{aligned}$$

Therefore,

$$X_{n,1} \oplus X_{n,2} \oplus ... \oplus X_{n,n} = f\left[T_n + n\,\mathrm{E}\, g(X_{n,1})\right] \tag{8.7}$$

where $T_n = \sum_{i=1}^{n} \left(g(X_{n,i}) - \mathrm{E}\, g(X_{n,i})\right)$. The Lindeberg–Feller theorem is used to find the asymptotic distribution of T_n. We first find the asymptotic variance of T_n. For $s > s_0$,

$$\begin{aligned} |sg(x/s) - x| &\le |sg(x/s) - x - ax^2/s| + |a|x^2/s \\ &\le \rho(x/s)x^2/s + |a|x^2/s \\ &\le x^2(M + |a|)/s, \end{aligned}$$

where the last two inequalities follow from assumptions (8.2) and (8.3), so

$$\lim_{s\to\infty} sg(x/s) = x \tag{8.8}$$

for all $x \in G$. From assumption (8.4), we have $|\sqrt{n}g(X_{n,1})| \le c_1|X_1|1(|X_1| \ge c_2) + c_3$ and $\left[\sqrt{n}g(X_{n,1})\right]^2 \le 2c_1^2X_1^2 + 2c_3^2$, so by dominated convergence and (8.8), $\mathrm{E}\left[\sqrt{n}g(X_{n,1})\right] \to \mathrm{E}\, X_1 = 0$ and $\mathrm{E}\left[\sqrt{n}g(X_{n,1})\right]^2 \to \sigma^2$, resulting in

$$\mathrm{Var}(T_n) = n\,\mathrm{Var}\left(g(X_{n,1})\right) = \mathrm{E}\left(\sqrt{n}g(X_{n,1})\right)^2 - \left(\mathrm{E}\,\sqrt{n}g(X_{n,1})\right)^2 \to \sigma^2.$$

We next check the Lindeberg condition. Fix $\varepsilon > 0$ and note that

$$\begin{aligned} &\sum_{i=1}^{n} \mathrm{E}\left[\left(g(X_{n,i}) - \mathrm{E}\, g(X_{n,i})\right)^2 1(|g(X_{n,i}) - \mathrm{E}\, g(X_{n,i})| > \varepsilon)\right] \\ &\le \mathrm{Var}(T_n) - \mathrm{E}\left[\left(\sqrt{n}g(X_{n,1}) - \mathrm{E}(\sqrt{n}g(X_{n,1}))\right)^2 1((\sqrt{n}g(X_{n,1}) - \mathrm{E}(\sqrt{n}g(X_{n,1})))^2 \le t)\right] \end{aligned}$$

provided $t \leq n\varepsilon^2$. The variance term above tends to σ^2 (as we have already seen). If t is a fixed continuity point of the distribution of X_1^2 then the last term above tends to $-\operatorname{E} X_1^2 1\{X_1^2 \leq t\}$ by the continuous mapping theorem and dominated convergence, which in turn tends to $-\sigma^2$ as $t \to \infty$ by dominated convergence. Therefore the Lindeberg condition holds and $T_n \xrightarrow{d} N(0, \sigma^2)$. The result then follows form (8.7) using Slutsky's lemma and the continuous mapping theorem provided we show $nEg(X_{n,1}) \to a\sigma^2$. Using the zero mean property of X_1 and assumption (8.3) we have

$$\begin{aligned} |n \operatorname{E} g(X_{n,1}) - a\sigma^2| &\leq n \operatorname{E} |g(X_{n,1}) - X_{n,1} - aX_{n,1}^2| \\ &\leq n \operatorname{E} \left[X_{n,1}^2 \rho(X_{n,1})\right] = \operatorname{E}\left[X_1^2 \rho(X_1/\sqrt{n})\right] \end{aligned}$$

which tends to zero by (8.2) and dominated convergence. □

Lemma 10

Suppose the conditions of Theorem 17 hold with (8.4) replaced by $\operatorname{E}(X_1^4) < \infty$. Then $n \operatorname{E} g(X_1/\sqrt{n})^2 \to \sigma^2$ and the conclusion of the theorem continues to hold. □

Proof: Assume that $e = 0$ as in the proof of Theorem 17. For $x \in G$ we have

$$\begin{aligned} ng\left(\frac{x}{\sqrt{n}}\right)^2 &= ng\left(\frac{x}{\sqrt{n}}\right)^2 \pm x^2 \pm \frac{a^2x^4}{n} \pm 2ax^2 g\left(\frac{x}{\sqrt{n}}\right) \\ &\quad \pm 2\sqrt{n}xg\left(\frac{x}{\sqrt{n}}\right) \pm \frac{2ax^3}{n} \\ &\leq \left|\sqrt{n}g\left(\frac{x}{\sqrt{n}}\right) - x - \frac{ax^2}{\sqrt{n}}\right|^2 - x^2 - \frac{a^2x^4}{n} + \frac{2ax^3}{n} \\ &\quad + 2\sqrt{n}xg\left(\frac{x}{\sqrt{n}}\right) + 2ax^2 g\left(\frac{x}{\sqrt{n}}\right) \\ &\leq \rho\left(\frac{x}{\sqrt{n}}\right)^2 \frac{x^4}{n} - x^2 - \frac{a^2x^4}{n} + \frac{2ax^3}{n} \\ &\quad + 2\sqrt{n}xg\left(\frac{x}{\sqrt{n}}\right) + 2ax^2 g\left(\frac{x}{\sqrt{n}}\right), \end{aligned}$$

where

$$\begin{aligned} 2\sqrt{n}xg\left(\frac{x}{\sqrt{n}}\right) &= 2\sqrt{n}xg\left(\frac{x}{\sqrt{n}}\right) \pm 2x^2 \pm \frac{2ax^3}{\sqrt{n}} \\ &\leq 2x\Big|\sqrt{n}g\left(\frac{x}{\sqrt{n}}\right) - x - \frac{ax^2}{\sqrt{n}}\Big| + 2x^2 + \frac{2x^3}{\sqrt{n}} \\ &\leq 2\rho\left(\frac{x}{\sqrt{n}}\right)\frac{x^3}{\sqrt{n}} + 2x^2 + \frac{2x^3}{\sqrt{n}}, \end{aligned}$$

and

$$\begin{aligned} 2ax^2 g\left(\frac{x}{\sqrt{n}}\right) &= 2ax^2 g\left(\frac{x}{\sqrt{n}}\right) \pm \frac{2ax^3}{n} \pm \frac{2a^2x^4}{n} \\ &\leq \frac{2ax^2}{n}\Big|\sqrt{n}g\left(\frac{x}{\sqrt{n}}\right) - x - \frac{ax^2}{\sqrt{n}}\Big| + \frac{2ax^3}{n} + \frac{2a^2x^4}{n} \\ &\leq \frac{2ax^4}{n^{3/2}}\rho\left(\frac{x}{\sqrt{n}}\right) + \frac{2ax^3}{n} + \frac{2a^2x^4}{n}. \end{aligned}$$

Using the above inequalities, we can construct a dominator of $ng(x/\sqrt{n})^2$ that does not depend on n. By (8.2), for n sufficiently large we have that $\rho(x/\sqrt{n}) \leq M$ for all $x \in G$, so a suitable dominator is given by

$$h(x) = (M^2 + 2|a|M + 2a^2)x^4 + 2(1 + 2|a| + M)|x|^3 + 2x^2.$$

The assumption that X_1 has a finite fourth moment guarantees that $\mathrm{E}\, h(X_1) < \infty$, so (8.8) gives $n\,\mathrm{E}\, g(X_1/\sqrt{n})^2 \to \sigma^2$ by dominated convergence. A similar argument, but only requiring finite second moment (and zero mean), shows that $\sqrt{n}\,\mathrm{E}\, g(X_1/\sqrt{n}) \to 0$. Inspection of the proof of Theorem 17 shows that (8.4) was only used to provide these two limits. □

We now proceed with a generalization of Theorem 2 in McKeague (2015). In this setting, $G = \mathbb{R}$ and the inverse isomorphism g is defined over all of $\mathbb{R}$. The classical Lindeberg–Feller theorem is extended by this second result. Unlike the results obtained in McKeague (2015), our second result does not contain Theorem 17 as a special case. For Theorem 18 to hold, the following assumptions are required:

A1. Let $\{X_{n,i}\}$ be a triangular array of mean-zero random variables that are independent across rows.

A2. $\sum_{i=1}^{n} \mathrm{E}\left(X_{n,i}^2 1(|X_{n,i}| > \eta)\right) \to 0$ for all $\eta > 0$.

A3. $\sum_{i=1}^{n} \mathrm{Var}(X_{n,i}) \to \sigma^2 < \infty$

The conditions $A1$-$A3$ are nothing more than the conditions of the classical Lindeberg Feller CLT. We now state Theorem 18.

Theorem 18

Suppose $A1$–$A3$ hold. Let $G = \mathbb{R}$ and suppose there exists $\rho : G \to \mathbb{R}^+$ where $\rho(x) \to 0$ as $x \to 0$ and $M > 0$ such that $\rho(x) \leq M$ for all $x \in G$, and

$$|g(x+e) - x| \leq \rho(x)x^2. \tag{8.9}$$

holds for all $x \in \mathbb{R}$. Then

$$X_{n,1} \oplus X_{n,2} \oplus ... \oplus X_{n,n} \xrightarrow{d} f(Z)$$

where $Z \sim N(0, \sigma^2)$. □

Proof: First, we have

$$X_{n,i} \oplus \cdots \oplus X_{n,n} = f\left[\sum_{i=1}^{n} g(X_{n,i})\right] \quad \text{and} \quad \sum_{i=1}^{n} g(X_{n,i}) = S_n + R_n$$

where $S_n = \sum_{i=1}^{n} X_{n,i}$ and $R_n = \sum_{i=1}^{n} [g(X_{n,i}) - X_{n,i}]$. We have $S_n \to N(0, \sigma^2)$ from the Lindeberg–Feller CLT and Slutsky's Lemma. We now show that $R_n \xrightarrow{P} 0$. We have

$$|R_n| \leq \sum_{i=1}^{n} |g(X_{n,i}) - X_{n,i}| \leq \sum_{i=1}^{n} \rho(X_{n,i}) X_{n,i}^2.$$

Let $\varepsilon > 0$ be arbitrarily chosen. We can choose an $\eta > 0$ such that $\sup_{\delta \in [-\eta, \eta]} \rho(\delta) < \varepsilon/\sigma^2$. We have

$$\sum_{i=1}^{n} \mathrm{E}\left(\rho(X_{n,i}) X_{n,i}^2\right) = \sum_{i=1}^{n} \mathrm{E}\left(\rho(X_{n,i}) X_{n,i}^2 1(|X_{n,i}| > \eta)\right)$$

$$+\sum_{i=1}^{n} \mathrm{E}\left(\rho(X_{n,i})X_{n,i}^2 1(|X_{n,i}|<\eta)\right)$$
$$\leq M\sum_{i=1}^{n} \mathrm{E}\left(X_{n,i}^2 1(|X_{n,i}|>\eta)\right) + \frac{\varepsilon}{\sigma^2}\sum_{i=1}^{n} \mathrm{E}\left(X_{n,i}^2\right)$$

where

$$M\sum_{i=1}^{n} \mathrm{E}\left(X_{n,i}^2 1(|X_{n,i}|>\eta)\right) + \frac{\varepsilon}{\sigma^2}\sum_{i=1}^{n} \mathrm{E}\left(X_{n,i}^2\right) \to \varepsilon$$

as $n \to \infty$. Therefore $\mathrm{E}\,|R_n| \to 0$ which shows $R_n \xrightarrow{P} 0$ and

$$\sum_{i=1}^{n} g(X_{n,i}) \xrightarrow{d} N(0,\sigma^2)$$

from Slutsky's Lemma. Our desired result follows from the continuous mapping theorem. □

The assumption that g has a parabolic approximation with a linear trend was crucial for Theorem 17 in the sense that it is the natural condition for the case of $\sqrt{n}$-normalization. We now show that higher-order approximations to g also lead to CLTs, provided the normalization matches the order of the leading term in the approximation, and the sum is centered by a "drift" term. When the approximation to g has no *linear* leading term, the deformation can cause the drift term to tend to infinity, so in general a tight limiting distribution is not possible without centering.

Suppose that g does not have a parabolic local approximation at the identity e. In this case we suppose that

$$|g(e+x) - \sum_{j=1}^{p} a_j x^{k_j}| \leq \rho(x)x^{k_p}$$

holds in place of (8.3) where $1 \leq k_1 < k_2 < \cdots < k_p$ with k_1 odd and $a_j \neq 0$ for $j = 1, ..., p$. Then

$$\lim_{s\to\infty} sg(e + x/s) = 0$$

when $k_1 > 1$ for all $x \in G$. The proof of Theorem 1 requires that the condition (8.3) implies that

$$\lim_{s\to\infty} sg(e + x/s) = x$$

holds for all $x \in G$. When g does not have a parabolic local approximation at the identity e, then the CLT can not be extended to $\oplus$-addition at $\sqrt{n}$ normalization. In Theorem 19, we show that the CLT can be extended to $\oplus$-addition where $X_{n,i} = e + n^{-1/k_1} X_1$.

Theorem 19

Suppose there exists a function $\rho : G_e \to \mathbb{R}^+$ satisfying (8.2) and

$$|g(e+x) - \sum_{j=1}^{p} a_j x^{k_j}| \leq \rho(x) x^{k_p} \tag{8.10}$$

for all $x \in G_e$, where the a_j and $1 \leq k_1 < k_2 < \cdots < k_p$ are prespecified, with $a_1 = 1$. Assume

$$|sg(e + s^{-1/k_1} x)| \leq c_1 |x|^{k_1} 1(|x| \geq c_2) + c_3 \tag{8.11}$$

for all $x \in G_e$ and $s > s_1$, where c_1, c_2, c_3 and $s_1 > 0$ are prespecified. Let $\{X_i\}$ be a sequence of iid G_e-valued random variables with $\mathrm{E}(X_1^{k_1}) = 0$ and $\sigma^2 = \mathrm{E}(X_1^{2k_1}) < \infty$. Let $X_{n,i} = e + n^{-1/(2k_1)} X_i$. Then

$$X_{n,1} \oplus X_{n,2} \oplus ... \oplus X_{n,n} \ominus f(\mu_n) \xrightarrow{d} f(Z) \tag{8.12}$$

where $Z \sim N(0, \sigma^2)$ and $\mu_n = n \,\mathrm{E}\, g(X_{n,1})$. □

Proof: The proof follows similar lines to the first part of Theorem 17, so we do not repeat all the details. Again assume that the identity $e = 0$. From (8.1), with T_n defined as before, but now with $n \,\mathrm{E}\, g(X_{n,1})$ moved to the other side of the equation, it suffices to use the Lindeberg–Feller theorem to find the asymptotic distribution of T_n. Conditions (8.2) and (8.10) give

$$\left| sg(s^{-1/k_1} x) - x^{k_1} - \sum_{j=2}^{p} a_j s^{1-k_j/k_1} x^{k_j} \right| \leq s^{1-k_p/k_1} \rho(s^{-1/k_1} x) x^{k_p} \to 0$$

as $s \to \infty$, so

$$\lim_{s\to\infty} sg(s^{-1/k_1}x) = x^{k_1} \tag{8.13}$$

for each $x \in G$. From (8.11),

$$\left[\sqrt{n}g(n^{-1/(2k_1)}x)\right]^2 \leq 2c_1^2 x^{2k_1} 1(|x| \geq c_2) + 2c_3^2$$

for all $n > s_1^2$, so by dominated convergence and (8.13) we have

$$\mathrm{E}\left[\sqrt{n}g(X_{n,i})\right]^2 \to \mathrm{E}(X_1^{2k_1}).$$

A similar argument shows that $\mathrm{E}[\sqrt{n}g(X_{n,i})] \to \mathrm{E}(X_1^{k_1}) = 0$. Thus,

$$\mathrm{Var}(T_n) = n\,\mathrm{Var}\left(g(X_{n,1})\right) = \mathrm{E}\left(\sqrt{n}g(X_{n,1})\right)^2 - \left(\mathrm{E}\,\sqrt{n}g(X_{n,1})\right)^2 \to \mathrm{E}(X_1^{2k_1}).$$

The Lindeberg condition is checked is the same way as before, so $T_n \xrightarrow{d} N(0, \sigma^2)$. □

8.3 Examples

Statistical systems that can be described in terms of Boltzmann–Gibbs entropy are associated with classical addition. Since both the logarithmic and exponential maps are the identity in this setting, the conditions of Theorem 17 are satisfied trivially. It is immediately seen that our main theorem generalizes the classical CLT. In this section we present several examples that go beyond the classical setting.

8.3.1 Kaniadakis addition

Our result can be used to derive a relativistic CLT given by McKeague (2015), who considered the case of Kaniadakis addition:

$$x \overset{\kappa}{\oplus} y = x\sqrt{1+\kappa^2 y^2} + y\sqrt{1+\kappa^2 x^2},$$

representing the addition of momenta in special relativity. The parameter $0 < \kappa \leq 1$ is the reciprocal of the speed of light in the ambient space (when all variables are expressed in

dimensionless units). The Lie group $(\mathbb{R}, \overset{\kappa}{\oplus})$ has exponential map $f_\kappa(x) = \sinh(\kappa x)/\kappa$, and logarithmic map

$$g_\kappa(x) = \frac{1}{\kappa}\sinh^{-1}(\kappa x) = \frac{1}{\kappa}\log(\kappa x + \sqrt{1+\kappa^2 x^2}).$$

Condition (8.3) can be checked using an inequality in McKeague (2015), which yields

$$|g_\kappa(x) - x| \leq x^2\rho(x)$$

with $\rho(x) = \kappa\min(\kappa|x|, 1)$ for all $x \in \mathbb{R}$. This ρ is bounded everywhere and $\rho(x) \to 0$ as $x \to 0$, so condition (8.2) holds. Further, $|g_\kappa(x)| \leq |x|$, so (8.4) holds. Therefore, all conditions of Theorem 17 are met, and we conclude that, for any iid sequence $\{X_i\}$ of mean-zero random variables with finite variance σ^2,

$$X_{n,1} \overset{\kappa}{\oplus} X_{n,2} \overset{\kappa}{\oplus} ... \overset{\kappa}{\oplus} X_{n,n} \xrightarrow{d} \frac{1}{\kappa}\sinh(\kappa Z)$$

where $Z \sim N(0, \sigma^2)$. In this setting, Z has mean zero since (8.3) is satisfied with $a = 0$. We have reached the same conclusion as (McKeague, 2015, Theorem 1).

McKeague (2015) also derived CLTs for velocity and energy using identities of Kaniadakis (2006) and the continuous mapping theorem to translate the corresponding CLT for momentum into velocity and energy. Our Theorem 1 provides a more direct approach. Velocities are combined according to the Einstein addition rule

$$x \overset{v}{\oplus} y = \frac{x+y}{1+\kappa^2 xy}$$

for $x, y \in G = (-1/\kappa, 1/\kappa)$, and the corresponding Lie group $(G, \overset{v}{\oplus})$ has exponential map $f_v(x) = \frac{1}{\kappa}\tanh(\kappa x)$ and logarithmic map

$$g_v(x) = \frac{1}{\kappa}\tanh^{-1}(\kappa x) = \frac{1}{2\kappa}\log\left(\frac{1+\kappa x}{1-\kappa x}\right).$$

We now verify that (8.3) holds:

$$|g_v(x) - x| \leq \rho(x)x^2$$

with $\rho(x) = |x/(1-\kappa|x|)|$. This ρ obviously satisfies condition (8.2). The function $h(x) = x^2\rho(x) - |g_v(x) - x|$ has derivative

$$h'(x) = \left(\frac{x^2}{1-\kappa|x|}\left(\frac{\kappa x^2}{|x|(1-\kappa|x|)} + 1\right) + \frac{\kappa^2 x^2}{1-\kappa^2 x^2} + \frac{2x^2}{1-\kappa|x|}\right)\text{sign}(x),$$

which is negative when $x < 0$, positive when $x > 0$. Since $h_v(0) = 0$, it follows that $h(x) \geq 0$ for all $x \in G$, so condition (8.3) holds as claimed. Similarly, the derivative of $x \mapsto \kappa|x| - g_v(x)$, namely

$$\kappa \left[1 - \frac{|x|}{\kappa^2 x^2 - 1} \right] \text{sign}(x),$$

is negative for $x < 0$ and positive for $x > 0$, so condition (8.4) holds with $c_1 = \kappa, c_2 = c_3 = 0$. All the conditions of Theorem 17 are satisfied, and we conclude that if $\{X_i\}$ is an iid sequence of mean-zero G-valued random variables with variance σ^2 (which is necessarily finite), then

$$X_{n,1} \overset{v}{\oplus} X_{n,2} \overset{v}{\oplus} ... \overset{v}{\oplus} X_{n,n} \xrightarrow{d} \frac{1}{\kappa} \tanh(\kappa Z)$$

where $Z \sim N(0, \sigma^2)$.

8.3.2 Tsallis addition

We next show that our theory leads to CLTs under addition associated with Tsallis entropy. Tsallis addition is a combination of standard addition and multiplication:

$$x \overset{q}{\oplus} y = x + y + (1-q)xy,$$

where $x, y \in G = (-1/(1-q), \infty)$, and $0 \leq q < 1$. The exponential map $f_q : \mathbb{R} \to G$ and respective logarithmic map g_q are given by

$$f_q(x) = \frac{\exp((1-q)x) - 1}{1-q}, \quad \text{and,} \quad g_q(x) = \frac{\log(1 + (1-q)x)}{1-q},$$

respectively. Condition (8.3) of Theorem 17 holds by a Taylor series expansion of g_q around $0 \in G$, namely

$$|g_q(x) - x + (1-q)x^2/2| \leq x^2 \rho(x), \quad x > -1,$$

where $\rho(x) = |x/(1+x)|$ and $a = -(1-q)/2$. This expansion follows from (8.6) in Remark 1, where we already noted that ρ satisfies condition (8.2). Let

$$h(x) = x^2 \rho(x) - |\log(1+x) - x + x^2/2|. \tag{8.14}$$

The derivative

$$h'(x) = \left(\frac{x}{x+1}\right)^3 \left|\frac{x+1}{x}\right| + 2x\left|\frac{x}{x+1}\right| - \frac{x^2}{x+1}\,\mathrm{sign}\left(x^2 - 2x + 2\log(1+x)\right)$$

is negative for $-1 < x < 0$ and positive for $x > 0$. Since $h(0) = 0$, we then have $h(x) \geq 0$ for all $x \in G$, so (8.6) holds. Next we check that (8.4) holds for g_q with $q = 0$, from which the case of general g_q follows immediately. First it is easy to check that $|s\log(1+x/s)| \leq |x|$ for all $s > s_0 > 1$ when $x > 0$. Second, suppose $-1 < x < 0$. From the monotonicity of the logarithm, $s\log(1-1/s) \leq s\log(1+x/s) \leq 0$. Fix $\varepsilon > 0$. As seen in the proof of Theorem 17, condition (8.3) implies that $sg(x/s) \to x$ as $s \to \infty$. Thus, for some positive s_1, we have

$$-1 - \varepsilon \leq s\log(1-1/s) \leq s\log(1+x/s) \leq \varepsilon$$

for all $s > s_1$. Therefore condition (8.4) holds with

$$s|\log(1+x/s)| \leq |x|1(|x| \geq 1) + 1 + \varepsilon.$$

All of the conditions of Theorem 17 are now verified for Tsallis addition, and we conclude that if $\{X_i\}$ is an iid sequence of mean-zero random variables with finite variance σ^2 then $X_{n,1} \overset{q}{\oplus} X_{n,2} \overset{q}{\oplus} ... \overset{q}{\oplus} X_{n,n} \xrightarrow{d} f_q(Z)$, where $Z \sim N(-(1-q)\sigma^2/2, \sigma^2)$.

Example 3.1. (*Tsallis addition and the product of positive random variables.*) The verification of the conditions of Theorem 17 for the product of iid positive random variables in Remark 1 overlaps with the verifications for Tsallis addition. This is because there is a direct connection between the two binary operations: $(1+x)(1+y) = 1 + x \overset{q}{\oplus} y$ for Tsallis addition with $q = 0$. We can then derive the limit distribution of the product as a shifted version of the limit in the CLT under Tsallis addition. To see this, express $X_{n,i}$ in Remark 1 as $1 + Y_{n,i}$, where $Y_{n,i} = X_i/\sqrt{n}$, so when $q = 0$ we have $\prod_{i=1}^n X_{n,i} = 1 + Y_{n,1} \overset{q}{\oplus} \cdots \overset{q}{\oplus} Y_{n,n}$.

It is now apparent that as a consequence of Theorem 17 distinct central limit theories are associated with Boltzmann–Gibbs, Kaniadakis, and Tsallis group entropies. Tsallis entropy is the only one of these to exhibit asymptotic bias in the sense that the normally distributed Z appearing in the limit $f(Z)$ has non-zero mean. The bias is due to the

presence of a second-order term in the Taylor expansion of the corresponding logarithmic map.

8.3.3 Deformations via exponentiation

We now provide an example that falls outside of the scope of Theorem 17, but that is covered by Theorem 19 which allows for more extreme types of deformations, provided the normalization of the summands is chosen appropriately. Consider the Lie group on $G = \mathbb{R}$ with binary operation

$$x \overset{\alpha}{\oplus} y = (x^\alpha + y^\alpha)^{1/\alpha}\,, \tag{8.15}$$

where $\alpha \geq 1$, the integer part of α is odd, and $x^\alpha = \exp\left[\alpha \log |x|\right] \text{sign}(x)$. The identity element is $e = 0$, the exponential map $f_\alpha(x) = x^{1/\alpha}$, and the logarithmic map $g_\alpha(x) = x^\alpha$. Condition (8.10) is satisfied with $\rho(x) = 0$, $p = 1$, $a_1 = 1$ and $k_1 = \alpha$. Condition (8.11) holds with $c_1 = c_2 = 1$ and $c_3 = 0$. Let $\{X_i\}$ be an iid sequence of random variables with $\mathrm{E}(X_1^\alpha) = 0$ and $\sigma^2 = \mathrm{E}(X_1^{2\alpha}) < \infty$ and put $X_{n,i} = n^{-1/(2\alpha)} X_i$. Then (8.12) holds, and since there is no drift in this case ($\mu_n = 0$), we conclude that $X_{n,1} \overset{\alpha}{\oplus} X_{n,2} \overset{\alpha}{\oplus} ... \overset{\alpha}{\oplus} X_{n,n} \xrightarrow{d} Z^{1/\alpha}$ where $Z \sim N(0, \sigma^2)$.

8.4 Random additive deformations

A basic assumption of the central limit theory we have developed is that the additive deformation is fixed. In particular, under Tsallis and Kaniadakis addition, the deformations are determined by the parameters q and κ. In this section, we present the results of a simulation study in which these parameters are allowed to be random. For applications of Kaniadakis addition, a random κ can arise when there are local variations in the ambient space through which (relativistic) particles are moving. In typical applications of Tsallis addition, q is regarded as a fitting parameter (Portes de Albuquerque et al., 2004), so treating it as random provides a way of adjusting for uncertainty about its actual value.

Suppose the iid mean-zero random variables X_i, normalized as $X_{n,i} = X_i/\sqrt{n}$, are combined according to

$$X_{n,1} \overset{\kappa_1}{\oplus} X_{n,2} \overset{\kappa_2}{\oplus} \cdots \overset{\kappa_{n-1}}{\oplus} X_{n,n} \tag{8.16}$$

where the κ_i are iid and $x \overset{\kappa}{\oplus} y = x + y + \kappa xy$, as in Tsallis addition with $\kappa = 1 - q$, or $x \overset{\kappa}{\oplus} y = x\sqrt{1+\kappa^2 y^2} + y\sqrt{1+\kappa^2 x^2}$ as in Kaniadakis addition. Associativity no longer holds, so we need to specify the order of operations in (8.16). The order is assumed to be from left to right, as in $((\ldots((X_{n,1} \overset{\kappa_1}{\oplus} X_{n,2}) \overset{\kappa_2}{\oplus} X_{n,3}) \overset{\kappa_3}{\oplus} \cdots) \overset{\kappa_{n-1}}{\oplus} X_{n,n}$. We have found from simulations that the sampling distribution appears to be the same in the reverse order, or in fact in any order, but we do not have a proof of this.

It would be interesting to establish the existence of limiting distributions of sums of the form (8.16), that are universal in the sense that they do not depend on the distributions of X_i or κ_i, but only on certain features of these distributions (such as their mean an variance) and on features of the deformation. This appears to be a very challenging problem. Our simulation studies, however, do shed some light on the question of whether such a universal limit exists.

A broad simulation study provides support for this finding across a wide range of scenarios. The behavior of sampling distributions for (8.16) is investigated for two data generating models with six additive parameter distributions each for both Tsallis and Kaniadakis addition. The sampling distributions corresponding to each scenario are constructed with one million samples of size $n = 2000$. The settings and empirical results are displayed in Table 8.1. It should be noted that the distribution of the X_i has been standardized and the additive parameter distributions have been shifted and scaled so that the mean is 1/2 and the standard deviation is 0.10. The densities of the sampled random sums from Table 8.1 are plotted in Figure 8.1. The curves in both panels of Figure 8.1 provide strong visual evidence for the existence of a universal limit law.

The numerical summaries in Table 8.1 further support the visual evidence in favor of the existence of a universal limit law. A Kolmogorov–Smirnov test between each sampling

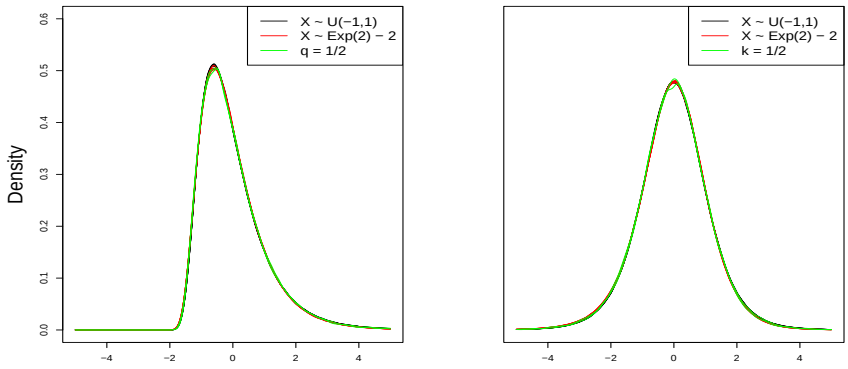

Figure 8.1: Evidence for the existence of a universal limit law. The sampling distributions for the simulation settings in Table 8.1 are plotted here. The left panel displays the density curves corresponding to the Tsallis case. The right panel displays the density curves corresponding to the Kaniadakis case. The green lines correspond to density curves for the fixed $q = \kappa = 1/2$ case for both data generating distributions and both addition operations.

distribution in Table 8.1 and a sampling distribution with fixed $\kappa = q = 1/2$ shows no significant difference at any reasonable testing level. Shapiro–Wilks tests between each sampling distribution in Table 8.1 and the asymptotic log-normal (Tsallis case) and sinh-normal (Kanidakis case) distributions also provide evidence in favor of a universal limit law. The `shapiro.test` function used to implement the Shapiro–Wilks tests in `R` can only handle a maximum of five thousand entries. As a result of this, we repeatedly sample five thousand entries from the million possible values a total of ten thousand times and report the proportion of p-values exceeding 0.05. What is striking about this procedure is the vast differences in the proportion of p-values exceeding 0.05 across addition operations and data generating distributions alike. The exponential data generating model and Tsallis addition are seen to be further away from asymptopia than the uniform data generating model and Kaniadakis addition respectively.

Figure 8.2 offers some additional explanation to the difficulties that arise when random deformations are considered. The left panel displays the results for Tsallis addition. In the Tsallis case, we consider fixed $q = 1$ (regular addition), $q = 1/2$, and $q = 0$ as reference distributions and we generate $q \sim U(0, 1)$ to form a random deformation. The black line depicts the sampling distribution of our random deformation where the additive parameter

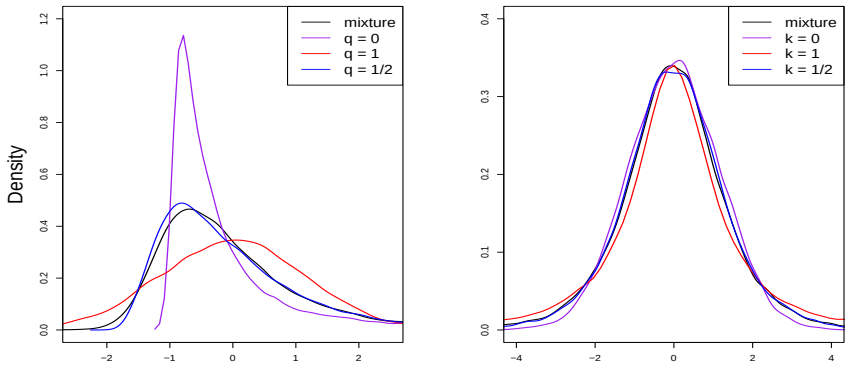

Figure 8.2: The random variables are generated as $X \sim U(-2, 2)$ for all sampling distributions in both panels. The sampling distributions are constructed with twenty thousand samples of size $n = 1000$. The left panel depicts sampling distributions for Tsallis addition at three fixed q values and one random deformation with $q \sim U(0, 1)$. The right panel depicts sampling distributions for Kaniadakis addition at three fixed κ values and one random deformation with $\kappa \sim U(0, 1)$.

has mean 1/2. The sampling distribution with q generated at random is similar in appearance to the sampling distribution with a fixed additive parameter equal to the mean of q. However, this similarity is not enough to suggest that a mathematical argument can be made to prove this observation true. This is because the sampling distribution takes on mass below the theoretical lower bound value of -2 when $q = 1/2$ is fixed.

The right panel of Figure 8.2 displays simulation results for Kaniadakis addition. In the Kaniadakis case, we consider $\kappa = 0$ (regular addition), $\kappa = 1/2$, and $\kappa = 1$ as reference distributions and we generate $\kappa \sim U(0, 1)$ to form a random deformation. The discrepancies between the sampling distributions in the Kaniadakis case are much less than those seen in the Tsallis case. Just as before, the sampling distribution with κ generated at random is similar in appearance to the sampling distribution with a fixed additive parameter equal to the mean of κ.

8.5 Discussion

Our theorems extend classical central limit theory to cases in which random variables are combined with a binary operation satisfying Lie group properties. We have shown that

different algebraic deformations with distinct isomorphisms yield different limiting distributions. The three statistical systems considered, the combination of velocity mentioned in McKeague (2015), and α-norms of random variables all arise as special cases of our extended central limit theorems.

Theorem 1 in McKeague (2015) provided the inspiration for the development of our theory. However, (McKeague, 2015, Theorem 1) arises as a very special case of our theorems. In particular, g has a local linear approximation instead of a local parabolic approximation, $g : \mathbb{R} \to \mathbb{R}$, and $\rho(x)$ is bounded everywhere. However, these properties do not hold in generality and they are relaxed in the present work. As a consequence, limiting normal distributions in (8.5) are not necessarily mean-zero and operations not defined over all of $\mathbb{R}$ have extensions. Theorem 19 then relaxes the requirement that g has a local parabolic approximation. In this Theorem, the approximation to g is then more general than a second order Taylor expansion.

The generality of our theory allows us to find the limiting distribution when random elements are combined via Tsallis addition. We are not the only authors to investigate limiting distributions in this setting. Umarov, et al. (2008) presents a q-central limit theory motivated by nonextensive statistical mechanics and Tsallis addition. In their setting, random variables are correlated and generalizations of independence (q_k-independence) are characterized by the Fourier transform defined within (Umarov, Tsallis, and Steinberg, 2008, section 2.4 and definition 3.2). They show that a q_k-independent sequence q_k converges to a q_{k-1}-normal distribution(Umarov, Tsallis, and Steinberg, 2008, Theorem 1). The statistical context of this result is not immediately apparent. Our theorems show that classical central limit theory can be extended to nonextensive statistical mechanics by exchanging standard addition with Tsallis addition when random variables meet classical assumptions.

The simulation studies within provide strong evidence in favor of the existence of a universal limit law. This universal limit law states that when additive parameters are themselves random, the sampling distribution of (8.16) will converge to that of (8.5) where the fitting parameter in (8.5) is the mean of the random additive parameters in (8.16). The evidence suggests that random deformations converge to the asymptotic distributions with

fixed parameters given by our theorems. In addition, the output in Table 8.1 suggests that some data generating mechanisms and addition operations approach the universal limit law faster than others.

Table 8.1: Simulation results. The first column displays the type of addition. The second column displays the data generating mechanism. The third column displays the additive parameter generating mechanism. The distributions in the third column have been scaled to have a mean of 0.5 and a standard deviation of 0.1. The random variables Y_1 through Y_3 are given below. The fourth column displays the p-values of the Kolmogorov–Smirnov test comparing to the fixed parameter setting $q = \kappa = 1/2$. The final column displays the proportion of Shapiro–Wilks p-values exceeding 0.05. A Shapiro–Wilks p-value greater than 0.05 suggests that the asymptotic distribution of the random combination is log-normal (Tsallis case) or sinh-normal (Kaniadakis case) where $q = \kappa = 1/2$.

Addition	distribution of data	distribution of κ or q	KS p-value	SW p-value proportion
Tsallis	$X \sim U(-1,1)$	$q \sim Y_1$	0.755	0.572
		$q \sim Y_2$	0.675	0.554
		$q \sim Y_3$	0.703	0.561
		$q \sim Beta(1/2, 1/2)$	0.648	0.529
		$q \sim Beta(1,3)$	0.764	0.557
		$q \sim Beta(3,1)$	0.781	0.565
	$X \sim Exp(2) - 2$	$q \sim Y_1$	0.347	0.066
		$q \sim Y_2$	0.465	0.058
		$q \sim Y_3$	0.565	0.048
		$q \sim Beta(1/2, 1/2)$	0.352	0.046
		$q \sim Beta(1,3)$	0.470	0.057
		$q \sim Beta(3,1)$	0.689	0.068
Kaniadakis	$X \sim U(-1,1)$	$\kappa \sim Y_1$	0.531	0.950
		$\kappa \sim Y_2$	0.728	0.941
		$\kappa \sim Y_3$	0.569	0.942
		$\kappa \sim Beta(1/2, 1/2)$	0.456	0.948
		$\kappa \sim Beta(1,3)$	0.399	0.952
		$\kappa \sim Beta(3,1)$	0.545	0.950
	$X \sim Exp(2) - 2$	$\kappa \sim Y_1$	0.336	0.423
		$\kappa \sim Y_2$	0.293	0.400
		$\kappa \sim Y_3$	0.212	0.415
		$\kappa \sim Beta(1/2, 1/2)$	0.291	0.444
		$\kappa \sim Beta(1,3)$	0.344	0.377
		$\kappa \sim Beta(3,1)$	0.312	0.424

$$Y_1 = \begin{cases} 1/3 & \text{w.p. } 1/2 \\ 2/3 & \text{w.p. } 1/2 \end{cases} \qquad Y_2 = \begin{cases} 1/3 & \text{w.p. } 1/3 \\ 2/3 & \text{w.p. } 2/3 \end{cases} \qquad Y_3 = \begin{cases} 1/3 & \text{w.p. } 2/3 \\ 2/3 & \text{w.p. } 1/3 \end{cases}$$

Appendix A

References

Albrecht, M., Nachtsheim, C., Albrecht, T., and Cook, R. D. (2013). Experimental Design for Engineering Dimensional Analysis. *Technometrics*, **55**, 251–271.

Amemiya, T. (1985). *Advanced Econometrics.* Harvard University Press, Cambridge, MA.

Andrews, D. W. K. (2002). Higher-Order Improvements of a Computationally Attractive k-Step Bootstrap for Extremum Estimators. *Econometrica*, **70**, 1, 119–162.

Barndorff-Nielsen, O. (1978). *Information and Exponential Families.* Wiley, Chichester.

Berk, R., Brown, L., Buja, A., Zhang, K., and Zhao, L. (2013). Valid post-selection inference. *Annals of Statistics*, **41**, 2, 802–837.

Bickel, P. J. and Freedman, D. A. (1981). Some Asymptotic Theory for the Bootstrap. *The Annals of Statistics*, **9**, 6, 1196-1217.

Billingsley, P. (1999). *Conergence of Probability Measures*, second edition. New York: Wiley.

Billingsley, P. (2012). *Probability and Measure.* Wiley, New Jersey.

Blows, M. W., and R. Brooks. (2003). Measuring nonlinear selection. *The American Naturalist* **162**:815–820.

Bluman, G. W. and Sukeyuki, K. (1989). *Symmetries of Differential Equations*, Springer-Verlag, New York.

Bridgman, P. W. (1931). *Dimensional Analysis* (2nd ed.) New Haven, CT: Yale University Press.

Breiman, L. (1996). Bagging Predictors. *Machine Learning*, **24**, 123–140.

Brown, L. D. (1986). *Fundamentals of Statistical Exponential Families: with Applications in Statistical Decision Theory.* Institute of Mathematical Statistics, Hayward, CA.

Buckingham, E. (1914) On Physically Similar Systems. *Physical Review*, **4**, 345–376.

Buckland, S. T., Burnham, K. P., and Augustin, N. H. (1997). Model Selection: An Integral Part of Inference. *Biometrics*, **53**, 603–618.

Bürger, R. and Lynch, M. (1995). Evolution and Extinction in a Changing Environment: A Quantitative-Genetic Analysis. *Evolution*, **49**, 151–163.

Burnham, K. P. and Anderson, D. R. (2004). Multimodel Inference. *Sociological and Methods Research*, **33**, 261–304.

Chang, S. I. (1994). Some Properties of Multiresponse D-optimal Designs. *Journal of Mathematical Analysis and Applications*, **184**, 256–282.

Charlesworth, B. (1980). *Evolution in age-structured populations.* Cambridge Univ. Press, Cambridge, U. K.

Charmantier, A., and P. Gienapp. (2014). Climate change and timing of avian breeding and migration: evolutionary versus plastic changes. *Evolutionary Applications*, **7**:15–28.

Chatterjee, S. and Bose, A. (2000). Variance Estimation in High Dimensional Models. *Statistica Sinica*, **10**, 497–515.

Childs, D. Z., M. Rees, K. E. Rose, P. J. Grubb, and S. P. Ellner. (2004). Evolution of size-dependent flowering in a variable environment: construction and analysis of a stochastic integral projection model. *Proceedings of the Royal Society B*, **271**:425–434.

Claeskens, G. and Hjort, N. L. (2008). *Model Selection and Model Averaging*. Cambridge University Press, Cambridge.

Clutton-Brock, T., and B. C. Sheldon. (2010). Individuals and populations: the role of long-term, individual-based studies of animals in ecology and evolutionary biology. *Trends in Ecology and Evolution*, **25**:562-573.

Cook, R. Dennis, and Nachtsheim, Christopher J. (1980). A Comparison of Algorithms for Constructing Exact D-Optimal Designs. *Technometrics*, **24**(1), 49–54.

Cook, R. Dennis, and Nachtsheim, Christopher J. (1982). Model Robust Linear-Optimal Designs. *Technometrics*, **22**(3), 315–324.

Cook, R. D. Li, B., and Chiaromonte, F. (2010). Envelope models for parsimonious and efficient multivariate linear regression. *Statistica Sinica*, **20**, 927–1010.

Cook, R. D. (2013). Course notes for Stat 8932 topics class on envelope models. `http://users.stat.umn.edu/~rdcook/Stat8932F13/`

Cook, R. D., Helland, I. S., and Su, Z. (2013), Envelopes and partial least squares regression. *Journal of the Royal Statistical Society* B, **75**, 791–910

Cook, R. D. and Su, Z. (2016). Scaled Predictor Envelopes and Partial Least Squares Regression. *Technometrics*, **58**, 155–165.

Cook, R. D. and Zhang, X. (2015a). Foundations for Envelope Models and Methods. *Journal of the American Statistical Association*, **110:510**, 599–611.

Cook, R. D. and Zhang, X. (2015b). Algorithms for Envelope Estimation. *Journal of Computational and Graphical Statistics*, `10.1080/10618600.2015.1029577`.

Csiszár, I. and Matúš, F (2005). Closures of Exponential Families. *Annals of Probability*, **33**, 582–600.

Diaconis, P. and Efron, B. (1983). Computer Intensive Methods in Statistics *Scientific America*, **248**.

Diamond, S. E., and J. G. Kingsolver. (2010a). Environmental dependence of thermal reaction norms: Host plant quality can reverse the temperature-size rule. *The American Naturalist*, **175**:1–10.

Diamond, S. E., and J. G. Kingsolver. (2010b). Fitness consequences of host plant choice: a field experiment. *Oikos*, **119**:542–550.

Douglas, P., Bergamini, S., and Renzoni, F. (2006). Tunable Tsallis Distributions in Dissipative Optical Lattices. *Physics Review Letters*, **96**, 110601.

Eck, D. J., Shaw, R., Geyer, C. J., and Kingsolver, J. G. (2015a). An Integrated Analysis of Phenotypic Selection on Insect Body Size and Development Time. *Evolution*, **69**, 2525-2532.

Eck, D. J., Shaw, R., Geyer, C. J., and Kingsolver, J. G. (2015b). Supporting Data Analysis for "An Integrated Analysis of Phenotypic Selection on Insect Body Size and Development Time." Technical Report no. 698. School of Statistics, University of Minnesota, `http://hdl.handle.net/11299/172272`

Eck, D. J. (2015). R package `envlpaster`, version 0.1-2, `http://cran.r-project.org/package=envlpaster`.

Eck, D. J., Geyer, C. J., and Cook, R. D. (2016a). Supporting Data Analysis for "An Application of Envelope Methodology and Aster Models." Technical Report No. 699. School of Statistics, University of Minnesota, `http://hdl.handle.net/11299/178384`

Eck, D. J., Geyer, C. J., and Cook, R. D. (2017). An Application of Envelope and Aster Models. *Submitted*.

Efron, B. (2014). Estimation and Accuracy After Model Selection. *Journal of the American Statistical Association*, **109:507**, 991–1007.

Etterson, J. R. and Shaw, R. G. (2001) Constraint to Adaptive Evolution in Response to Global Warming. *Science*, **294**, 151–154.

Everitt, B. S. and Skrondal, A. (2010). *The Cambridge Dictionary of Statistics*, 4th Edition. Cambridge University Press.

Federov, V. V. (1972). Theory of Optimal Experiments, translated and edited by W. J. Studden and E. M. Klimko. New York: Academic Press.

Fisher, R. A. (1930). *The Genetical Theory of Natural Selection.* The Clarendon Press.

Freedman, D. A. (1981). Bootstrapping Regression Models. *The Annals of Statistics*, **9**, 6, 1218-1228.

Freedman, D. A. and Peters, S. C. (1984). Bootstrapping a Regression Equation: Some Empirical Results *Journal of the American Statistical Association*, **79**, 97–106.

Friedberg, S. H., Insel, A. J., and Spence, L. E. (2003). *Linear Algebra 4th ed.* Prentice Hall, Upper Saddle River, NJ.

Fukuda, K. (2008). cddlib library, version 094f. `http://www.ifor.math.ethz.ch/~fukuda/cddhome/cdd.html`

Fisher, R. A. (1930). *The genetical theory of natural selection.* Clarendon Press, Oxford, U. K.

Geyer, C. J. (1990). Likelihood and Exponential Families. PhD thesis, University of Washington. `http://conservancy.umn.edu/handle/11299/56330`.

Geyer, C. J., Wagenius, S., and R. G. Shaw. (2007). Aster models for life history analysis. *Biometrika* **94**:415–426.

Geyer, C.J. and Meeden, G. D. (2008). R package rcdd (C Double Description for R), version 1.1. Incorporates code from Fukuda (2008). `http://www.stat.umn.edu/geyer/rcdd/`

Geyer, C. J. (2009). Likelihood inference in exponential families and directions of recession. *Electronic Journal of Statistics*, **3**, 259–289.

Geyer, C. J. and Shaw, R. G. (2009). Model Selection in Estimation of Fitness Landscapes. Technical Report No. 671. School of Statistics, University of Minnesota. `http://conservancy.umn.edu/handle/11299/56219`.

Geyer, C. J. (2010). A Philosophical Look at Aster Models. Technical Report No. 676. School of Statistics, University of Minnesota. `http://purl.umn.edu/57163`.

Geyer, C. J. (2010). R package `aster2` (Aster Models), version 0.1. `http://cran.r-project.org/package=aster2`.

Geyer, C. J., Ridley, C. E., Latta, R. G., Etterson, J. R., and Shaw, R. G. (2013). Local Adaptation and Genetic Effects on Fitness: Calculations for Exponential Family Models with Random Effects. *Annals of Applied Statistics*, **7**, 1778–1795.

Geyer, C. J. (2013). Course slides for Stat 8931 topics class on aster models. `http://www.stat.umn.edu/geyer/8931aster/slides/`.

Geyer, C. J. (2014). R package `aster` (Aster Models), version 0.8-30. `http://cran.r-project.org`.

Halmos, P. R. (1958). *Finite-Dimensional Vector Spaces 2nd ed.* Van Nostrand Reinhold Company, New York, N.Y. 10001.

Hjort, N. L. and Claeskens, G. (2003). Frequentist Model Average Estimators. *Journal of the American Statistical Association*, **98:464**, 879–899.

Hjort, N. L. (2014). Discussion of Efrons paper, Estimation and accuracy after model selection. *Journal of the American Statistical Association*, **109:507**, 1017–1020.

Islam, M. F., and Lye, L. M., (2009). Combined use of dimensional analysis and modern experimental design methodologies in hydrodynamics experiments. *Ocean Engineering*, **36**, pp. 237–247.

Ji, H. and Muller, H.-G., 2016 Optimal Designs for Longitudinal and Functional Data *Journal of the Royal Statistical Society B*, in press. `10.1111/rssb.12192`.

Kaniadakis, G. (2006). Towards a relativistic statistical theory. *Physica A: Statistical Mechanics and its Applications*, **365** (1), 17–23.

Kaniadakis, G. (2013). Theoretical Foundations and Mathematical Formalism of the Power-Law Tailed Statistical Distributions. *Entropy*, **15**, 3983–4010.

Kass, R. K. and Raftery, A. E. (1995). Bayes Factors. *Journal of the American Statistical Association*, **90:430**, 775–795.

Kelley, J. L. (1955). *General Topology.* Springer-Verlag, New York. Originally published by Van Nostrand.

Kenward, M. G. (1987). A method for comparing profiles of repeated measurements. *Journal of the Royal Statistical Society* C, **36**, 296–308.

Khuri, A., Mukherjee, B., Sinha, B. K., and Ghosh, M. (2006). Design Issues for Generalized Linear Models: A Review *Statistical Science*, **21**, No. 3, 376–399.

Kingsolver, J. G., H. E. Hoekstra, J. M. Hoekstra, D. Berrigan, S. N. Vignieri, C. E. Hill, A. Hoang, P. Gilbert, and P. Beerli. (2001). The strength of phenotypic selection in natural populations. *The American Naturalist*, **157**:245–261.

Kingsolver, J. G., and S. E. Diamond. (2011). Phenotypic selection in natural populations: What limits directional selection? *The American Naturalist*, **177**:346–357.

Kingsolver, J. G., S. E. Diamond, S. A. Seiter, and J. K. Higgins. (2012). Direct and indirect phenotypic selection on developmental trajectories in *Manduca sexta*. *Functional Ecology*, **26**:598–607.

Lai, T., Robbins, H., and Wei, V. (1979). Strong Consistency of least squares estimated in multiple regression. *Journal of Multivariate Analysis*, **9**, 343-361.

Lande, R., and S. Arnold. (1983). The measurement of selection on correlated characters. *Evolution*, **37**:1210–1226.

Lehmann, E. L. (1959). *Testing Statistical Hypotheses.* Wiley, New York. MR0107933.

Lenski, R. E., and P. M. Service. (1982). The statistical analysis of population growth rates calculated from schedules of survivorship and fecundity. *Ecology*, **63**:655–662.

Liang, H., Zou, G., Wan, A. T. K., and Zhang, X. (2011). Optimal Weight Choice for Frequentist Model Average Estimators. *Journal of the American Statistical Association*, **106:495**, 1053–1066.

Lin, D., Shen, W. (2013) Comments: Some Statistical Concerns on Dimensional Analysis. *Technometrics*, **55**, 3.

Lowry, D. B. and Willis, J. H. (2010). A Widespread Chromosomal Inversion Polymorphism Contributes to a Major Life-History Transition, Local Adaptation, and Reproductive. *PLoS Biol*, **8(9)**, e1000500, `10.1371/journal.pbio.1000500`.

McKeague, I. W. (2015). Central limit theorems under special relativity. *Statistics and Probability Letters*, **99**, 149–155.

Mitchell-Olds, T. and Shaw, R. G. (1987). Regression analysis of natural selection: statistical inference and biological interpretation. *Evolution*, **41**, 1149–1161.

Ozgul, A., D. Z. Childs, M. K. Oli, K. B. Armitage, D. T. Blumstein, L. E. Olson, S. Tuljapurkar, and T. Coulson. (2010). Coupled dynamics of body mass and population growth in response to environmental change. *N*ature, **466**:482–485.

Ozgul, A., S. Tuljapurkar, T. G. Benton, J. M. Pemberton, T. H. Clutton-Brock, and T. Coulson. (2009). The dynamics of phenotypic change and the shrinking sheep of St. Kilda. *Science*, **325**:464-467.

Portes de Albuquerque, M., Esquef, I. A., Gesualdi Mello, A. R., and Portes de Albuquerque, M. (2004). Image thresholding using Tsallis entropy. *Pattern Recognition Letters*, **25** (2004) 1059–1065.

Potirakis, S.M., Minadakis, G., and Eftaxias, K. (2012). Analysis of electromagnetic pre-seismic emissions using Fisher information and Tsallis entropy. *Physica A: Statistical Mechanics and its Applications*, **391** (2012) 300–306.

R Development Core Team (2017). R: A language and environment for statistical computing. R Foundation for Statistical Computing, Vienna, Austria. `http://www.R-project.org`

Rockafellar, R. T. 1970. *Convex Analysis*. Princeton University Press, Princeton, NJ.

Rockafellar, R. T., and Wets, R. J.-B. (1998). *Variational Analysis*, Springer-Verlag, Berlin. (The corrected printings contain extensive changes. We used the 3rd corrected printing, 2010.)

Roff, D. A. (2002). *Life history evolution*. Sinauer Associates, Sunderland MA.

Rudin, W. (1973). *Functional Analysis 2nd ed.* McGraw-Hill.

Shaw, R. G., and C. J. Geyer. (2010). Inferring fitness landscapes. *Evolution*, **64**:2510–2520.

Shaw, R. G., C. J. Geyer, S. Wagenius, H. Hangelbroek, and J. R. Etterson. (2008). Unifying life-history analyses for inference of fitness and population growth. *The American Naturalist*, **172**:E35–E47.

Siepielski, A. M., J. D. DiBattista, and S. M. Carlson. (2009). It's about time: the temporal dynamics of phenotypic selection in the wild. *Ecology Letters*, **12**:1261–1276.

Singh, V. P. and Cui, H. (2015). Modeling sediment concentration in debris flow by Tsallis entropy. *Physica A: Statistical Mechanics and its Applications*, **vol. 420**, issue C, pages 49–58.

Sonin, A. (2001) *The Physical Basis of Dimensional Analysis*, Cambridge, MA: Department of Mechanical Engineering, MIT.

Su, Z. and Cook, R. D. (2011). Partial envelopes for efficient estimation in multivariate linear regression. *Biometrika*, **98**, 133-146.

Su, Z. and Zhu, G. and Chen, X. and Yang, Y. (2016). Sparse Envelope Model: Efficient Estimation and Response Variable Selection in Multivariate Linear Regression. *Biometrika*, **103**, 579–593.

Tempesta, P. (2011). Group entropies, correlation laws and zeta functions. *Physical Review E*, **84**, 021121.

Tsague, G. N. (2014). On Optimal Weighting Scheme in Model Averaging. *American Journal of Applied Mathematics and Statistics*, **2**, 3, 150–156.

Tsallis, C. (1988). Possible generalization of Boltzmann–Gibbs statistics. *Journal of Statistical Physics*, **52**, Issue 1–2, pp 479–487.

Umarov, S., Tsallis, C., and Steinberg, S. (2008). On a q-Central Limit Theorem Consistent with Nonextensive Statistical Mechanics. *Milan Journal of Mathematics*, **76**, 307–328.

Vignaux, G. A., and Scott, J. L. (1999), Simplifying Regression Models Using Dimensional Analysis. *Australia and New Zealand Journal of Statistics*, **41**, 31–34.

Wehn, D. (1962). Probabilities on Lie groups. *Proceedings of the National Academy of Sciences*, **48**, 791–795.

Weisberg, S. (2005). *Applied Linear Regression third edition*. Wiley, New Jersey.

Weyl, H. (1912). Das asymptotische Verteilungsgesetz der Eigenwerte linearer partieller Differentialgleichungen (mit einer Anwendung auf die Theorie der Hohlraumstrahlung). *Mathematische Annalen*, **71**, no. 4, 441-479.

White, F. M. (1999). *Fluid Mechanics fourth edition*. McGraw-Hill Companies, Inc.

Yamamoto, R. T. (1969). Mass rearing of the tobacco hornworm. II. Larval rearing and pupation. *Journal of Economic Entomology*, **62**:1427–1437.

Yamauchi, H., and N. Yoshitake. (1984). Developmental stages of ovarian follicles of the silkworm, *Bombyx mori* L. *Journal of Morphology*, **179**:21–31.